UNIVERSITY OF ADELAIDE
31·10·02
LIBRARY

THE UNIVERSITY OF ADELAIDE

Department of Applied Mathematics

Evaluating and Applying Contaminant Transport Models to Groundwater Systems

Masters Thesis
November 2001

Carl Purczel

Contents

List of Figures

List of Tables

Abstract

This thesis examines the use of random walk techniques to model the transport of a contaminant in groundwater. These techniques involve the distribution of a plume of contaminant into a discrete number of particles. These particles are then individually subjected to advective and dispersive forces and their progress though the model domain tracked over time.

In general, pollution of groundwater is characterised by:
1) being difficult to detect,
2) being complicated and expensive to investigate and monitor, and
3) being expensive to clean up.

These factors make the modelling of groundwater contamination an important area of investigation.

This thesis presents the principles of groundwater flow and contaminant transport, along with their governing equations (namely, the groundwater flow equation and the advection dispersion equation); methods for the solution of the advection dispersion equation are discussed. These methods include analytic, finite difference and random walk techniques.

Three random walk techniques are presented and compared with the analytic solutions for the following cases:
1) one dimensional dispersion
2) one dimensional advection dispersion
3) two dimensional dispersion
4) two dimensional advection dispersion

Results of the comparisons have showed that all three random walk schemes presented produce computed results which are consistent with the analytic solution in each of the cases considered.

Two finite difference schemes are presented and applied to the case of two dimensional advection dispersion. Through doing so, the problem of numerical diffusion has been highlighted.

Random walk techniques have been applied to two physical problems. In the first case, a model has been developed to simulate the movement of a plume of chloride in an aquifer in the province of Saskatchewan, Canada. Results are compared for each of the three random walk schemes, namely time histories and

breakthrough curves which plot the concentration of particles at a location in space over the time period modelled. All three random walk techniques have produced results that are very similar, with each modelling the movement of the plume acceptably.

The second model uses data from The South Australian Department of Mines and Energy to simulate the movement of salt in the groundwater in a vine growing region near Naracoorte, South Australia. This model produces results which are consistent with available measured data.

Statement of Originality

This work contains no material which has been accepted for the award of any other degree or diploma in any university or other tertiary institution and, to the best of my knowledge and belief, contains no material previously published or written by another person, except where due reference has been made in the text.

I give consent to this copy of my thesis, when deposited in the University Library, being available for loan and photocopying.

Carl Purczel Date

Acknowledgments

This thesis would not have been possible without the help and support of a number of people.

I'd like to thank my supervisor, Dr Michael Teubner, firstly for taking me on as his student, and secondly for his helpful, and almost endless support, without which I would have lost my focus on countless occasions.

I would also like to thank my family: firstly, to my parents Les and Roslyn, for their support and encouragement throughout my academic life and for being understanding when things were going not so well. Their support, both in emotional and financial terms, has made it possible for me to study at university. Secondly to my brother Paul who kept me sane by talking to me on some of those late nights.

I would like to thank Jenny Williamson; for her love, patience and support and for giving me confidence in myself and the motivation to finish this thesis.

I'd like to thank my close friends James Conn, Joshua Perrie, Andrew Grein, and Cameron Miller, all of whom have been my friends for longer than I care to remember and have been supportive of my academic career.

Finally, thank you to the staff and students in the Pure and Applied Mathematics departments at Adelaide University, without whom my experience at university would not have been as enjoyable as it has been.

Chapter 1

Introduction

1.1 Overview

The objective of this thesis is to examine the solution of the two dimensional advection dispersion equation, with particular application to the modelling of contaminants in groundwater, using particle tracking techniques. The more common numerical solution methods of solving this equation, namely finite difference methods, are presented and discussed briefly.

Three different particle tracking techniques are compared against known analytic solutions for a variety of problems, and then used to model the movement of contaminants in two groundwater systems.

1.2 The Groundwater Flow System and Groundwater Pollution

1.2.1 Groundwater Flow

Figure 1.1 shows the hydrologic cycle, of which groundwater flow is a significant part. From the diagram it can be seen that water enters the system in the form of precipitation which falls on the land surface. A portion of this water evaporates and some of this water moves along the land surface in the form of surface runoff. The rest of the water percolates through the soil, where it eventually reaches the water table (the uppermost level of subsurface water). The additional water creates localised increases in the surface of the water table which in turn creates gradients over the surface of the water table.

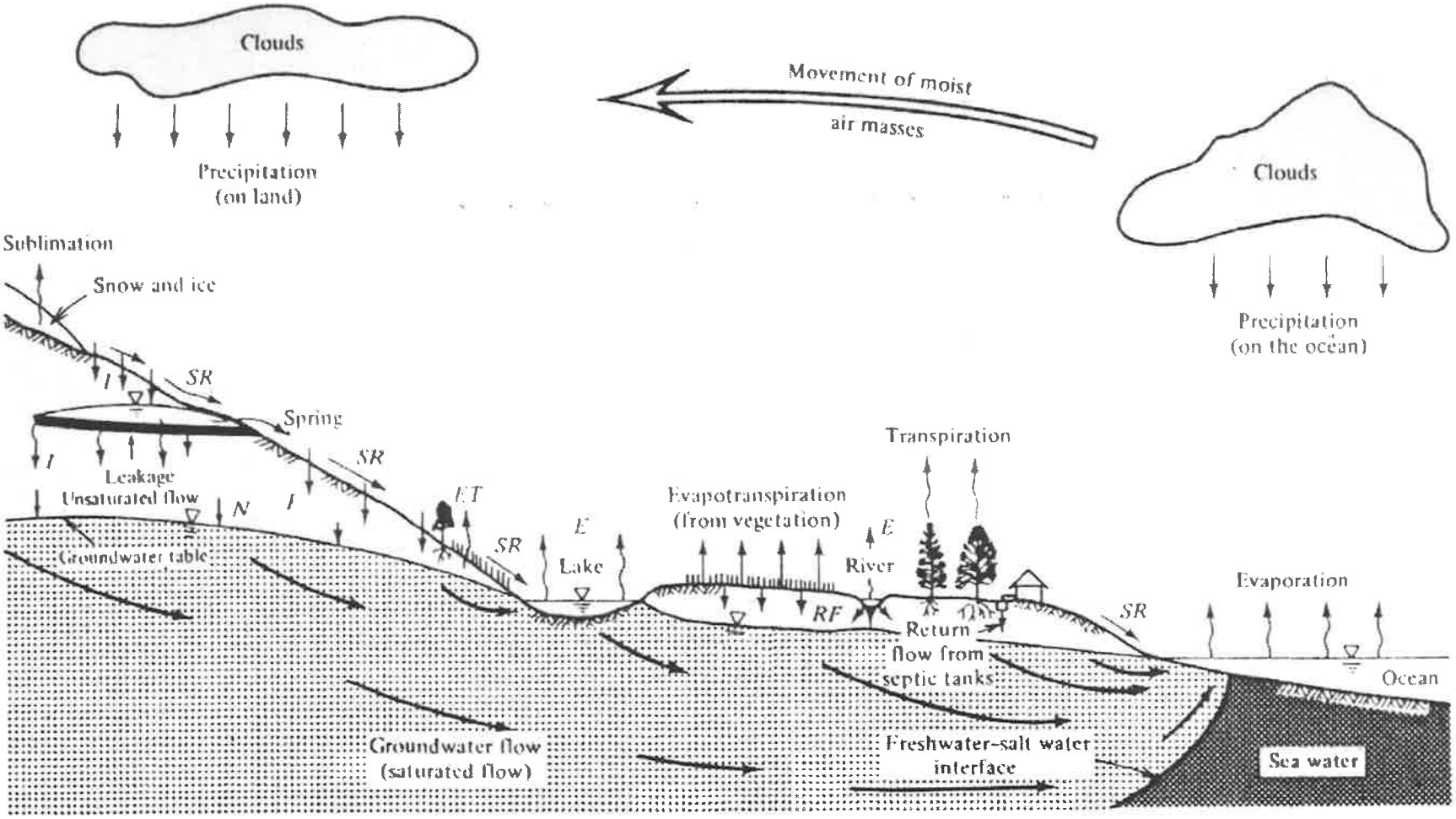

Figure 1.1: The Hydrologic Cycle, where SR = Surface runoff, N = Natural replenishment, E = Evaporation, ET = Evapotranspiration, RF = Return flow from irrigation and I = Infiltration [4].

Groundwater flows down gradient until it reaches a discharge point which may be a lake, river, sea or perhaps a man made well.

1.2.2 Groundwater Pollution

Suppose a contaminant is introduced into the system; for example, a contaminant is spilled on the land surface. (Some possible sources of contamination are given in Section 1.2.4). The contaminant leeches into the soil, eventually reaching the water table. Once in the groundwater it travels down gradient with the flow of groundwater. The velocity of the contaminant transport may not be the same as the groundwater flow velocity due to the properties of the contaminant and the soil.

Groundwater pollution has three main characteristics [8], these being:

- Groundwater pollution is not readily detectable, possibly delaying its discovery until many years past the initial contamination of the groundwater.
- Groundwater contamination is complicated and expensive to investigate and monitor.
- Cleaning up groundwater contamination is expensive, and there are limitations as to the amount of contaminant that can be removed.

It is therefore highly desirable to avoid groundwater contamination wherever possible, since in general the cost of cleaning up the contaminant is significantly higher than the cost of taking preventative action. There are some situations where groundwater pollution is tolerated, generally when the groundwater is already of poor quality or when the benefits to the community provided by the activities which contaminate the groundwater outweigh the cost of preventing the contamination.

Modelling of groundwater pollution is a cost effective method by which predictions of a contaminant plume's position may be made, and allows a variety of scenarios to be tested to determine the most effective clean up strategy.

1.2.3 Modelling Groundwater Flow and Pollution

Modelling groundwater flow involves the study of the flow of subsurface water through porous media, and the development of computer codes to simulate this flow. These models may be used to predict changes in groundwater levels and distribution. The modelling of contaminant transport in groundwater involves the

study of, and code development for, the movement of substances, both natural and artificial, which have been introduced into the groundwater system.

The benefits of modelling groundwater flow are that we are able to determine the long term effects of groundwater usage in a region and to evaluate the long term viability of the resource. By coupling this with modelling the transport of contaminants in the groundwater we may develop solutions to problems concerning groundwater quality, and where appropriate, take preventative action or develop an effective clean up strategy.

The modelling of groundwater flow in regions which have a high agricultural value allows us to determine the effects of changes in groundwater usage, for example increases in the pumping of groundwater, and increases in the irrigation of the land. By doing so we are able to maximise the crop productivity and quality in a region, while at the same time preserving the long term viability of the groundwater resource. The modelling of transport of contaminants in these same regions allows us to predict any potential problems associated with, for example, increases in salinity in the groundwater, or a hazardous chemical which has leeched into the groundwater system. By having an accurate model of the movement of these contaminants, we are able to determine, via the running of the model reflecting different scenarios, the best strategies for dealing with the contaminant problem.

1.2.4 Sources of Groundwater Pollution

There are many sources of groundwater pollution, ranging from naturally occurring pollutants, such as salt, to hazardous, man made contaminants. Table 1.1 gives a list of many sources of groundwater pollution, and the classifications given to them according to the U.S. Office of Technology Assessment [8]. Clearly, groundwater contamination occurs in areas of concentrated human activity, either through the direct discharge of pollutants into the groundwater system, or by the accumulation of naturally occurring pollutants (such as salt) as a side effect of human activity.

This thesis discusses the modelling of two different types of groundwater contamination: Chapter 4 discusses a Category II source of contamination (specifically disposal of chloride), while Chapter 5 discusses a Category VI source of contamination (natural leeching of salt) based on Table 1.1.

Category I: Sources designed to discharge substances

- Subsurface percolation (e.g. septic tanks and cesspools)
- Injection Wells
  - Hazardous waste
  - Non-hazardous waste (e.g. brine disposal and drainage)
  - Non-waste (e.g. enhanced recovery, artificial recharge, solution mining and in-situ mining)
- Land Application
  - Wastewater (e.g. spray irrigation)
  - Wastewater byproducts (e.g. sludge)
  - Hazardous waste
  - Non-hazardous waste

Category II: Sources designed to store, treat, and/or dispose of substances: discharge through unplanned release

- Landfills
  - Industrial hazardous waste
  - Industrial non-hazardous waste
  - Municipal sanitary
- Open dumps including illegal dumping (waste)
- Residential (or local) disposal (waste)
- Surface impoundments
  - Hazardous waste
  - Non-hazardous waste
- Waste tailings
- Waste piles
  - Hazardous waste
  - Non-hazardous waste
- Materials stockpiles (non-waste)
- Graveyards
- Animal burial
- Aboveground storage tanks
  - Hazardous waste
  - Non-hazardous waste
  - Non-waste
- Underground storage tanks
  - Hazardous waste
  - Non-hazardous waste
  - Non-waste
- Containers
  - Hazardous waste
  - Non-hazardous waste
  - Non-waste
- Open burning and detonation sites
- Radioactice disposal sites

Category III: Sources designed to retain substances during transport or transmission

- Pipelines
  - Hazardous waste
  - Non-hazardous waste
  - Non-waste
- Materials transport and transport operations
  - Hazardous waste
  - Non-hazardous waste
  - Non-waste

Category IV: Sources discharging substances as consequence of other planned activities

- Irrigation practices (e.g. return flow)
- Pesticide applications
- Fertilizer applications
- Animal feeding operations
- De-icing salts applications
- Urban runoff
- Percolation of atmospheric pollutants
- Mining and mine drainage
  - Surface mine-related
  - Underground mine-related

Table 1.1: Sources of Groundwater Contamination [8]

Category V: Sources providing conduit or inducing discharge through altered flow patterns

- Production Wells
  - Oil (and gas) wells
  - Geothermal and heat recovery wells
  - Water supply wells
- Other wells (non-waste)
  - Monitoring wells
  - Exploration wells
- Construction excavation

Category VI: Naturally occuring sources whose discharge is created and/or exacerbated by human activity

- Groundwater-surface water interactions
- Natural leeching
- Salt-water intrusion/brackish water upconing (or intrusion and other poor-quality natural water)

Table 1.1 (continued): Sources of Groundwater Contamination [8]

1.3 Cleaning Up Groundwater Pollution

Once the presence of a contaminant has been identified in the groundwater system, decisions regarding the removal of the contaminant must be made. The level of action taken depends upon a number of factors, such as the risk to public health, the value of the groundwater resource to the community, the extent of the contamination and the cost of removing the contaminants from the groundwater. Based upon these factors, it may be decided to either do nothing, or to investigate the problem further. In any such investigation, the modelling of the transport of contaminants is an important step in deciding what action is required. Actions may range from simply monitoring the area to a full scale clean up and prohibition of certain polluting activities [8]. The ability to model the transport of contaminants in groundwater allows the monitoring of the effects of particular clean up strategies, so as to allow the best choice to be made, as well as making long term predictions about the extent of contamination if no clean up strategy is undertaken.

1.4 Summary of this Thesis

This thesis discusses techniques that have been applied to model the movement of contaminants through a groundwater system. An outline of each chapter follows.

In Chapter 2, equations which govern both the flow of groundwater and the movement of contaminants are presented, and the processes of advection, dispersion, and diffusion are introduced and defined. Techniques which can be used to solve the advection dispersion equation numerically are discussed, in particular the finite difference method and Lagrangian/random walk techniques.

Two finite difference methods are applied to an example problem, and their results discussed. Eulerian and Lagrangian techniques are considered and their differences highlighted. Lagrangian/random walk models for solving the advection dispersion equation are described and their advantages and disadvantages noted.

A brief outline of the computer code RNDWALK2D [23] is given, and further developments of the code mentioned.

In Chapter 3, three Lagrangian/random walk techniques are presented. Each of the three techniques are applied to problems with known analytic solutions, and their results compared to these known solutions.

In Chapter 4 the computer code RNDWALK2D and modifications to employ other methods are applied to a contaminant transport problem in Saskatchewan, Canada. A model is developed which simulates the movement of chloride in the aquifer underlying the city of Regina using all three random walk techniques discussed in Chapter 3, and their results compared against measured data.

In Chapter 5, using data obtained from the Department of Mines and Energy in South Australia, a model which simulates the movement of salt in groundwater in a vine growing region in the south-east of South Australia is developed, and simulated results over a ten year period are presented.

Finally, Chapter 6 presents some conclusions based on the work contained within this thesis.

Chapter 2

Modelling Contaminant Transport in Groundwater Systems

2.1 Overview

This chapter looks at modelling the movement of contaminants in groundwater systems.

The governing equations for the flow of groundwater and the movement of contaminants are presented and briefly discussed, and methods for the numerical solution of the advection dispersion equation are mentioned before discussing random walk dispersion techniques, and the computer program RNDWALK2D.

2.2 The Governing Equations

The flow of subsurface water is governed by the two dimensional groundwater flow equation [26]

$$S\frac{\partial h}{\partial t} + Q_F = \frac{\partial}{\partial x}\left(T_x\frac{\partial h}{\partial x}\right) + \frac{\partial}{\partial y}\left(T_y\frac{\partial h}{\partial y}\right), \tag{2.1}$$

where

t = time $(years)$,
x, y = x and y coordinates (m),
h = groundwater level relative to some datum or potentiometric surface (m),
T_x, T_y = transmissivity in the x and y directions $(m^2/year)$,
S = storage coefficient,

Q_F = source/sink term $(m^3/year/m^2)$.

The transport of contaminants in groundwater is controlled by the advection dispersion equation. In two dimensions this is [10]:

$$\frac{\partial C}{\partial t} + u\frac{\partial C}{\partial x} + v\frac{\partial C}{\partial y} = \frac{\partial}{\partial x}\left(D_x\frac{\partial C}{\partial x}\right) + \frac{\partial}{\partial y}\left(D_y\frac{\partial C}{\partial y}\right) + K_e C + Q_T, \tag{2.2}$$

where

u, v = contaminant velocities in the x and y directions $(m/year)$,
D_x, D_y = hydrodynamic dispersion coefficients in the x and y directions $(m^2/year)$,
K_e = decay coefficient $(years^{-1})$,
Q_T = term representing sources and sinks of contaminant $(m^3/year/m^3)$,
C = the concentration of contaminant (m^3/m^3).

Additionally, the hydrodynamic dispersion coefficient in the x direction (D_x) may be expressed as [23],

$$D_x = d_L u + D_x^*, \tag{2.3}$$

where

d_L = the longitudinal dispersion coefficient (m),
D_x^* = the coefficient of molecular diffusion$(m^2/year)$.

A similar relationship holds for the hydrodynamic dispersion coefficient in the y direction (D_y).

To determine the transport of contaminants in a groundwater system Equation 2.2 is applied. Equation 2.2 requires that a velocity distribution is available for the model domain. To accomplish this, Equation 2.1 is solved to produce a distribution of potentiometric levels over the domain. By considering the rate of change of potentiometric levels with respect to space, a groundwater velocity profile can be determined using Darcy's law [4] which in the x direction can be written:

$$u_D = -K_x \frac{dh}{dx}, \tag{2.4}$$

where

$$\begin{aligned} u_D &= \text{Darcy velocity in the x direction,} \\ K_x &= \text{the conductivity of the soil in the x direction } (m/year), \\ &= \frac{T_x}{b}, \text{ where } b \text{ is the thickness of the aquifer.} \end{aligned}$$

A similar equation holds for v_D (Darcy velocity in the y direction).

To find the contaminant velocities u, v as required by the advection dispersion equation (Equation 2.2), the Darcy velocities u_D and v_D are divided by the porosity of the soil [23], giving

$$\begin{aligned} u &= \frac{u_D}{porosity}, \\ v &= \frac{v_D}{porosity}. \end{aligned} \tag{2.5}$$

2.2.1 Advective and Dispersive Processes

Contaminants present in a groundwater system are moved by a number of processes, specifically, advection, diffusion and dispersion. Each of these processes is discussed below.

Advection of a contaminant is the process by which a contaminant moves with the groundwater flow. As long as the groundwater is flowing, the flow velocity is non zero. Contaminants within the groundwater travel with the groundwater flow at some velocity which is related to the groundwater flow velocity. In the most simple case the advection of a contaminant is at the same velocity as the groundwater flow; however, this is not always necessarily the case, and it is quite possible for the flow of a contaminant to be retarded in relation to the groundwater flow velocity due to the contaminant's interaction with the soil particles or the physical properties of the contaminant. Where there is a non zero flow velocity, advection is generally the dominant process in the movement of a contaminant.

Dispersion and Diffusion are the two processes by which a contaminant plume spreads over time. An everyday example of this is the dispersion of smoke in the

air. If an observer were to watch smoke rising from a smoke stack on a windless day, rather than seeing the smoke stay clumped together, it would be seen to spread out, eventually having a concentration so small that it would not be visible.

Likewise with a pollutant in a groundwater flow: if a contaminant is introduced into a groundwater system, even without any flow, then it would be expected that the contaminant would spread throughout the system. This is due to the interactions between contaminant particles and the soil particles.

The process of *dispersion* or *mechanical dispersion* (d_L in Equation 2.3) is defined to be the random spread of contaminant particles caused by variations in velocity at the microscopic level as shown in Figure 2.1. This requires that some mean flow is present in the system.

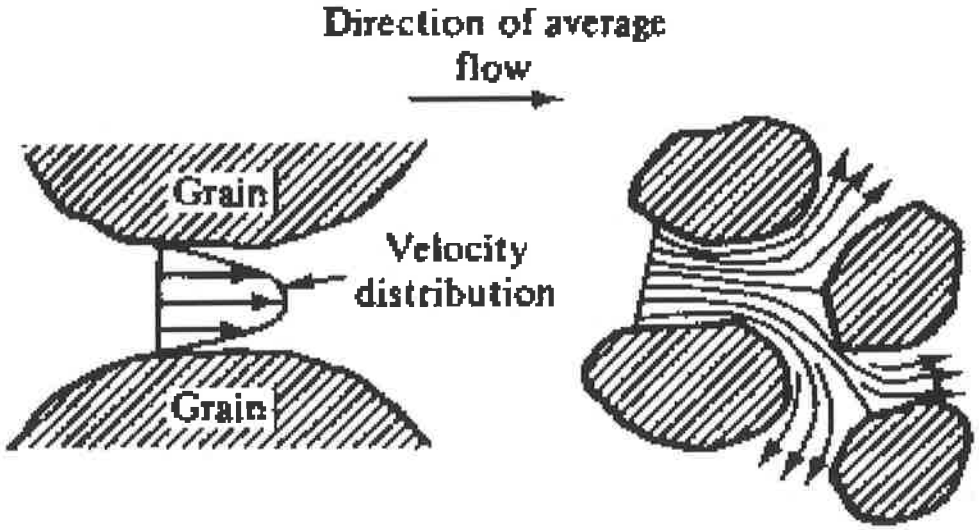

Figure 2.1: Velocity distribution between soil particles and the spread of contaminant due to dispersion [4].

On the other hand, the process of *diffusion* or *molecular diffusion* (D_x^* in Equation 2.3) is defined to be the random spread of contaminant particles caused by the random interactions of particles at the microscopic level as shown in Figure 2.2. These interactions themselves produce velocity variations between particles, resulting in the transport of a contaminant. The effect of diffusion is more prominent when the mean flow velocity is low or zero.

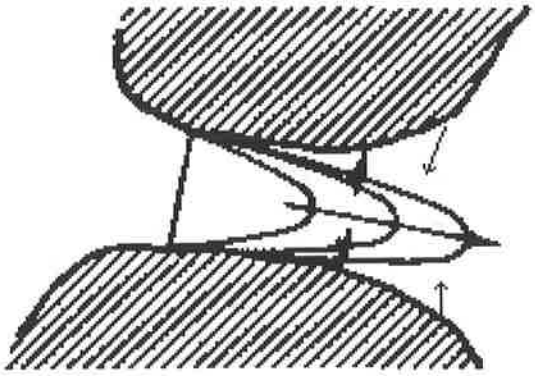

Figure 2.2: Velocity distribution between soil particles due to soil particle interactions [4].

The two processes of dispersion and molecular diffusion are quite similar in that they both cause the spread of a contaminant through variations of velocity between soil particles. Bear [3] describes the separation of dispersion and molecular diffusion as being an artificial one, since hydrodynamic dispersion contains both processes. Therefore, in this thesis where there is a mean velocity present the two processes have been considered as one, and have been referred to simply as *dispersion*.

2.3 Analytic Solutions

Analytic solutions can be found for the advection dispersion equation for simplified problems, with non-complex boundaries, and simplified conditions, the most common being to drop the source/sink and the decay terms.

The inability to handle complex (and thus real life) boundaries easily, limits the usefulness of analytic solutions; however, where applicable, they are the preferred method of solution for the advection dispersion equation since they have the advantage of being exact and of being the easiest of all the solution methods to implement in a computer code. Analytic solutions are also commonly used in the development of a numerical model, to verify the accuracy of the results obtained from the model.

In Chapter 3 some analytic solutions to simple problems are presented for the purpose of evaluating numerical random walk methods.

2.4 Numerical Solutions

The advection dispersion equation (Equation 2.2) may be solved numerically via a number of methods. These include finite difference, finite element, and finite volume methods, each of which have their own particular advantages and disadvantages. Of these methods, the most commonly used and easiest to implement and investigate is the finite difference method.

2.4.1 Finite Difference Method

The finite difference method is a common and effective method with which to solve partial differential equations numerically.

There exist a number of different finite difference methods which may be applied to solve the advection dispersion equation (Equation 2.2). The advantages of using a finite difference method over the finite volume or finite element methods for the solution of Equation 2.2 are:

- The equations to solve for a finite difference method are easy to develop and solve,
- Incorporating such methods into a computer code is relatively easy.

The disadvantages of using finite difference methods for the solution of Equation 2.2 are:

- Difficulties in applying boundary conditions,
- Poor handling of irregular boundaries,
- Introduction of numerical diffusion which can significantly alter results,
- Stability criteria may need to be satisfied.

2.4.2 Application of the Finite Difference Method

The application of the finite difference method to solve Equation 2.2 numerically requires that the entire solution domain be discretised into a grid in both space

(x,y) and time (t).

Given a rectangular spatial domain of dimensions $I \times J$ metres, then overlaying a grid of step size Δx in the x direction and Δy in the y direction (ensuring that $\frac{I}{\Delta x}$ and $\frac{J}{\Delta y}$ are integers), leads to the grid shown in Figure 2.3.

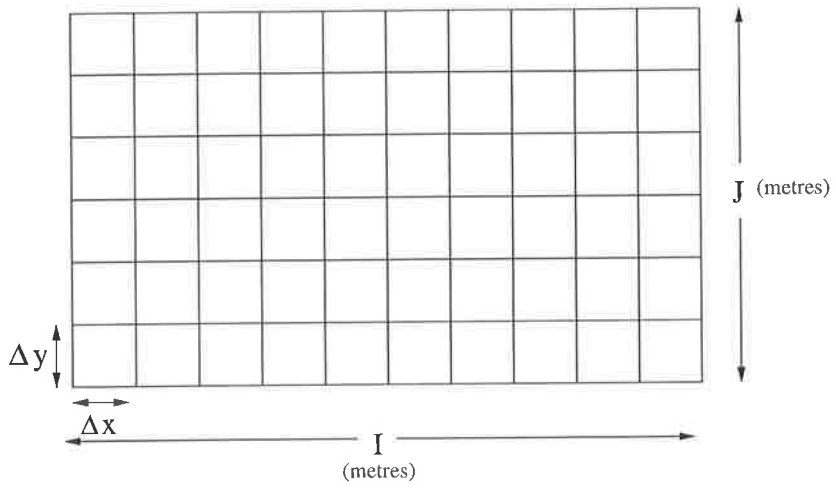

Figure 2.3: Example of a spatial domain with a finite difference grid superimposed.

The finite difference formula to be applied then refers to grid points via their (i,j) coordinate, where $0 \leq i\Delta x \leq I$ and $0 \leq j\Delta y \leq J$. Similarly, if the finite difference method is to be applied for a length of time T, then using a time step of Δt, the time is identified by its n "coordinate" where $0 \leq n\Delta t \leq T$. Combining these two, a point can be identified in space and time by specifying its (i, j, n) coordinate. Points surrounding the $(i, j)^{th}$ point at time step n are referenced as shown in Figure 2.4.

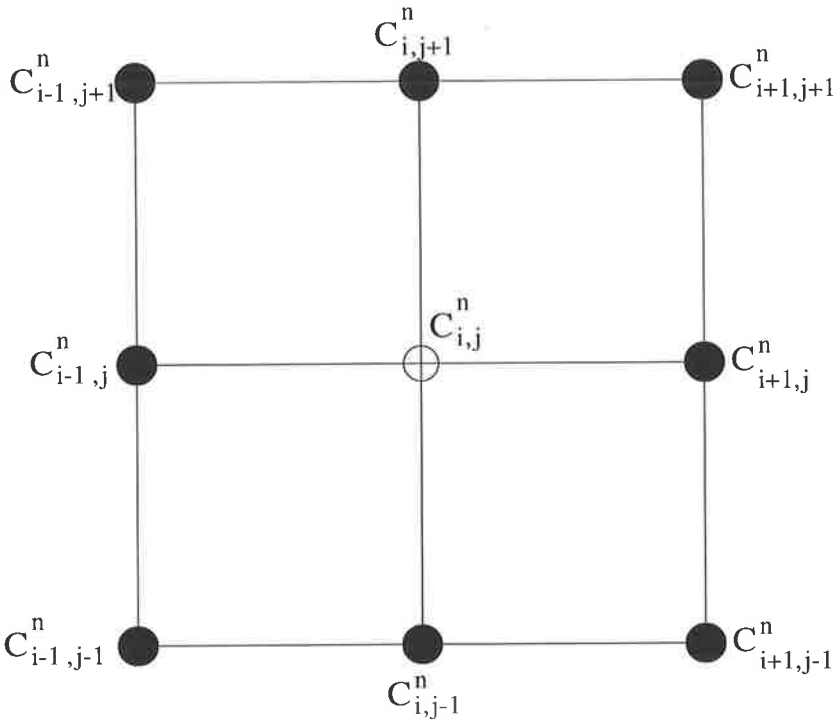

Figure 2.4: Finite difference grid, showing the n^{th} time level and the distribution of grid points around the $C^n_{i,j}$ grid point.

Forward time, centred space (FTCS) type formula

The first finite difference formula to consider is a forward time, centred space type (explicit) formula. Using a forward time approximation for the time derivative, a centred space approximation for the space derivatives at the grid point (i, j) at the n^{th} time level, and assuming no source/sink or decay terms (and that D_x, D_y, u and v are constant throughout the domain), an approximation for the concentration of contaminant at grid point (i, j) at the $n+1^{th}$ time level using the points $(i-1, j), (i, j), (i+1, j), (i, j-1), (i, j+1)$ at the n^{th} time level (as shown in Figure 2.4) can be developed, which yields the following finite difference approximation for the advection dispersion equation

$$\begin{aligned} C^{n+1}_{i,j} &= (\frac{c_x}{2} + s_x)C^n_{i-1,j} \\ &+ (\frac{c_y}{2} + s_y)C^n_{i,j-1} + (1 - 2s_x - 2s_y)C^n_{i,j} \\ &- (\frac{c_x}{2} - s_x)C^n_{i+1,j} - (\frac{c_y}{2} - s_y)C^n_{i,j+1}, \end{aligned} \tag{2.6}$$

where

$$\begin{aligned} c_x &= \frac{u\Delta t}{\Delta x}, \\ c_y &= \frac{v\Delta t}{\Delta y}, \\ s_x &= \frac{D_x\Delta t}{(\Delta x)^2}, \\ s_y &= \frac{D_y\Delta t}{(\Delta y)^2}. \end{aligned}$$

Performing a von Neumann stability analysis [18] to determine the numerical stability of Equation 2.6 yields the following relations that need to be satisfied simultaneously for stability [15]

$$s_x + s_y \leq \frac{1}{2}, \tag{2.7}$$

$$\frac{(c_x)^2}{s_x} + \frac{(c_y)^2}{s_y} \leq 2. \tag{2.8}$$

Presented below are results produced by the computer program listed in Appendix A, using choices of parameters that satisfy the above stability relations.

Results and Discussion

A listing of a FORTRAN 77 program is given in Appendix A. This program solves the two dimensional advection dispersion equation, using a forward time, centred space approximation, for a situation where a slug of contaminant is injected into a 300 $ft \times 300\ ft$ domain at grid point (5,15) with parameters as given in Table 2.1.

Clearly these satisfy the requirements for von Neumann stability given above, since

$$\begin{aligned} s_x + s_y &= \frac{4.5 \times 0.5}{10^2} + \frac{1.125 \times 0.5}{10^2} \\ &= 0.028125 \\ &< \frac{1}{2} \end{aligned}$$

Parameter	Value
Δx	$10\ ft$,
Δy	$10\ ft$,
Δt	$0.5\ days$
Longitudinal Dispersivity (D_x)	$4.5\ ft^2/day$
Transverse Dispersivity (D_y)	$1.125\ ft^2/day$
X velocity (u)	$1\ ft\ day^{-1}$
Y velocity (v)	$0\ ft\ day^{-1}$
Initial concentration	$300\ ppm.$
Boundary concentrations	$0\ ppm$

Table 2.1: Parameter values used in the FTCS program presented in Appendix A.

and, using the same parameters

$$\begin{aligned} \frac{(c_x)^2}{s_x} + \frac{(c_y)^2}{s_y} &= \frac{(\frac{0.5}{10})^2}{0.0225} \\ &= 0.11111111 \\ &< 2 \end{aligned}$$

Figure 2.5 shows the computed results after 150 days of simulation time. It is noted that the contaminant has been advected approximately $150ft$ in the x direction (as expected), and the slug has spread to cover an area which is over $100ft$ long in the x direction and approximately $50ft$ in the y direction.

Upwind Formula

The second finite difference formula that will be considered is an upwind type (explicit) formula. Using a forward time approximation for the time derivative, a centred space approximation for the dispersive terms, and a backward space approximation for the advective terms (assuming that the velocities u and v are positive) at the point (i, j) at the n^{th} time level yields the following finite difference approximation for the advection dispersion equation

$$\begin{aligned} C_{i,j}^{n+1} &= (s_y + c_y)C_{i,j-1}^n + (s_x + c_x)C_{i-1,j}^n \\ &+ (1 - 2s_x - 2s_y - c_x - c_y)C_{i,j}^n \\ &+ s_x C_{i+1,j}^n + s_y C_{i,j+1}^n. \end{aligned} \tag{2.9}$$

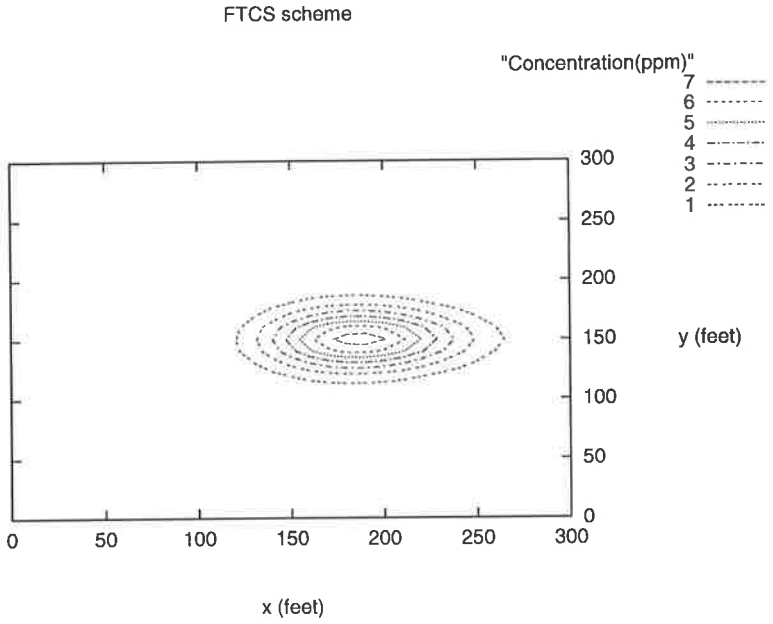

Figure 2.5: Concentration of contaminant after 150 days using the FTCS type formula. Contours indicate the concentration of contaminant $(1-7\ ppm)$ over a 30×30 grid with $\Delta x = \Delta y = 10ft$. The initial position of the contaminant plume was $(50, 150)$.

Von Neumann stability requires for this case [20]

$$2s_x + 2s_y + c_x + c_y \leq 1. \tag{2.10}$$

However, this finite difference method incorporates numerical diffusion, which means that there will be more dispersion than that prescribed by the parameters D_x and D_y. This can be seen by examining the modified equivalent partial differential equation [21] which indicates numerical diffusion coefficients of $\alpha_x^n = u\Delta x(1-c_x)/2$ and a similar term α_y in the y direction [4]; for the parameters used, this gives a numerical diffusion coefficient in the x direction of $4.75\ ft^2/day$. This means that there will be approximately double the required amount of dispersion.

Results and Discussion

A listing of a FORTRAN 77 program may be found in Appendix B. This program solves the two dimensional advection dispersion equation using the upwind method for a situation where a slug of contaminant is injected into a 300 $ft \times$ 300 ft domain at grid point (5,15) with the same parameters as used for the FTCS type formula.

Clearly these parameters satisfy the requirements for Von Neumann stability as given above since

$$\begin{aligned} 2s_x + 2s_y + c_x + c_y &= 2\left(\frac{4.5 \times 0.5}{10^2}\right) + 2\left(\frac{1.125 \times 0.5}{10^2}\right) + \frac{0.5}{10} \\ &= 0.10625 \\ &< 1 \end{aligned}$$

Figure 2.6 shows the computed results after 150 days of simulation time. Comparing Figure 2.5 with Figure 2.6, it is clear that Figure 2.6 displays far more dispersion than that shown in Figure 2.5 despite both having used exactly the same parameters. It is clear that the slug's maximum concentration after 150 days is somewhat reduced than that shown in Figure 2.5, and that there is an increased amount of spread of the material. This is a clear demonstration of the numerical dispersion that is present within the explicit upwind type finite difference formula (Equation 2.9).

When the dispersion coefficient D_x is increased by 4.75 ft^2/day and the FTCS scheme run with a D_x of $9.25 ft^2/day$, then the results are very similar to those using the upwind formula. Figure 2.7 shows these results. The similarities between these results and those presented in Figure 2.6 can be seen easily.

The presence of numerical diffusion in the upwind solution, as shown in Figure 2.6, gives motivation to seek an alternative method of solution to the advection-dispersion equation (Equation 2.2). One such method is the Random Walk method, discussed below.

2.4.3 Lagrangian/Random Walk Methods

The previous sections have discussed the solution of the advection dispersion equation (Equation 2.2) using an *Eulerian* approach to describe the flow regime. This involves the consideration of a particular point in space, and observing the

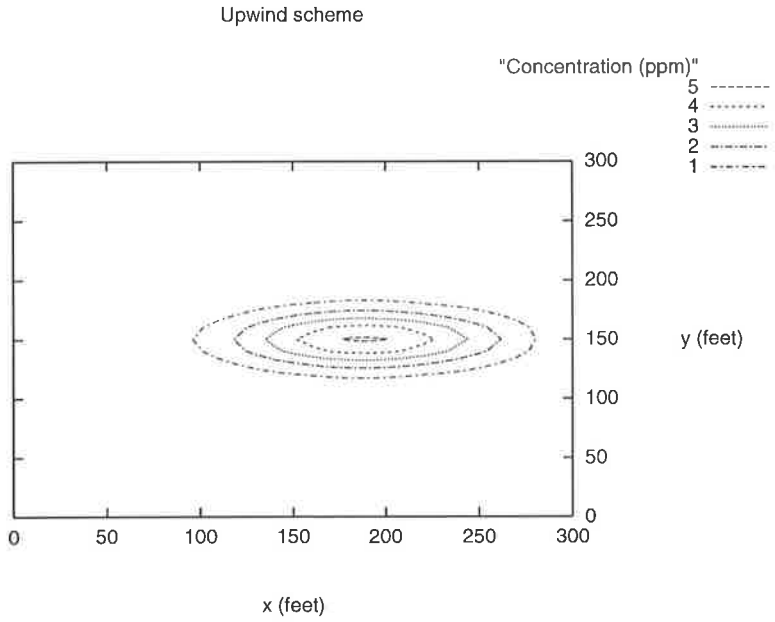

Figure 2.6: Concentration of contaminant after 150 days using the upwind formula. Contours indicate the concentration of contaminant $(1-5\ ppm)$ over a 30×30 grid with $\Delta x = \Delta y = 10ft$. The contaminant plume was initially located at $(50, 150)$.

changes in concentration of the fluid as the fluid passes that point.

As shown in Woods [30, 31], computer codes which employ finite difference, finite element and finite volume methods as their method of solution may lead to incorrect simulated results due to inconsistency, numerical diffusion (as demonstrated in Figure 2.7) or stability problems in the solution technique. Therefore, an alternative method of solution is sought.

An alternate description of the flow regime is the *Lagrangian* approach. This considers the entire fluid to be a mass of part-icles, each of which can move independently. The overall flow is assessed by considering each particle separately and tracking its changing position over time. The movement of the fluid is simulated by the movement of the particles, and the concentration within the fluid at a particular point in space is determined by the number of particles present in the

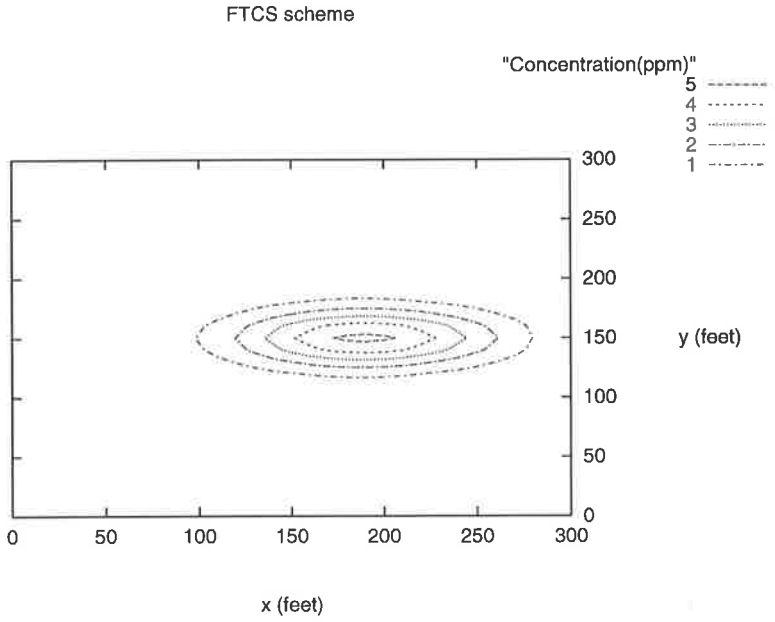

Figure 2.7: Concentration of contaminant after 150 days using the FTCS type formula with $D_x = 9.25 ft^2/day$. Contours indicate the concentration of contaminant $(1-5\ ppm)$ over a 30×30 grid with $\Delta x = \Delta y = 10 ft$. The initial position of the contaminant plume was $(50, 150)$.

vicinity of that point.

Description of Lagrangian/random walk models

The advection dispersion equation (Equation 2.2) may be solved using a Lagrangian/random walk technique. This is a very different technique to those described in Section 2.4.1, due to the treatment of the contaminant plume in a Lagrangian manner.

The underlying assumptions behind random walk techniques are the following: firstly, the dispersion of a fluid through a porous media (for example, soil) is a random process [23]; secondly, a plume of contaminant consists of a large number of molecules; and thirdly, the movement of the contaminant is determined by considering the movement of each particle, and then summing the number of par-

ticles present in a particular region to determine the concentration of contaminant.

This technique considers the contaminant plume as a collection of a large number of particles, each of which represents a predetermined quantity of contaminant and is acted upon independently by advective and dispersive forces. In doing so, the technique is much more closely related to the physical process of a contaminant travelling through a groundwater system. Figure 2.8 shows how contaminant particles travelling in a groundwater flow are dispersed through their movement through the soil.

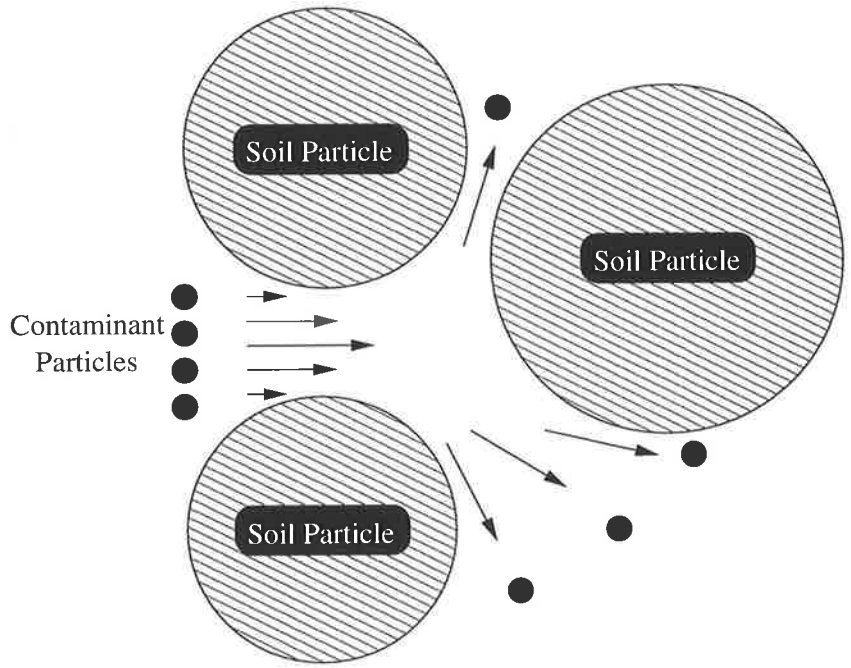

Figure 2.8: Dispersion of contaminant particles in a porous medium, highlighting the widely varying final positions (in both x and y directions) of particles which were initially in close proximity.

As can be seen in Figure 2.8, the final position of a particle relies not only on the groundwater flow, but also on the random interactions with the soil particles. Given some mean flow, the particles will move with the flow. Their final position in the medium is determined by the interactions of these particles with the soil particles. In this way, particles may be spread perpendicular to the mean flow (transverse dispersion) or some particles may have their motion retarded at a different rate compared to other particles (longitudinal dispersion). The random walk

technique is an attempt to mathematically model this aspect of the movement of contaminants through porous media, by the application of random perturbations in the particles' movement.

In its most basic form, a Lagrangian/random walk scheme can be expressed as

$$x_{n+1} = x_n + \delta x + R_1, \tag{2.11}$$
$$y_{n+1} = y_n + \delta y + R_2, \tag{2.12}$$

where

x_n, y_n	are the x and y positions of the particle at time step n,
$\delta x, \delta y$	are the advective components of the particle's movement in the x and y directions ($\delta x = u\Delta t$ and $\delta y = v\Delta t$ where Δt is the time step length),
R_1, R_2	are some random movement terms incorporating D_x, D_y, the dispersion coefficients.

This describes the method which is used to determine a particle's position at the $n+1^{th}$ time step given the position of the particle at the n^{th} time step.

Concentrations of contaminant are calculated on the basis of how many particles are present near a grid point, and how much contaminant each particle represents. This directly reflects the physical processes involved in measuring the concentrations of contaminant in a groundwater flow.

Application to the Advection Dispersion Equation

To simulate the advective components of the advection dispersion equation ($u\frac{\partial C}{\partial x}$ and $v\frac{\partial C}{\partial y}$ terms), a particle is moved a distance of δx in the x-direction and δy in the y-direction at each time step where:

$$\delta x = u\Delta t,$$
$$\delta y = v\Delta t.$$

This assumes that the velocities u and v are available, or can be calculated by some means. Most commonly, velocities are known, or have been calculated, for specific points in a domain, such as every node of a finite difference grid, or perhaps at the midpoint between each node as is used in RNDWALK2D discussed in Section 2.5. However, the probability of a particle lying on a point where the velocities are defined is small so some method is required to be able to find the

velocities u and v at any point in the domain. To find the velocity components u, v at any other point requires that an interpolation scheme be used. Such a scheme usually uses the closest defined velocities to calculate a particle's velocity.

To model the effect of dispersion in the advection dispersion equation ($D_x \frac{\partial^2 C}{\partial x^2}$ and $D_y \frac{\partial^2 C}{\partial y^2}$ terms), a particle is moved some random distance, in some random direction at each time step. This is in keeping with the physical process of dispersion through porous media, which is considered to be a random process [23].

The Lagrangian/Random Walk Algorithm

In this section the algorithm for using a Lagrangian/random walk technique is presented. It is assumed that there is an initial distribution of M particles at time $t = 0$. Figure 2.9 shows the steps required to implement a random walk algorithm.

The algorithm as shown assumes that there exists a number of particles in the model area representing some contaminant. Each particle is uniquely identified by a number. Likewise, each time step is identified by a number. To start the algorithm the current time step is set to 0 and the current particle number is set to 1. Starting from these conditions, the algorithm is applied in the following manner: the location of particle number 1 is scanned and velocities at its location determined or calculated. Using this velocity information the particle is advected, and then dispersed, resulting in a new location for the particle. The location is then stored, and the particle number incremented. Similarly for the rest of the particles. When the final particle has been moved the time step number is incremented, the current particle number set to 1 and the process repeated. This procedure is repeated until all required time steps are completed.

Advantages and Disadvantages of Using a Random Walk Technique

The advantages of using a random walk technique to solve the advection dispersion equation over other numerical techniques are many. For example:

- By using a random walk technique, we eliminate the numerical diffusion that may occur when using a finite difference method.
- If the contaminant plume occupies only a fraction of the model domain, then significant simulation time can be saved in calculating the movement of a plume when compared to finite difference methods, particularly in three

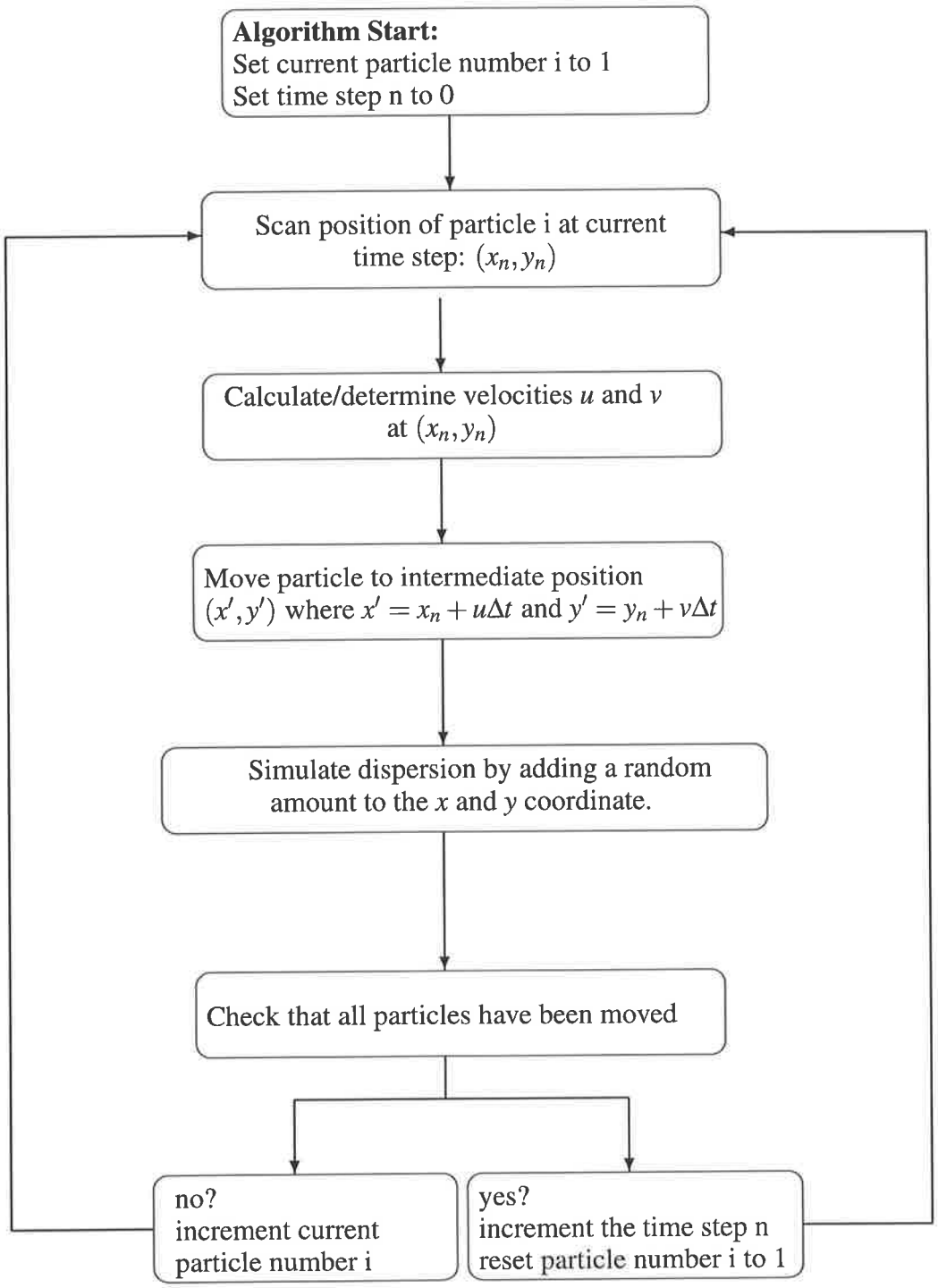

Figure 2.9: The random walk algorithm.

dimensions, due to the lower number of computations required at each time step. This is because the number of particles, in general, is much less than the number of grid points.

- A solution can have as much resolution as required by the user, or as dictated by other factors such as time and money. By using fewer particles, less computer time is expended in producing a solution, with the trade-off of having a lower resolution solution.

- Solutions obtained using random walk methods are additive. If more resolution is required, the model only needs to be run again with the additional particles required and the two (or more) solutions combined [23].

- Particle tracking (Lagrangian) techniques can be a valuable tool for tracing problems in flow models, and for the visualisation of a flow through the plotting of particle pathlines [2].

- Decay can be easily implemented by allowing the removal of particles.

There are, however, some disadvantages to using a Lagrangian/random walk technique, such as:

- The output of a Lagrangian/random walk technique requires some interpretation since a single particle represents a certain quantity of contaminant, and particles may cover the domain sparsely, in particular if a small number of particles are used [23].

- Possible problems may occur around low yield pumping wells [33] if the grid size is inappropriate, or if the method for estimating velocities is not sufficiently accurate. In such a situation, particles may not be extracted from the system when in the vicinity of a such a well, resulting in inaccurate contaminant concentration results.

- It is possible to have concentrations greater than initial concentrations at some grid points [23]. Figure 2.10 shows a situation of an initial concentration of three particles per grid space, representing some concentration of contaminant. After one time step, grid space (5,3) contains four particles, which is greater than the initial concentration of three. This situation is difficult to avoid; however, the magnitude of this error can be minimised by using more particles.

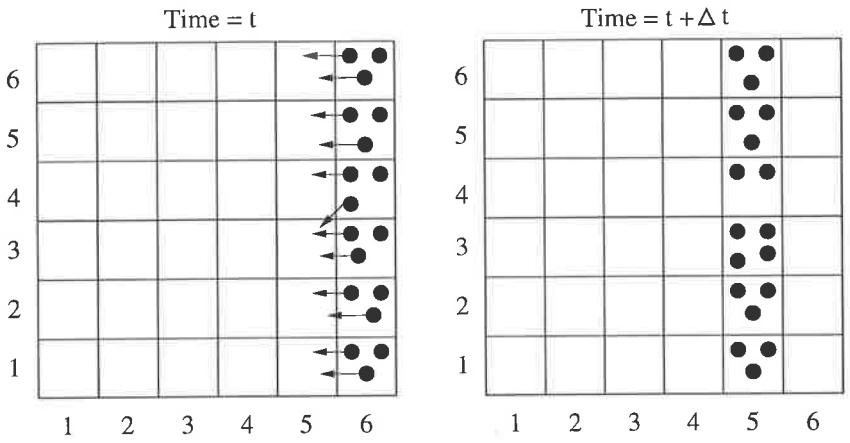

Figure 2.10: Diagram showing how concentrations greater than initial concentrations are possible.

2.4.4 Previous Users of Random Walk Techniques

T.A. Prickett, T.G. Naymik and C.G. Lonnquist [23]

Published in 1981, *"A "Random-Walk" Solute Transport Model for Selected Groundwater Quality Evaluations"* is an extension of PLASM [22], adding a contaminant transport component to the widely used groundwater modelling computer code PLASM. This code (RNDWALK2D) is used in the modelling of groundwater and test problems throughout this thesis.

J.R. Hunter [16]

The paper *"The application of Lagrangian particle-tracking techniques to modelling of dispersion in the sea"* examines the computational efficiency of random walk methods as compared to the more widely used finite difference techniques. It is determined that random walk techniques are more accurate, for a given computational cost, if the number of particles is small, the model is of higher dimension, and the contaminant does not cover the entire model. Random walk techniques are used to model the movement of an oil slick near Anglesey, North Wales, and thermal discharge of a proposed power plant in Koombana Bay, Western Australia. In the case of the oil slick model, a mere 10 particles were used to give an indication of the oil slick's position and size.

W.C. Walton [29]

"Numerical Groundwater Modeling: Flow and Contaminant Migration" contains details of modified versions of the groundwater flow program PLASM [22] and RNDWALK2D [23] (referred to as GWFL3D and GWTR3D respectively. The "3D" part of each code's name refers to the quasi three dimensional models to which both PLASM and RNDWALK2D can be extended). Of primary interest, in relation to this thesis, is the modified version of RNDWALK2D. GWTR3D is an attempt to create a RNDWALK2D-based code which contains more user friendly features such as frequent on-screen prompts, helpful on-screen directions and choices of output type (printer or disk files). Additionally, much of RNDWALK2D has been rewritten, new situation specific subroutines added, and some subroutines modified to produce a more readable code.

J. Bear and A. Verruijt [4]

"Modeling Groundwater Flow and Pollution" contains a brief introduction to random walk techniques, highlighting their advantage of having no numerical dispersion like finite difference or finite element models. A random walk scheme is developed, initially in one dimension and then extended to two dimensions, and a code presented, showing its application in the case of a plume of contaminant being contained within the capture zone of a pumping well.

A.H. Al-Rabeh and N. Gunay [1]

"On the Application of a Particle Dispersion Model" details the development of a random walk technique, later used by Lewis, Noye and Evans [19] and Grzechnik and Noye [13]. The technique is tested against a problem which has a known analytic solution, before being applied in an environmental impact study in the release of pollutants into the sea from an offshore platform.

A.L. Fogelson [9]

"Particle-Method Solution of Two-Dimensional Convection-Diffusion Equations" uses random walk techniques to model the transport of the chemical adenosine diphosphate (ADP) which is released by a type of blood cell (platelets). As with a fast moving groundwater flow, the flows in which ADP is being transported are advection dominated. It is shown that in this situation random walk techniques are accurate, without the oscillations of some finite difference techniques or the numerical diffusion of others. The lack of numerical diffusion in this application is important since the size of the actual diffusion coefficient is small. Likewise,

in some groundwater contaminant transport problems the dispersion may be quite small, which could be overwhelmed by large numerical diffusion.

C. Zheng [33]

"Analysis of Particle Tracking Errors Associated with Spatial Discretization" details errors that can arise from using random walk techniques to model contamination of groundwater. It is shown that problems can arise if the grid used is too coarse, and if a low extraction pumping well exists, then inaccuracies can arise due to the velocity interpolation scheme not correctly defining velocities around the well. Solutions to this problem are considered, including the use of a finer sub-grid around such wells, or the use of a more accurate velocity interpolation scheme.

A.K. Easton, J.M. Steiner and D.F. Zhang [6]

"Domain and Cell Effects in Diffusion Models for Oil Spills in the Ocean" examines the solution of the two dimensional diffusion equation by use of random walk techniques as later used in [7]. Additionally, this paper discusses the use of Gaussian Kernel Weighting in random walk methods to convert known particle positions into mass concentrations.

A.K. Easton, J.M. Steiner and D.F. Zhang [7]

"Random Walk Methods for the Solution of the Diffusion Equation" presents a random walk scheme (referred to in this thesis as the Easton, Steiner and Zhang scheme) and compares results with those obtained by analytic finite difference solutions for the diffusion equation. An analysis of the effect of the number of particles and the grid size on the accuracy of the results obtained by using a random walk scheme is presented, showing that the accuracy of concentrations increases with the number of particles, but decreases with an increase in the area of the grid. Area weighting, a technique used to more accurately distribute the contaminant represented by a particle amongst the surrounding grid nodes, is used to reduce the error in the computed concentrations using random walk techniques.

G.D. Lewis, B.J. Noye and P.L. Evans [19]

"A Comparison of Finite Difference and Lagrangian-Stochastic Methods for Oil Slick Tracking" uses the random walk technique as presented in Al-Rabeh and Gunay [1], and compares it with the use of a finite difference approach when modelling an oil spill in the Northern Spencer Gulf, South Australia. It is noted that both finite difference and random walk techniques give similar results, with

the random walk technique producing its results faster due to the lower number of computations required at each time step. A technique is mentioned that uses random walk initially until the spill is sufficiently large, then changing to a finite difference approach; however no results for this method are given. The random walk technique employed in this paper is referred to as the "Lewis, Noye and Evans scheme" in this thesis.

M. Grzechnik and J. Noye [14]

"A Lagrangian-Stochastic Particle Tracking Procedure for Coastal Seas" discusses the development of a procedure, based on the random walk technique presented in [7]. A procedure for specifying velocities at large time intervals ΔT and using interpolation to determine the required random walk time step Δt (for the purpose of decreasing storage requirements, or where velocity information is sparse) is developed and discussed.

D.F. Zhang, A.K. Easton and J.M. Steiner [32]

"Modelling the Kirki Oil Spill" discusses the development of a computer model which simulates the release of oil into the sea from a damaged oil tanker. Of interest is the method used to model a moving source of contaminant. (However, this has no equivalent counterpart in groundwater modelling.) Results obtained from this model matched well with observations at the time. This model shows that random walk techniques can be used to produce accurate predictions of the movement of contaminants.

C. Purczel and M. Teubner [24]

"Comparison of three techniques for modelling the advection/dispersion equation" compares the results of three random walk techniques (Prickett et al. [23], Easton et al. [7], and Lewis et al. [19]) for the cases of one and two dimensional advection-dispersion and one dimensional dispersion. A model of the release of chloride from a waste water reservoir in Canada is developed and the computed results presented and compared with known measured results.

M. Grzechnik and J. Noye [13]

"Alternative Boundary Conditions for a Lagrangian Particle Tracking Routine for Coastal Seas" considers the behaviour of particles near two types of boundaries in the modelling of prawn larvae dispersion, namely open sea boundaries and closed boundaries. These can be directly equated with constant head boundaries and no flow boundaries in groundwater modelling. While the issues surrounding

the behaviour near no flow boundaries are relevant to groundwater modelling, those mentioned for open boundaries (eg. particles leaving the model domain and returning later) are less likely to happen in groundwater modelling since the likelihood of a reversal of groundwater velocities is not high (except possibly in the case where a pumping well is switched on very close to a boundary).

M. Grzechnik and J. Noye [12]

"Lagrangian-Stochastic Particle Tracking Applied to Prawn Larvae Dispersion in Gulf St. Vincent, South Australia" shows the development of a method to model the dispersion of prawn larvae. Additionally, examination of two types of grid definition is undertaken, namely Arakawa type A and Arakawa type C grids. In this thesis, as in Prickett et al.[23], an Arakawa type C grid is used in the definition of the velocity components, wherein the velocities are defined midway between nodes. It was determined that both types give similar results, with a type C grid being more useful where barrier boundary conditions are present such as coast lines or, in groundwater, impermeable rock formations, indicating that the grid type used in Prickett et al. [23] is the more suitable type of grid definition to use. Examination of three types of random walk schemes is performed which is an extension (and correction of) work done by Purczel and Teubner [24]. Finally, results from a model using the Easton, Steiner and Zhang scheme are presented for comparison.

2.4.5 Comparison with Eulerian techniques

Given two different methods to solve the advection dispersion equation, it is of interest how the two compare in various aspects, such as accuracy, and their respective advantages and disadvantages. The following sections discuss these aspects.

Accuracy of Lagrangian/random walk techniques

In choosing a Lagrangian/random walk method over the more traditional Eulerian approach, it is clearly desirable that it is at least as accurate as the Eulerian approach.

Two main sources of error are present within a Lagrangian/random walk technique, the first being introduced via the estimation of the particle velocities, and the second being small errors due to the random nature of the technique.

Errors due to the use of random numbers to represent the physical process of dispersion in the technique are unavoidable. These will only be of great concern when a large number of time steps are used, since at each time step a small error may be introduced, causing the numerical solution to depart slightly from the true solution. Of greater importance are the errors introduced via the estimation of velocities since for most cases the advective component is the dominant process in a particle's movement. The advective component of a particle's movement is dependent on the velocity and is determined via the equations

$$\begin{aligned} \delta x &= u\Delta t \\ \delta y &= v\Delta t. \end{aligned}$$

Clearly the accuracy of the velocities u and v will directly influence the accuracy of the advective components δx and δy, and thus an accurate way of determining u and v is required to minimise the errors. It should be noted that this problem is not unique to the random walk method since finite difference methods, such as those mentioned in Section 2.4.1, similarly require that accurate velocities be available or the numerical solutions generated will be inaccurate.

Estimating Velocities u and v

The most accurate way of determining u and v would be through the application of a known analytic solution. For real life situations, such a solution is unlikely to exist; however for test cases (such as for evaluating a technique) these could be specified and used. The advantage of using an analytic solution is that velocities are exact, and are defined over the whole of the solution domain.

More realistically, groundwater head levels are likely to be known at particular points in the domain, either from being measured, or by being calculated via a groundwater model. In the former case head levels are likely to be known at a small number of irregularly spaced points in the model domain, while in the latter case the heads are likely to be known at a larger number of regularly spaced points. In either situation internodal groundwater velocities are calculated via the application of Darcy's law (Equation 2.4), which determines groundwater velocities at a discrete number of points in the domain.

The likelihood of a particle's position being at a point in the domain where the groundwater velocity is know is small, and thus a method which can be used to determine a particle's velocity at any point in the domain is required.

Given some particle at a point whose velocities are unknown, surrounding points whose velocities are known are used to estimate the velocity of the particle through the use of interpolation.

The importance of using an accurate velocity interpolation scheme is highlighted in Zheng [33]. It is shown that in the case where there exists a low extraction pumping well, an inaccurate velocity interpolation scheme leads to particles not being removed from the model. This would lead to inaccurate concentration readings in the model. Zheng[33] suggests that an alternative, more accurate velocity interpolation scheme should be implemented within grid spaces that contain low yield wells to eliminate this problem.

Of interest also is when a particle tracking scheme will be more accurate than a finite difference method. This is of interest since it is desirable to use the best technique for a given situation, and by knowing under what conditions a Lagrangian/random walk technique is more accurate than a finite difference method, parameters such as the number of particles can be chosen to provide the most accurate solution. For a given computational cost, a Lagrangian/random walk method has been shown [16] to be more accurate for:

- Higher model dimensions
- Small numbers of particles
- Situations where the contaminant does not cover the whole model.

2.5 RNDWALK2D

In this section, the groundwater flow and contaminant transport computer code RNDWALK2D [23] which employs a Lagrangian/random walk technique and is used to model groundwater contaminant problems in Chapters 4 and 5, is discussed.

2.5.1 Introduction to RNDWALK2D

RNDWALK2D is a groundwater flow and contaminant transport code written by Prickett, Naymik and Lonnquist in 1981 [23]. The code is an extension of the groundwater flow code PLASM written by Prickett and Lonnquist in 1971 [22]. Essentially, RNDWALK2D is PLASM with additional routines added to calculate the movement of contaminants. In addition, the code is in the public domain, so

further modifications may be incorporated into RNDWALK2D by the inclusion of appropriate subroutines. Details of how to compile, run and modify RNDWALK2D are given in Appendix F.

2.5.2 Groundwater Flow Component

RNDWALK2D can simulate a wide variety of groundwater flow situations. Some features of RNDWALK2D are

- Numerical solution of steady and non-steady groundwater flow,
- Variable sized grids,
- Time varying pumping and recharge,
- Injection wells,
- Natural and artificial recharge,
- Evapotranspiration.

The first step in a groundwater contaminant transport model is to solve for the head levels in the domain; these are used to generate a velocity field via the application of Darcy's law (Equation 2.4). In the RNDWALK2D computer code, PLASM is used to solve for the head levels at each time step before applying the contaminant transport component.

To develop a distribution of heads over the model domain, Equation 2.1 is solved using an alternating direction implicit (ADI) finite difference formula. This technique is applied iteratively within each timestep until the solutions obtained converge to within some predetermined tolerance.

2.5.3 Contaminant Transport Component

RNDWALK2D is able to simulate the movement of contaminants in groundwater by the application of a Lagrangian/random walk technique. Some features of RNDWALK2D's contaminant transport code are:

- Injection of contaminated water into wells,
- Leakage of contaminants from water sources of differing water quality into the aquifer, for example from a contaminated river,
- Decay of contaminants,

- Tabulation of concentration of contaminants entering sinks.

Using the heads developed by the groundwater flow component, internodal velocities are calculated using Darcy's law (Equation 2.4).

The initial condition of the contaminant is incorporated by placing predetermined numbers of particles into the model according to the initial concentrations required. Every particle is moved for each random walk time step, using the appropriate random walk formula.

Particles are added to the model depending on the situation being modelled. For example, a discrete number of particles may be introduced into the flow at a point at every time step to simulate a continuous release of contaminant into the system, or a particular number of particles may need to be maintained at particular points to simulate a constant concentration boundary.

At any point in time the concentration at a point can be determined by counting the number of particles present within half a grid length of the point in the x and y directions as shown in Figure 2.11 by the shaded area, and calculating the mass of water present in that same area. Calculating the concentration of contaminant in this way reflects the physical process of measuring the concentration of contaminant in groundwater.

Contaminant particles can be removed from the model by the use of a sink. Where a sink is defined, any particles residing within half a grid space of the sink location are removed from the model. Sinks can be used to remove particles from the model where a pumping well is located, or if a line of sinks is placed along a boundary, to remove particles which leave the model; this will prevent particles building up near the boundaries. Another method which might be used to remove particles from the model is through the modelling of decay (depending on the contaminant being modelled). To model decay, particles are removed at time intervals depending on the half life of the substance.

These results suggest that the advective and dispersive terms of the contaminant transport equation may be modelled using random walk techniques.

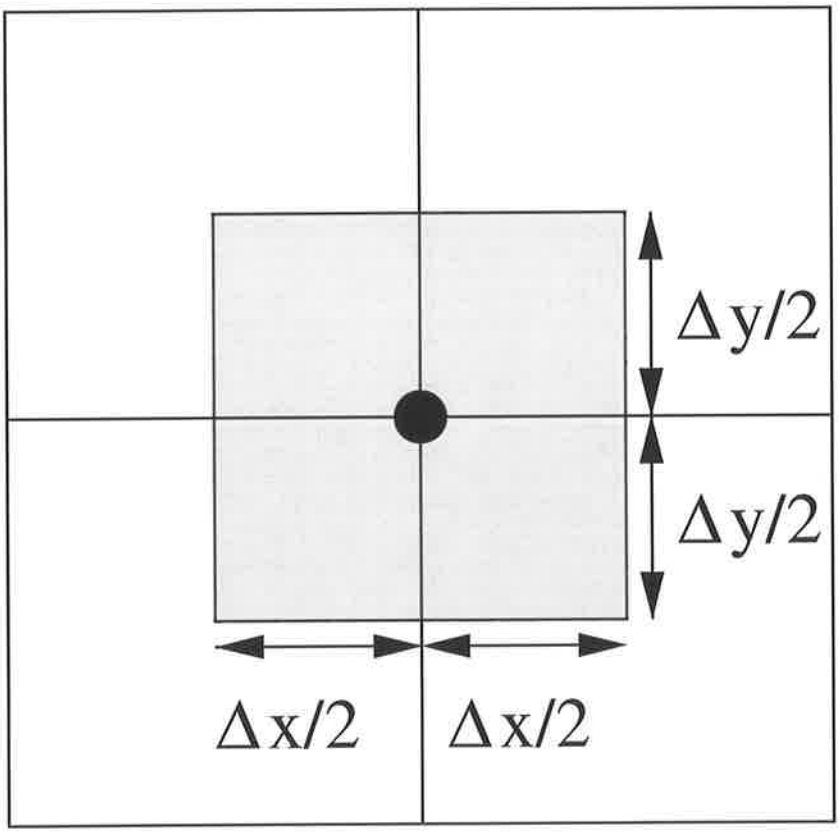

Figure 2.11: Diagram showing the area used to determine the concentration at a point.

Chapter 3

Comparison of Random Walk Schemes

3.1 Overview and Objective

This chapter introduces and discusses a number of different random walk schemes that may be used to model the effect of dispersion. These schemes are compared against known analytic solutions for the cases of one and two dimensional dispersion, and one and two dimensional advection dispersion.

The aim of making these comparisons between the computed results for each of these schemes and our known analytic solutions is to highlight any inaccuracies that may be present in the use of a random walk scheme to simulate the effects of dispersion. In addition, it was desirable to determine whether the use of a different random walk scheme would produce appreciably different results. In this respect, one would hope that by simply implementing different random walk schemes to a groundwater contamination problem, the results produced would be extremely close to one another (allowing for minor differences, due to the random aspect of the techniques).

3.2 Equations for Three Random Walk Schemes

Three techniques are presented in this section for the computational solution of the advection dispersion equation in one and two dimensions. Each of these techniques uses a Lagrangian approach to model the advective component, and a random walk technique to model the dispersive component. As discussed in Section 2.4.3, a random walk technique considers a contaminant plume as a num-

ber of representative particles, and assumes that the dispersion of a contaminant through a porous medium is a random process, an assumption which is realised in these three techniques via the use of random numbers. In each of the following subsections, equations have been presented which allow the computation of an individual contaminant particle's position at the $n+1^{th}$ time step. These equations are then repeated for each particle in our contaminant plume, for each time step.

3.2.1 Prickett, Naymik and Lonnquist Scheme.

In this technique [23], the following equations are used to determine the location of a contaminant particle at time step $n+1$:

$$\begin{aligned} x_{n+1} &= x_n + \delta x + R_L \delta x + R_T \delta y, \\ y_{n+1} &= y_n + \delta y + R_L \delta y - R_T \delta x. \end{aligned} \tag{3.1}$$

where:

x_n, y_n are x and y coordinates of the particle at time $t = n\Delta t$,

$\delta x, \delta y$ are the advective components of the particle's movement in the x and y directions ($\delta x = u\Delta t, \delta y = v\Delta t$),

$$RL = R_1 \sqrt{\frac{2d_L}{DD}},$$

$$RT = R_2 \sqrt{\frac{2d_T}{DD}},$$

$$DD = \sqrt{\delta x^2 + \delta y^2},$$

R_1, R_2 are two normally distributed random numbers (mean 0, variance 1),

d_L, d_T are the longitudinal and transverse dispersivities respectively.

Figure 3.1 (a) shows the method used to determine a particle's position at the $n+1^{th}$ time step. From the diagram it can be seen that starting from the particle's initial position at (x_n, y_n) the particle is initially moved to an intermediate position (x', y') by adding δx $(= u\Delta t)$ to the x coordinate, and δy $(= v\Delta t)$ to the y coordinate, to simulate the effect of advection.

The quantity $(RL\ \delta x + RT\ \delta y)$ is added to the x coordinate and $(RL\ \delta y - RT\ \delta x)$ is added to the y coordinate to simulate the effect of dispersion, resulting in the particle's new position at the $n+1^{th}$ time step, (x_{n+1}, y_{n+1}).

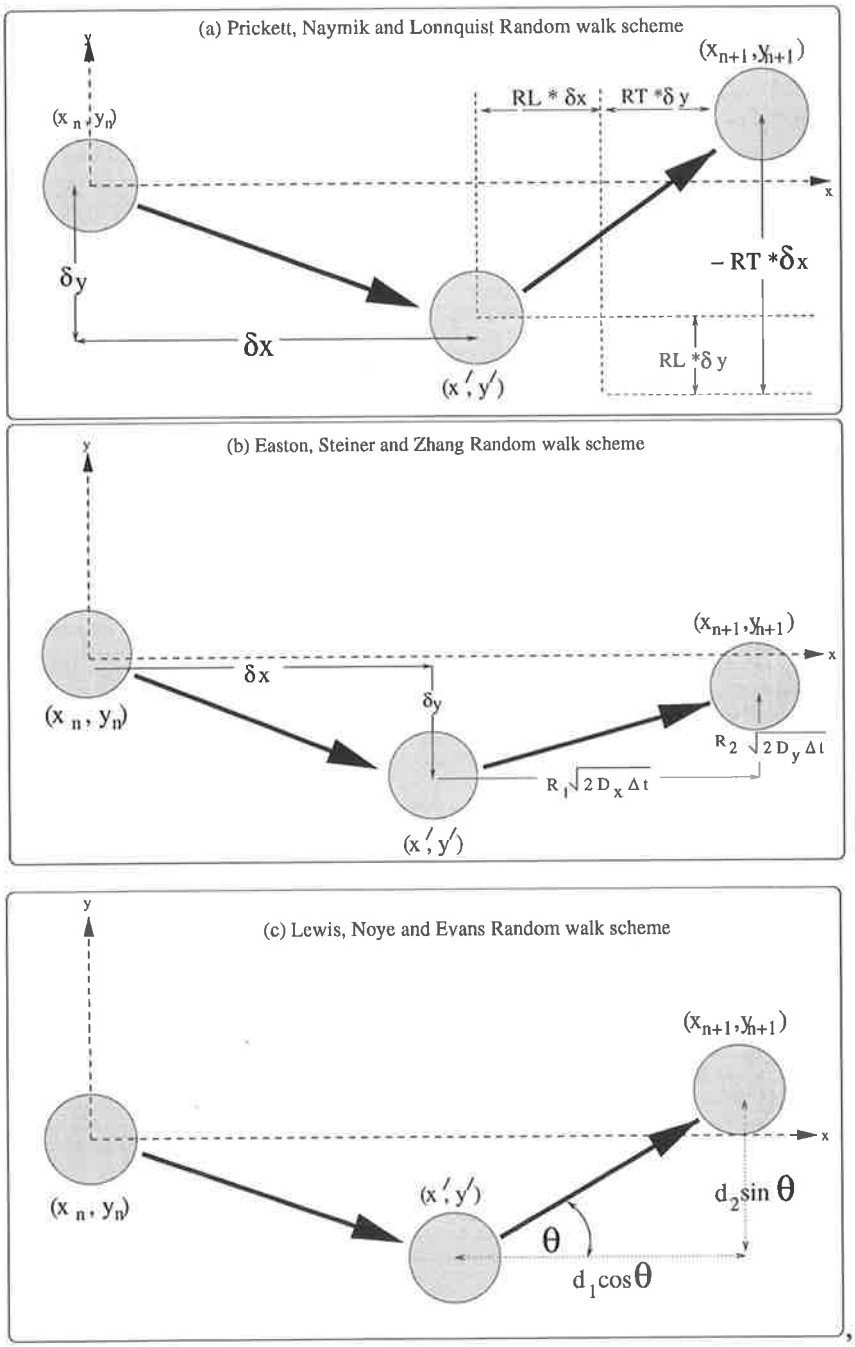

Figure 3.1: Three random walk schemes used to determine a particle's position at the $n+1^{th}$ time step: (a) Prickett, Naymik and Lonnquist scheme, (b) Easton, Steiner and Zhang scheme, (c) Lewis, Noye and Evans scheme.

3.2.2 Easton, Steiner and Zhang Scheme.

In this scheme the following equations are used to determine the location of a contaminant particle at time step $n+1$. This is a modified version of the scheme presented in Easton et al. [7] allowing for the situation where $D_x \neq D_y$:

$$\begin{aligned} x_{n+1} &= x_n + \delta x + R_1\sqrt{2D_x\Delta t}, \\ y_{n+1} &= y_n + \delta y + R_2\sqrt{2D_y\Delta t}. \end{aligned} \tag{3.2}$$

Figure 3.1 (b) shows the method used to determine a particle's position at the $n+1^{th}$ time step. It can be seen that, like the Prickett, Naymik and Lonnquist scheme, the particle is initially moved to an intermediate position (x',y') by adding δx $(= u\Delta t)$ to the x coordinate, and δy $(= v\Delta t)$ to the y coordinate, to simulate the advective component of motion. To simulate the effect of dispersion, the x and y coordinates are perturbed by $R_1\sqrt{2D_x\Delta t}$ and $R_2\sqrt{D_y\Delta t}$ respectively, with the particle's new position at the $n+1^{th}$ time step being given by the coordinate (x_{n+1},y_{n+1}).

3.2.3 Lewis, Noye and Evans Scheme.

In this technique the following equations are used to determine the location of a contaminant particle at time step $n+1$. Similar to the scheme presented in the previous section, the scheme presented in Lewis et al. [19] has been modified to allow for the situation $D_x \neq D_y$:

$$\begin{aligned} x_{n+1} &= x_n + \delta x + d_1 cos\theta, \\ y_{n+1} &= y_n + \delta y + d_2 sin\theta. \end{aligned} \tag{3.3}$$

where

$$\begin{aligned} \theta &= 2\pi R_1, \\ d_1 &= \sqrt{3}R_2\sqrt{4D_x\Delta t}, \\ d_2 &= \sqrt{3}R_2\sqrt{4D_y\Delta t}, \\ R_1, R_2 &\quad \text{are uniformly distributed random numbers in [0,1].} \end{aligned}$$

Figure 3.1 (c) shows the method used to determine a particle's position at the $n+1^{th}$ time step. As with the two previous schemes the particle is initially moved to an intermediate position (x',y') by addition of δx and δy to the x and y coordinates respectively, to simulate the effect of advection. To simulate the effect of dispersion $d_1 cos\theta$ is added to the x coordinate and $d_2 sin\theta$ is added to the y coordinate. As with the previous two methods, the particle's new position at the $n+1^{th}$ time step is given by (x_{n+1},y_{n+1}).

3.2.4 Similarities

In certain situations, some or all of these schemes are the same. These situations are detailed below.

When there is no dispersion present, that is $D_x = 0$ and $D_y = 0$, then all three equations reduce to that of pure advection, namely:

$$\begin{aligned} x_{n+1} &= x_n + \delta x, \\ y_{n+1} &= y_n + \delta y. \end{aligned}$$

In one dimension, when the velocity $u \neq 0$ and dispersion is present then the Easton, Steiner and Zhang and the Prickett, Naymik and Lonnquist schemes become identical. This is due to the following:
the Prickett, Naymik and Lonnquist scheme in one dimension uses the equation:

$$x_{n+1} = x_n + \delta x + RL\ \delta x. \tag{3.4}$$

Recall that:

$$\begin{aligned} RL &= R_1\sqrt{\frac{2d_L}{DD}}, \text{where } R_1 \text{ is some random number, and} \\ DD &= \sqrt{\delta x^2 + \delta y^2} \\ &\Rightarrow DD = \delta x, \text{ since } \delta y = 0 \end{aligned}$$

giving:

$$\begin{aligned} x_{n+1} &= x_n + \delta x + R_1\sqrt{\frac{2d_L}{\delta x}}\delta x \\ &= x_n + \delta x + R_1\sqrt{2d_L\delta x} \\ &= x_n + \delta x + R_1\sqrt{2d_L u\Delta t}. \end{aligned} \tag{3.5}$$

The Easton Steiner Zhang scheme in one dimension is:

$$x_{n+1} = x_n + \delta x + R_1\sqrt{2D_x\Delta t}$$

Substituting Equation 2.3 into the above yields:

$$x_{n+1} = x_n + \delta x + R_1\sqrt{2(d_L u + D_x^*)\Delta t} \tag{3.6}$$

It can be seen that if $D_x^* = 0$ (i.e. if diffusion is neglected) then Equation 3.6 is the same as Equation 3.5.

3.3 Comparison of Results against Analytic Solutions

Presented in this section are the results of four simulations which have been used to verify that the three random walk techniques introduced in Section 3.2 accurately model the advection dispersion equation.

In the problems discussed below, values for the dispersion coefficients provided in Prickett, Naymik and Lonnquist [23] are used, namely $D_x = 4.5 ft^2/day$ and $D_y = 1.125 ft^2/day$. Where an advective force is present, molecular diffusion is ignored (ie $D_x^* = D_y^* = 0$).

Additionally, where used, the one dimensional version of each scheme is simply the x component of the schemes presented in Equations 3.1 – 3.3.

3.3.1 One Dimensional Dispersion

Consider the case of one dimensional dispersion. This is governed by the equation:

$$\frac{\partial C}{\partial t} - D_x \frac{\partial^2 C}{\partial x^2} = 0. \tag{3.7}$$

Problem Description

Suppose we have a slug of tracer, which is injected into the middle of a region $300 ft$ long with a grid length of $10 ft$ (i.e., the tracer is injected at grid point 15, see Figure 3.2) , and with a dispersivity of $D_x = 4.5 ft^2/day$. The dispersion of this tracer material will be given by [23]:

$$C(x,t) = \frac{C_0 \Delta x}{\sqrt{4 D_x \pi t}} exp\left(-\frac{(x-150)^2}{4 D_x t}\right), \tag{3.8}$$

where C_0 is the initial concentration of the tracer.

Results

Given an initial concentration corresponding to 300 particles, Figure 3.3 shows the analytic solution plotted against the numerical solution determined using the Easton, Steiner and Zhang scheme and the Lewis, Noye and Evans scheme for two different time periods. In each case, the numerical solutions show good agreement

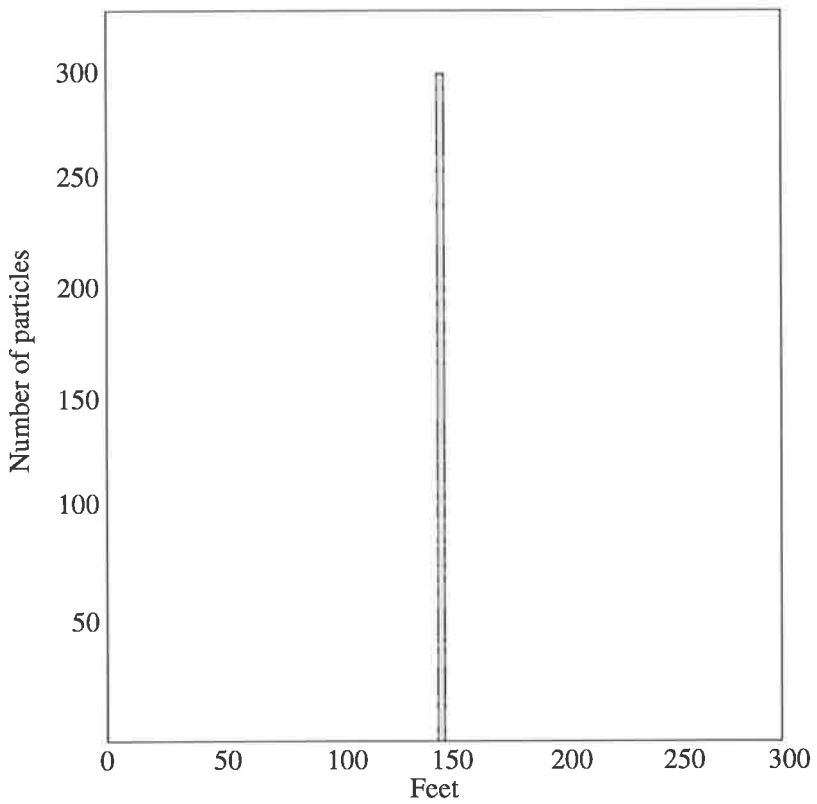

Figure 3.2: Initial conditions for one dimensional dispersion, where the shaded region is the initial (point source) concentration of tracer material.

with the analytic solution. Both solutions oscillate slightly around the exact solution, but match the maximum and minimum values and their locations well.

The Prickett, Naymik and Lonnquist scheme is completely dependent on advection, since, if $\delta x = \delta y = 0$ (i.e., zero advection), equations (3.1) reduce to:

$$\begin{aligned} x_{n+1} &= x_n \\ y_{n+1} &= y_n \end{aligned} \tag{3.9}$$

For this reason, this scheme cannot be compared with the other schemes for pure dispersion. For our modelling purposes, this should not pose any problem, since the subsurface water which we will be considering will be moving, even if only with a small velocity. It does, however, impact on our ability to compare results against analytic solutions in cases where there is no advection.

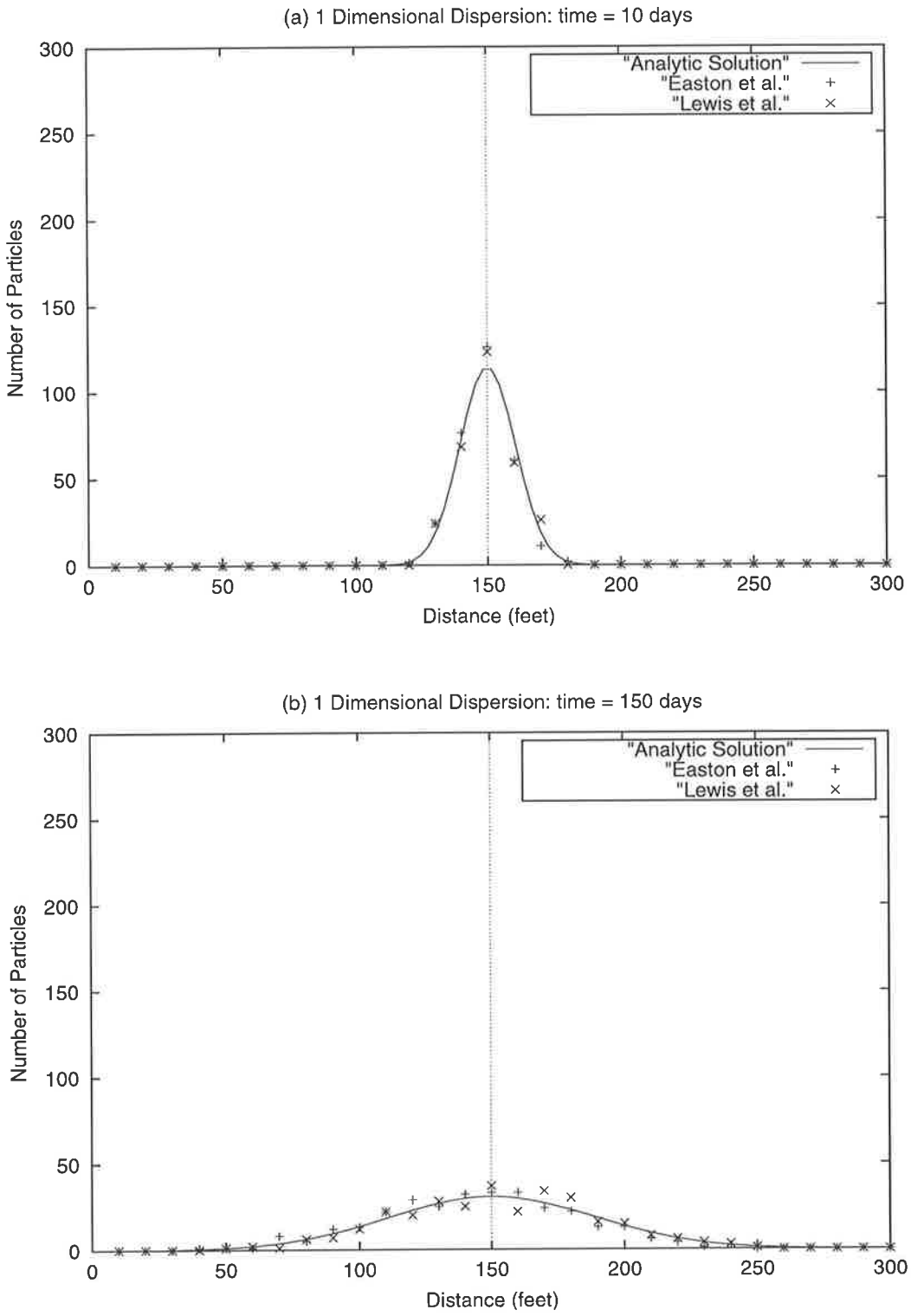

Figure 3.3: Comparison of analytic vs. computed solutions for the case of 1-D dispersion after 10 and 150 days. The x axis represents the distance from the origin (feet), the y axis represents the concentration of contaminant (number of particles).

3.3.2 One Dimensional Advection Dispersion

Consider the problem of one dimensional advection dispersion. This is governed by the equation:

$$\frac{\partial C}{\partial t} + u\frac{\partial C}{\partial x} - D_x\frac{\partial^2 C}{\partial x^2} = 0. \tag{3.10}$$

Problem Description

Given a flow velocity of $1 ft/day$, and a dispersivity of $D_x = 4.5 ft^2/day$ (and with $D_x^* = 0.0$), a slug of tracer consisting of 300 particles is injected at position $x = 0$ into a region 300 feet long. The analytic solution for the distribution of particles is given by [23]:

$$C(x,t) = \frac{C_0 \Delta x}{\sqrt{4\pi D_x t}}\, exp\left(\frac{-(x-ut)^2}{4D_x t}\right), \tag{3.11}$$

where C_0 is some initial concentration of particles representing the slug, u is the velocity, D_x is the dispersion coefficient and Δx is the grid length. Figure 3.4 shows the initial conditions of this problem.

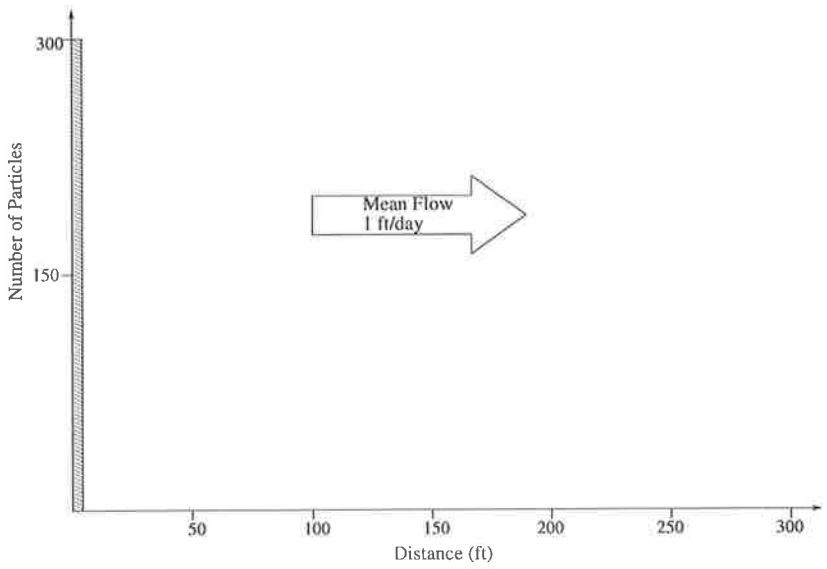

Figure 3.4: Initial conditions for the problem of one dimensional advection dispersion.

Results

Figure 3.5 shows the analytic solution (Equation 3.11) plotted against the numerical solutions for all three schemes after 10 and 150 days. It can be seen at each time period that the results for the Easton, Steiner and Zhang and Prickett, Naymik and Lonnquist schemes are identical (as expected from Section 3.2.4) and compare well to the analytic solution.

At 10 days all three schemes show good agreement with the analytic solution, although the concentration in the middle of the slug is too high for each of the three schemes. It can be seen that the Lewis, Noye and Evans scheme displays slightly better reproduction of this peak.

At 150 days once again all three schemes display good agreement with the analytic solution, with the three computed solutions being close to the analytic solution throughout the solution domain. Some variation from the analytic solution can be seen, especially near the centre of the slug; however, these deviations are considered to be acceptably small.

3.3.3 Oscillations in the numerical solutions

Examining the numerical results from both of the one dimensional test cases (Figures 3.3 and 3.5) shows that the computed solutions appears to oscillate around the analytic solution. This is particularly noticeable near the peaks of both the solutions after 150 days. Such oscillations are the result of the number of particles and the size of the grid used. Both of these variables influence the resolution of the computed results. The oscillations occurring due to the grid size are present as a result of the process through which the particles are counted and assigned a grid node. Particles within half a grid length of a node are included in the particle count for that node. If the grid is coarse, then the distance that the particles can be from a node to be included in that node's particle count is obviously larger. By using a smaller grid size, these oscillations can be reduced.

Prickett et al. [23] mentions such problems with accuracy and suggests using additional particles, a smaller grid or to accept the results and use "engineering judgment" in interpreting the results. Figure 3.6 shows the use of the Easton, Steiner and Zhang scheme using an increased number (2000) of particles. While the results shown in Figure 3.6(a) are virtually the same as in Figure 3.5(a), it can be seen that the oscillations present in Figure 3.6(b) are smaller than those in Figure 3.5(b). This indicates that with an increase in the number of particles, the computed solution converges to the analytic solution.

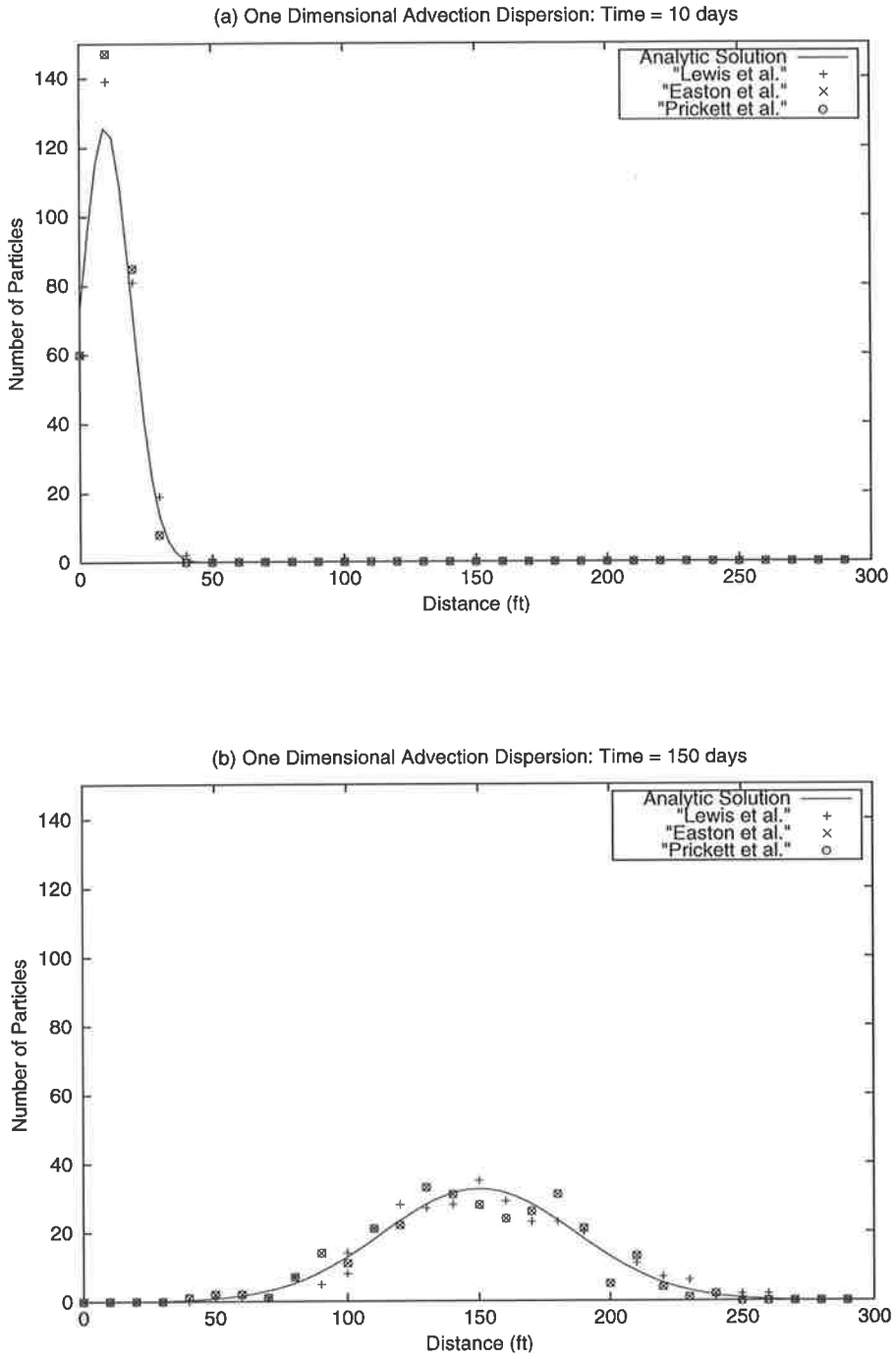

Figure 3.5: Comparison of analytic vs. computed solution for the case of 1-D advection dispersion after 10 and 150 days. The x axis represents the distance from the origin (feet), the y axis represents the concentration of contaminant (number of particles). Easton, Steiner and Zhang and Prickett, Naymik and Lonnquist results are identical.

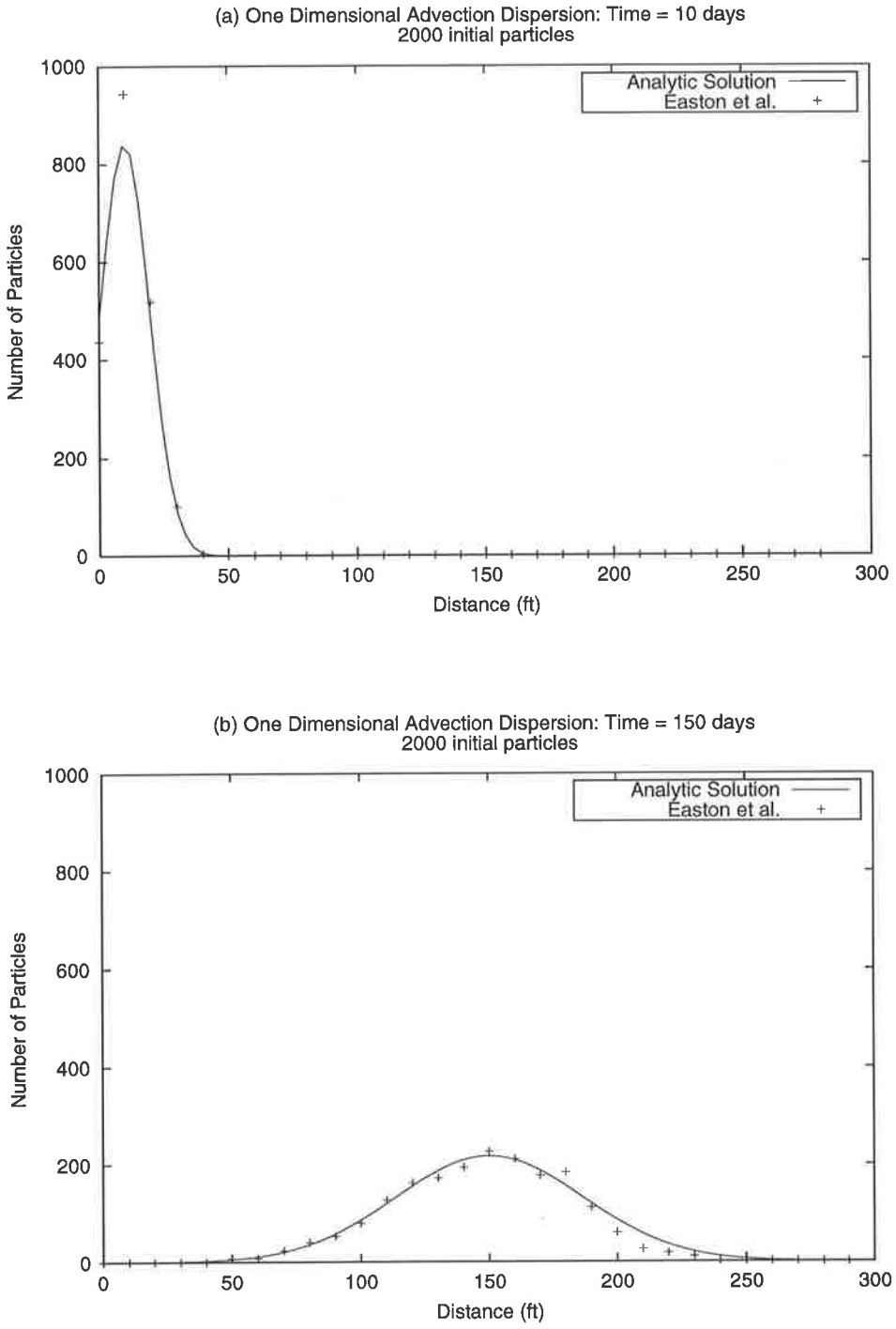

Figure 3.6: Comparison of analytic vs. computed solution for the case of 1-D advection dispersion after 10 and 150 days using 2000 initial particles and the Easton, Steiner and Zhang random walk scheme.

3.3.4 Two Dimensional Dispersion

Consider the problem of two dimensional dispersion. This is governed by the equation:

$$\frac{\partial C}{\partial t} - D_x \frac{\partial^2 C}{\partial x^2} - D_y \frac{\partial^2 C}{\partial y^2} = 0. \tag{3.12}$$

Problem Description

Consider a problem domain $300ft \times 300ft$, with zero flow, into which a slug of tracer is deposited at the centre. Dispersion coefficients are set at $D_x = 4.5\ ft^2/day$ and $D_y = 1.125\ ft^2/day$.

The analytic solution to such a problem is given by [12]:

$$C(x,y,t) = \frac{C_0 \Delta x \Delta y}{4\pi t \sqrt{D_x D_y}}\ exp\left(-\frac{(x-150)^2}{4D_x t} - \frac{(y-150)^2}{4D_y t}\right). \tag{3.13}$$

Figure 3.7 shows the initial position of the particles for this problem. The objective of this section is to show that random walk techniques can be used to model the spread of a contaminant from this initial position to an acceptable degree of accuracy.

As with one dimensional dispersion (Section 3.3.1), the Prickett, Naymik and Lonnquist scheme could not be used to compute a numerical solution due to the lack of advection.

Results

Figures 3.8 and 3.9 show the computed results after 150 days for the two schemes that are applicable to this problem (i.e. Easton, Steiner and Zhang and Lewis, Noye and Evans schemes) when 2000 particles are injected into the centre of the computational domain.

From Figures 3.8(a) and (b) it can be seen that the two schemes applied to the case of two dimensional dispersion give a good representation to the analytic solution with regard to the spread of the slug. It can also be seen that the maximum concentration of particles in each of the computed solutions is larger than that of the analytic solution. Table 3.1 shows the maximum, minimum and average error in the model domain using each of the schemes. Both of the maximum errors occur near the centre of the domain while the minimum errors occur near the edges of the domain.

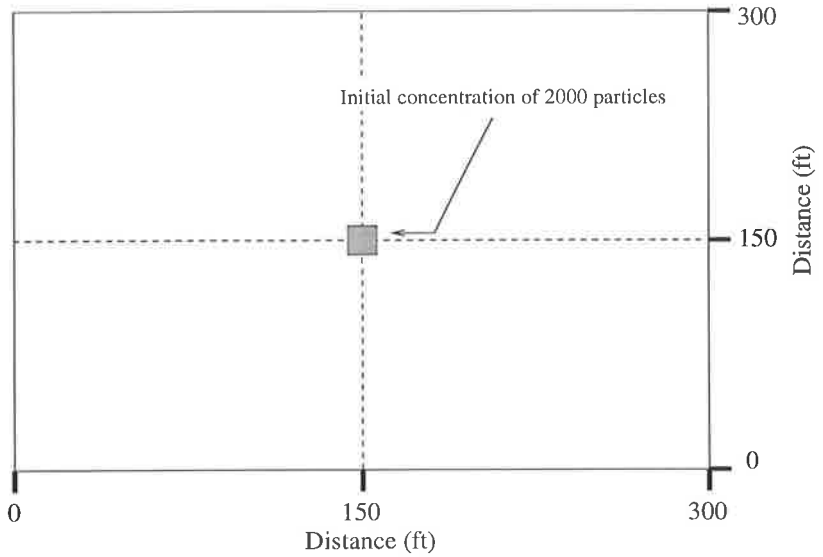

Figure 3.7: Initial position of 2000 particles for the problem of two dimensional dispersion.

RW Scheme	Max Abs Error	Max Rel Error	Min Abs Error	Av Abs Error
Easton et al.	12.18	1.99	0.00	0.47
Lewis et al.	15.33	3.46	0.00	0.59

Table 3.1: Maximum, minimum and average errors for each of the random walk schemes used to model two dimensional dispersion for 150 days.

These errors can be seen in more detail in Figures 3.9(a) and (b). These figures show cross sectional plots of both schemes in the x and y directions through the middle of the plume.

By inspection of Figure 3.9 it can be seen that the Lewis, Noye and Evans scheme exhibits a slightly higher peak near the centre of the computed contaminant plume for this time period; however, the spread of the contaminant plume remains consistent with the Easton, Steiner and Zhang scheme and the analytic solution.

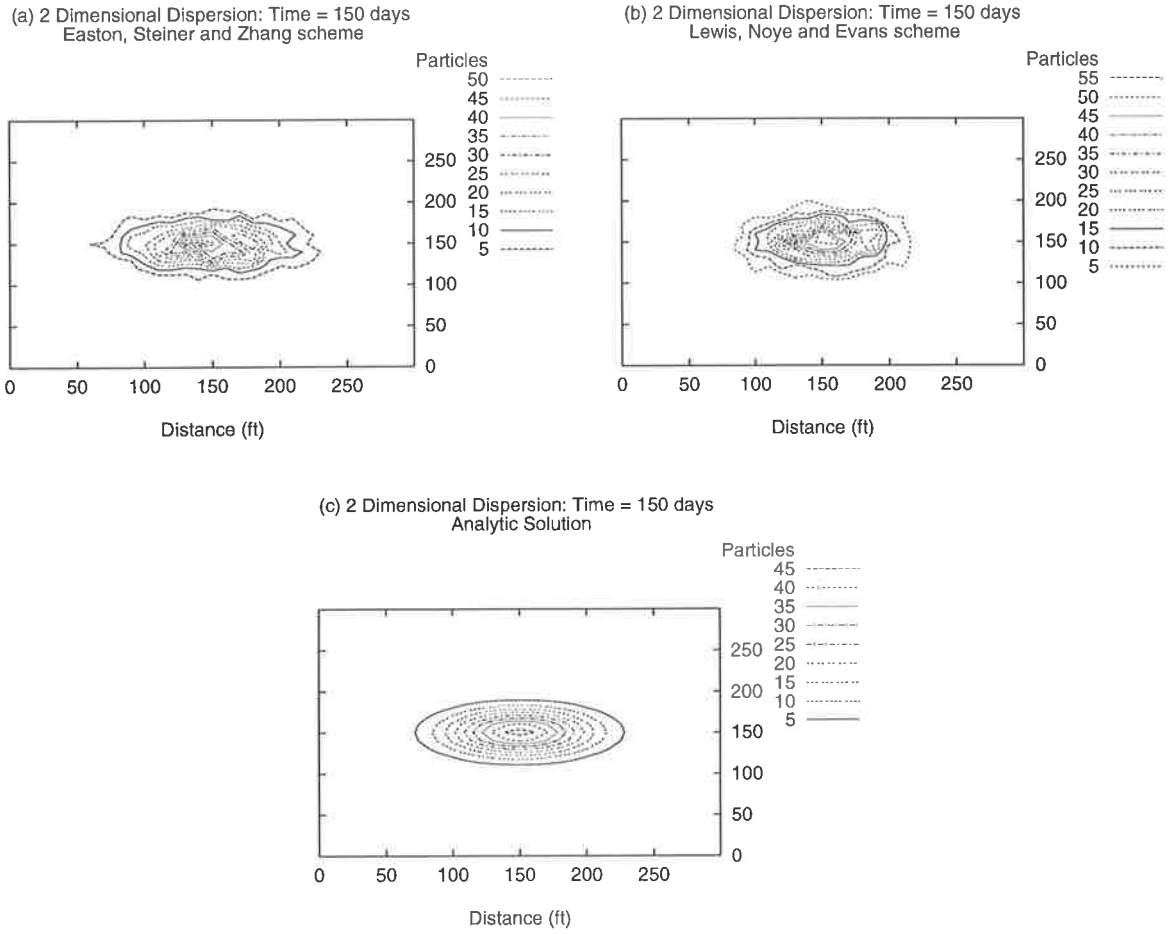

Figure 3.8: Comparison of Easton, Steiner and Zhang and Lewis, Noye and Evans random walk schemes applied to the case of two dimensional dispersion, compared to (c) the analytic solution. Contours indicate the number of particles present within each region.

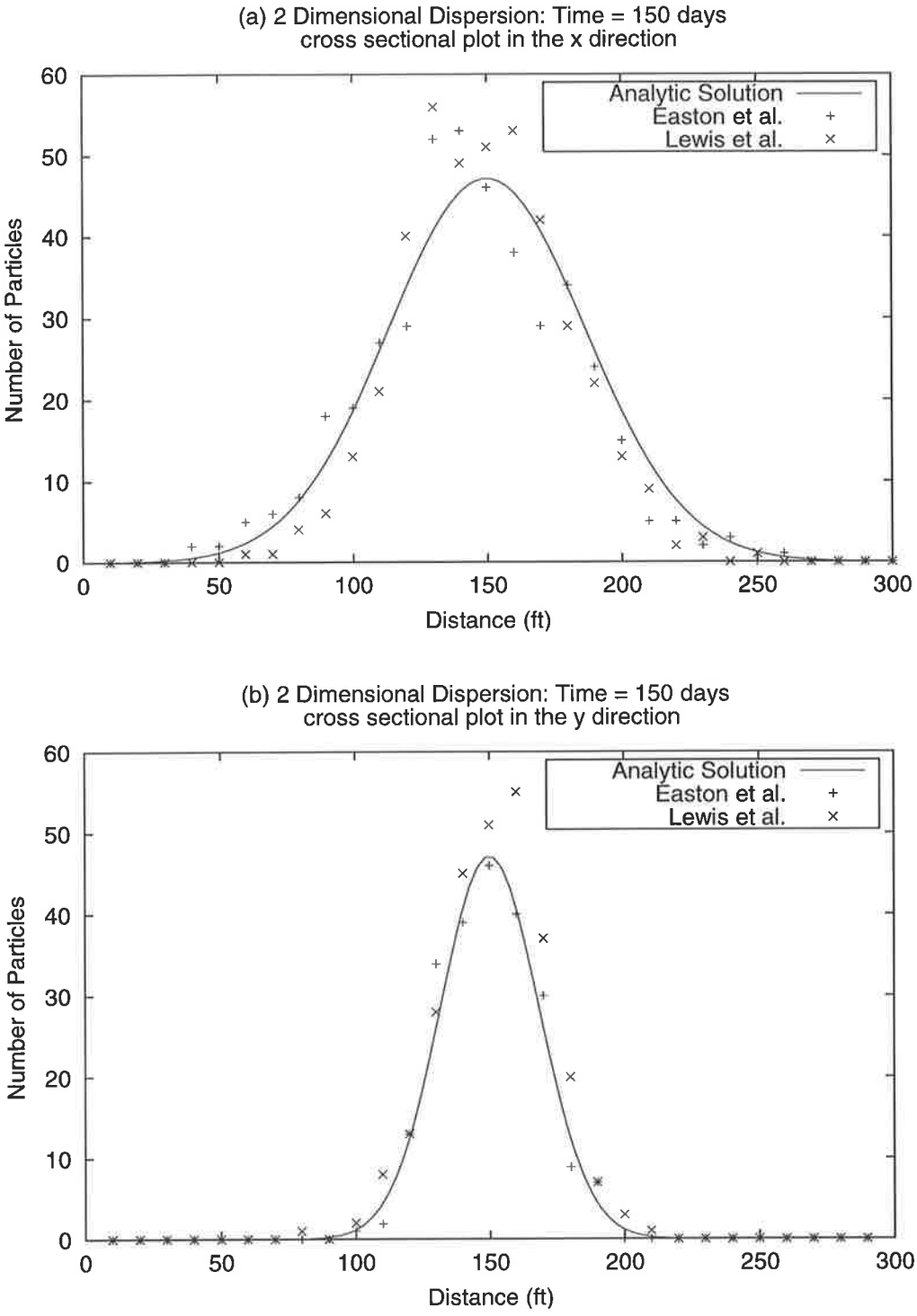

Figure 3.9: Cross sectional plots in the (a) x direction and (b) y direction after 150 days.

Figure 3.9 shows that on the edges of the plume there is definitely good agreement with the analytic solution, with differences being only a few particles at most. As mentioned above, however, there are some noticeable differences at particular points, mostly near the centre of the plume. This is not unsurprising since with a larger number of particles there exists a greater chance for differences from the analytic solution. Most of these differences are within 5 particles of the analytic solution, which can be considered to be within acceptable limits, especially near the centre of the slug where the greatest number of particles reside.

The method by which particle numbers are calculated may also have an effect on these results, since a group of particles may have passed into an adjoining grid square, decreasing substantially the particle count in a particular square. It can be seen that where there is a particularly low particle count compared with the analytic solution the grid squares around it generally have an excess, and vice versa.

As far as the accuracy of the schemes is concerned, it should be noted that with the use of any random walk scheme it is unlikely that there will be an exact match to the analytic solution due to the discrete nature of the computed solutions. In addition, the randomness of the computations may produce some results which seem out of place, such as peaks greater than those present at the exact centre of the slug.

3.3.5 Two Dimensional Advection Dispersion

Consider the problem of two dimensional advection dispersion. This is governed by the equation:

$$\frac{\partial C}{\partial t} + u\frac{\partial C}{\partial x} + v\frac{\partial C}{\partial y} - D_x\frac{\partial^2 C}{\partial x^2} - D_y\frac{\partial^2 C}{\partial y^2} = 0. \tag{3.14}$$

This is an extension of the one dimensional problem discussed in Section 3.3.2.

Problem Description

Consider the case of two dimensional advection and dispersion, over a 300 $ft \times$ 300 ft domain, with a flow velocity of $1 ft/day$ in the x direction, and with dispersion coefficients of $D_x = 4.5 ft^2/day$ and $D_y = 1.125 ft^2/day$. The distribution of particles is given by the analytic solution [23]:

$$N(x,y,t) = \frac{N_0 \Delta x \Delta y}{4\pi t\sqrt{D_x D_y}}\, exp\left(-\frac{((x-50)-ut)^2}{4D_x t} - \frac{(y-150)^2}{4D_y t}\right). \tag{3.15}$$

The objective of this section is to show that random walk techniques can be used to model the advection and dispersion of a contaminant in groundwater.

Results

Figure 3.10 shows the computed results after 150 days for the three schemes in addition to the analytic solution for this problem, when an initial slug of 2000 particles is injected into the flow at the point (50,150).

The results show that all three schemes compare well against the known analytic solution. The transport and general spread of each plume is consistent with the analytic solution.

In the x cross section (Figure 3.11(a)) it is seen that the Easton, Steiner and Zhang and the Prickett, Naymik and Lonnquist methods give solutions that are identical, much like in the one dimensional case (see Figure 3.5) and the solutions compare favourably with the analytic solution. In general, the difference between the analytic and computed solutions using the Easton, Steiner and Zhang and the Prickett, Naymik and Lonnquist schemes is less than five particles, with the maximum difference occuring near the centre of the plume. In the case of the Lewis, Noye and Evans scheme, there seems to be a good match at the edges of the plume with a greater variation from the analytic solution near the centre of the plume much like the other two solutions. It is noted that the results presented show some spikes in the solution. In general, however, the solution is a good match with the analytic solution, with many of the points lying on or extremely close to the analytic curve.

In the y cross section (Figure 3.11(b)) the match between the computed and analytic solutions is not as good, with some overshoot near the centre of the plume. In this plot it can be seen that the Lewis, Noye and Evans scheme produces a result which is a better match with the analytic solution, with most differences being less than five particles. The other two schemes produce results that are close to the analytic solution, with most differences being within five particles.

Figures 3.11(a) and (b) show cross sectional curves of the slug after 150 days, comparing the three schemes to the analytic solution. The cross sections are taken through the center of the slug in the x and y directions, i.e. through y=150 for the x cross section and through x=200 for the y cross section.

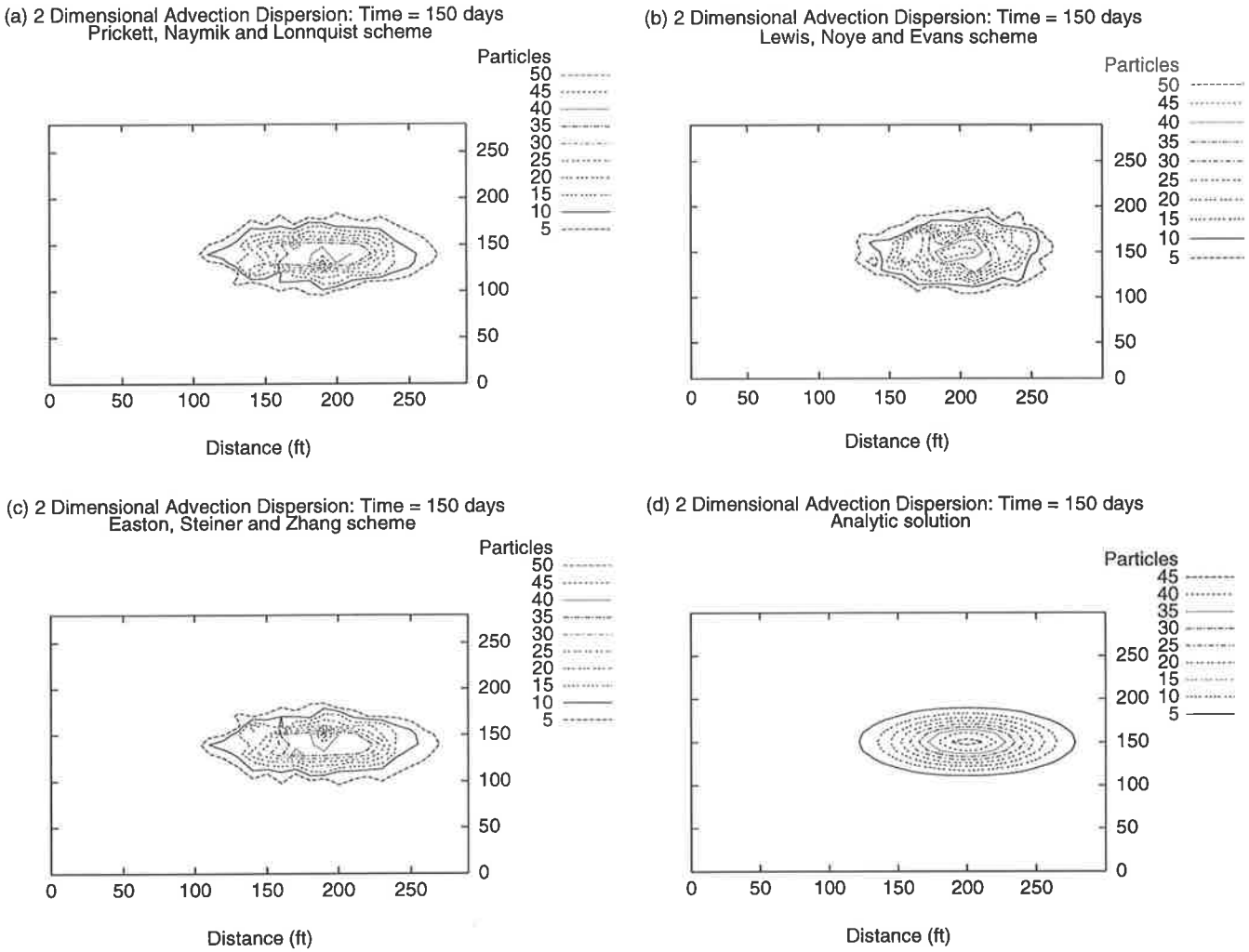

Figure 3.10: Comparison of (a) Prickett, Naymik and Lonnquist, (b) Lewis, Noye and Evans and (c) Easton, Steiner and Zhang schemes applied to the case of two dimensional advection dispersion. Analytic solution (d) (Equation 3.15) is presented for comparison. Contours indicate the number of particles present within each region.

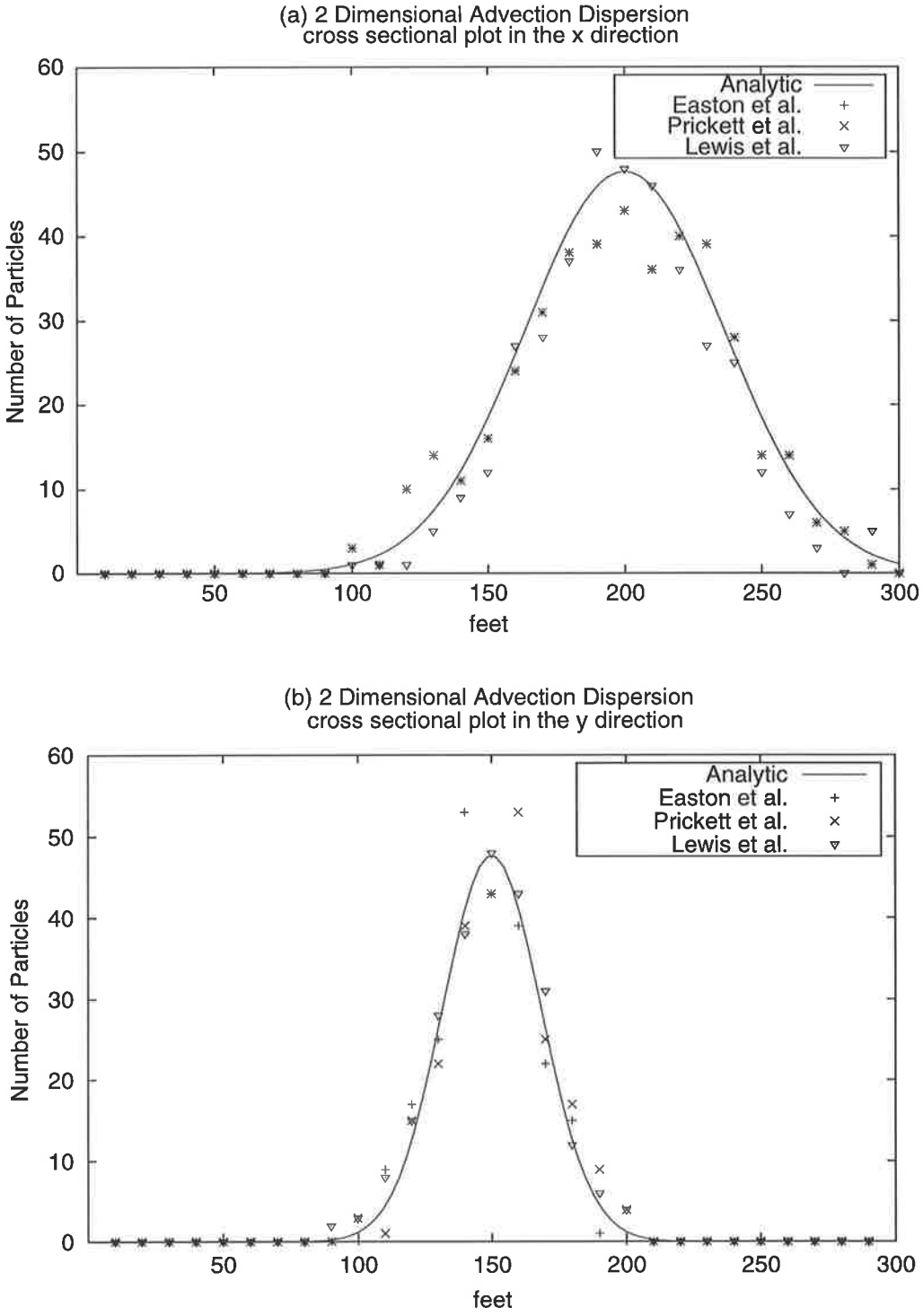

Figure 3.11: Cross sectional plots in the (a) x direction and (b) y direction after 150 days.

3.4 Finite Difference Schemes

As shown in Chapter 2 the advection dispersion equation can be numerically solved using the more widely used finite difference method. Figure 3.12 shows the results from the two finite difference techniques presented in Section 2.4.2, using the same parameters as in Section 3.3.5, compared against the analytic solution.

It can be seen that the solution using the upwind finite difference scheme exhibits a large amount of numerical dispersion, while the FTCS scheme shows good agreement with the analytic solution.

The use of the FTCS finite difference technique to solve the two dimensional advection dispersion equation clearly produces excellent results; however if the size of the modelled domain were to be increased substantially, not unlikely in a field situation, then the number of calculations required to produce a solution would increase dramatically, and hence the time required to run the model would increase. On the other hand, by using a random walk technique the number of calculations remains the same if the model domain is extended, thus requiring no further model execution time.

3.5 Discussion

In Sections 3.3.1–3.3.5 random walk techniques were used to model the cases of one and two dimensional dispersion and advection dispersion. Through the examination of the numerical results and comparing them with analytic solutions it has been determined that the random walk technique can be used to model dispersion and advection with acceptable accuracy. It was noted that the numerical results exhibited a tendency to oscillate about the analytic solution in each case. Possible solutions are to use a finer grid for the display of the results or to use greater numbers of particles, which in both cases would effectively increase the resolution of the transport model. The characteristic of oscillating solutions is something which is noted by Prickett et al [23] who suggest that "engineering judgment is an absolute requirement in arriving at an acceptable solution". This means that a user of one of these techniques should be aware of this particular characteristic before making any conclusions based on model results.

Having determined that random walk techniques can be used to numerically solve the advection dispersion equation, these methods will now be applied to simulate the advection and dispersion of contaminants in groundwater.

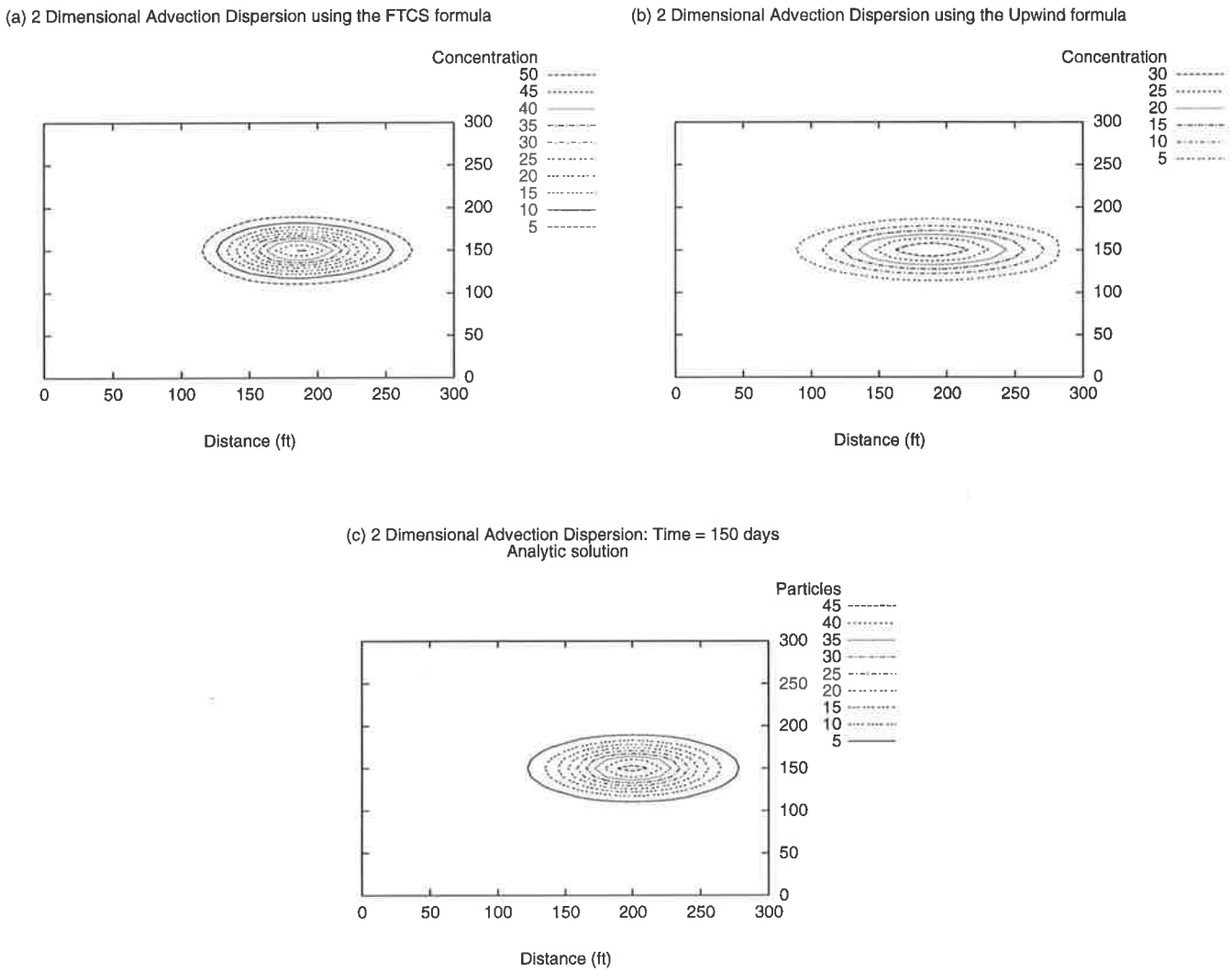

Figure 3.12: (a) FTCS and (b) Upwind finite difference methods applied to the advection dispersion equation in two dimensions and compared to (c) the analytic solution.

Chapter 4

An Application of Random Walk to Saskatchewan, Canada

4.1 Overview and Objective

In this chapter the groundwater modelling program RNDWALK2D developed by Prickett et al. [23] is applied to a contaminant transport problem in Saskatchewan, Canada [28] involving the transport of a long and narrow contaminant plume. In this problem, the contaminant occupies a small fraction of the model domain, and hence, as mentioned in Section 2.4.3, is an ideal situation for the random walk technique to be used. The objective of this chapter is to apply RNDWALK2D and modifications made to implement other random walk methods to this physical problem, and to determine its effectiveness under field conditions.

4.2 Background

The area of interest is near the city of Regina, located in the south east of the province of Saskatchewan, Canada (see Figure 4.1). Underlying Regina is the Condie Aquifer, which consists primarily of coarse sand and gravel-like material. There exists a Provincial Corrections Facility near the city of Regina whose water supply source is the Condie Aquifer. From 1964, water used in the Provincial Corrections Facility was subjected to a water softening procedure, in which sodium chloride is used, resulting in elevated levels of chloride in the effluent expelled from the Facility. Effluent from this Facility was released into a sewage reservoir, resulting in this reservoir having a high concentration of chloride. The chloride-contaminated water from the sewage reservoir seeped into the soil underneath the reservoir, eventually penetrating the Condie Aquifer after approximately two years [28]. Once in the aquifer, the chloride moved with the groundwater flow,

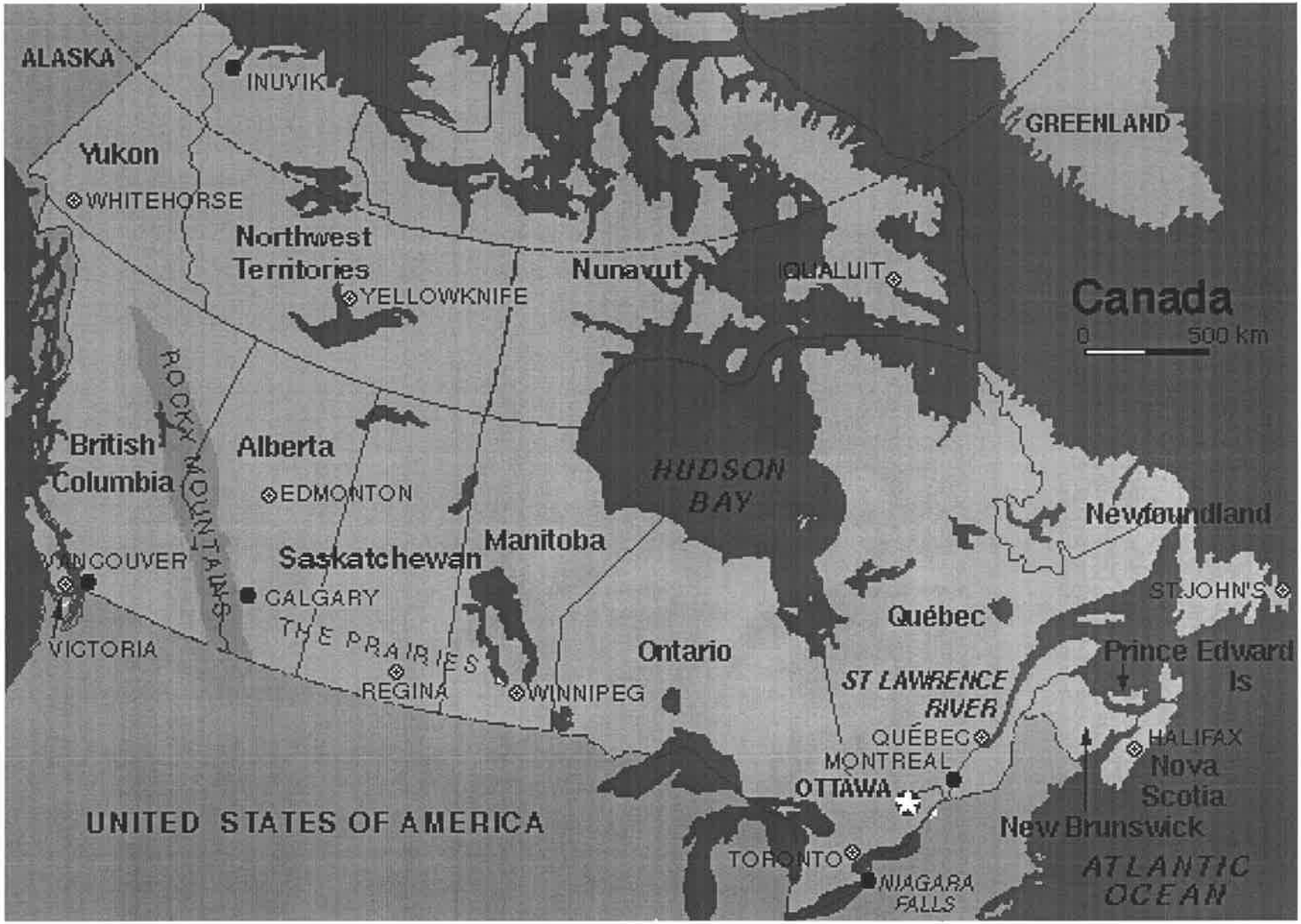

Figure 4.1: Location map showing the province of Saskatchewan and the city of Regina in the south of Canada.

Parameter	Value
Transmissivity ($T_x = T_y$)	1728 to 2160 $m^2\ day^{-1}$
Hydraulic conductivity ($K_x = K_y$)	216 to 268 $m\ day^{-1}$
Longitudinal dispersivity (d_L)	60-120 m
Transverse dispersivity (d_T)	0.10 m
Molecular diffusion (D_x^*, D_y^*)	0.0 $m^2\ day^{-1}$
Porosity	0.35 to 0.40
Storativity	0.40

Table 4.1: Model parameters for the Condie aquifer, Saskatchewan, Canada [28].

estimated to be approximately 410 to 580 metres per year.

4.3 Model Development and Calibration

In this section, the development of the Saskatchewan model is discussed, firstly detailing the flow model parameters and calibration, and then the modelling of the contaminant plume.

In setting up the model, two aspects of the model were required to be developed, the first being the head distribution and the second the introduction and movement of the contaminant plume. Figure 4.2 shows the measured heads taken from various monitoring wells in the area, with contours of equipotentials developed from these measurements. Also shown is the approximate path of the plume, based on measured chloride levels.

4.3.1 Model Input Data

The problem domain as shown in Figure 4.2 has been discretised into a uniform 64×41 grid, with a grid length of 200 metres. The model input data is presented in Table 4.1. These values have been derived through field measurements [28]. As can be seen, there is some variation in the values for some parameters. Where appropriate a number of parameter values have been tried so as to determine the effect on the model of variations in each of the parameters.

4.3.2 Flow Model and Flow Model Calibration

The first step in the development of a model using RNDWALK2D is to produce a head distribution which matches as closely as possible the measured values shown

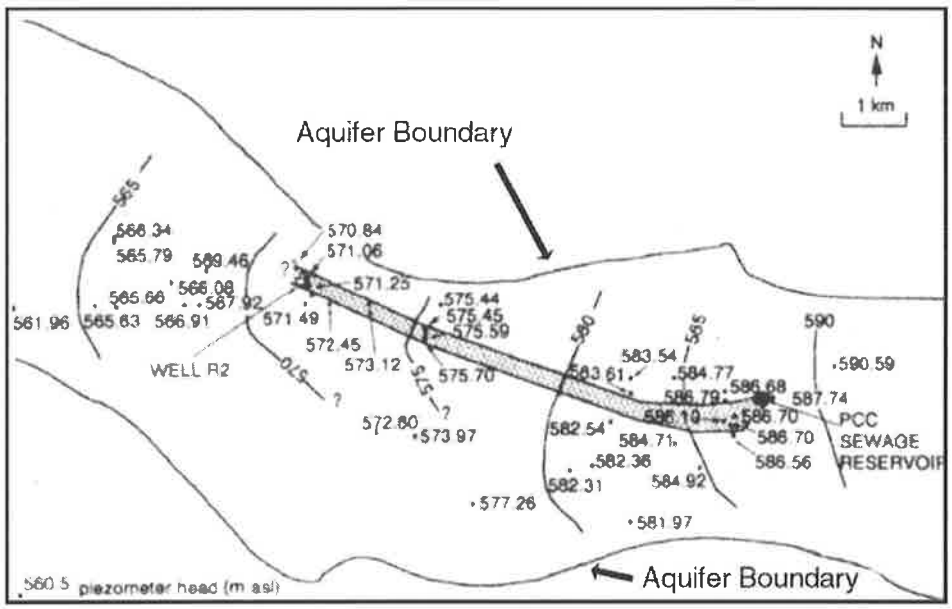

Figure 4.2: Measured values of head for the Condie Aquifer [28]. The estimated extent of the chloride plume is shaded.

in Figure 4.2. The accuracy of the flow model is important since the transport of the contaminants is dependent on the velocity of the groundwater flow, which in turn is dependent on the head distribution through the application of Darcy's law (Equation 2.4).

As an initial input to the model, the northern and southern aquifer boundaries have been defined as being no flow boundaries ($\frac{\partial h}{\partial n} = 0$). These conditions are consistent with physical conditions, those being that the aquifer being modelled is separated from the surrounding aquifers by a clayey aquitard. Constant head boundary conditions have been defined on the western and eastern boundaries, with values of 560 and 590 metres respectively. Initially, the transmissivity was set to 1728 m^2/day. The nature of the groundwater flow in the Condie Aquifer is such that it can be considered to be essentially steady [28]; thus RNDWALK2D was made to produce a steady state head distribution by setting the time step to a large value (10^{30} days was used) and running the flow model until the change in head values is less than some prespecified amount (0.01 metres in this case) at each grid point.

Inspection of the results suggested that while the computed heads were similar to the measured heads, they were not entirely consistent; in particular, the head distribution in the western part of the model did not reflect the measured head distribution.

Re-examination of the measured data suggested that the western boundary would be better represented as a constant head boundary with head values ranging from 565 metres on the southern extent to 560 metres on the northern extent. On running the model, the results presented in Figure 4.3 were achieved. These heads appear to be in good agreement with the heads shown in Figure 4.2.

Transmissivity was changed to various values between 1728 m^2/day and 2160 m^2/day with few noticeable differences in the computed heads, showing that the flow model is not particularly sensitive to changes in this parameter. This was to be expected since the head model in this case is controlled by the boundary conditions. Therefore a value of 1728 m^2/day was used in the model.

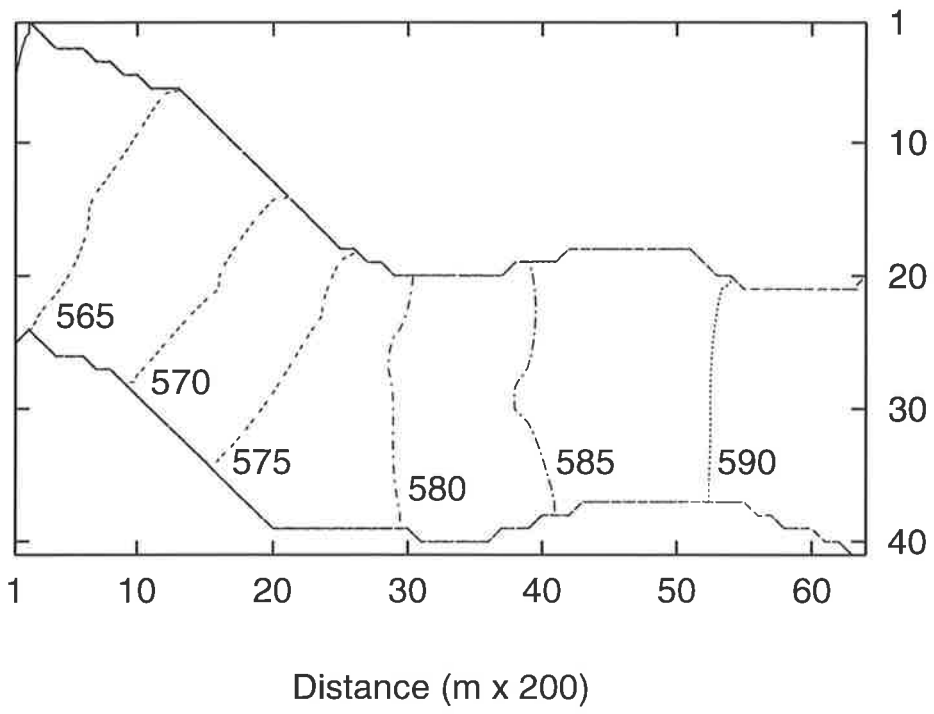

Figure 4.3: Computed head distribution using parameters from Table 4.1.

4.3.3 Contaminant Plume Model and Calibration

The second step in the development of the model is the simulation of the movement of chloride within the Condie Aquifer. Of interest here is the ability to be able to accurately model the path taken by the plume of chloride once it has entered the aquifer beneath the sewage reservoir.

In the area there is a background chloride level which has been omitted since it has no effect on the model outcome. Of interest is the plume created by the release of water containing high levels of chloride into the aquifer, and so the background concentration can be safely left out and the increase in chloride over background levels modelled.

In this model the chloride has been modelled by allowing particles representing the chloride to move within the simulated groundwater flow via both advective and dispersive processes. The dispersive process is simulated via the random walk technique. In modelling this plume it has been assumed that the chloride enters the aquifer at a constant rate, and that the concentration of chloride under the sewage reservoir remains constant (van der Kamp et al. [28] calculates the concentration under the reservoir as 374 mg/l) . This concentration has been simulated by keeping the number of particles present at grid point (52,27) constant at 100 particles. This number of particles was chosen so as to give acceptable resolution for the computed contaminant plume.

Using parameters shown in Table 4.1 as the initial input parameters to the model, it was found that the computed contaminant plume exhibited the same characteristics as shown in Figure 4.2, that being the tendency to form a narrow (approximately 200 metres wide) plume of contaminant as the chloride moved down gradient.

While this aspect was consistent with the measured values presented in Figure 4.2, the computed contaminant plume was located south of the measured plume as shown in Figure 4.4. The simulated contaminant plume was located in the centre of the aquifer, as one would expect from a one dimensional flow situation. However, Figure 4.2 suggests that the plume moved such that it was closer to the northern aquifer boundary, indicating that something other than one dimensional flow was occurring. This behaviour clearly needed to be modelled in order to provide an accurate representation of the movement of the contaminant plume within the aquifer.

The technique used to correct the path of the contaminant plume involved

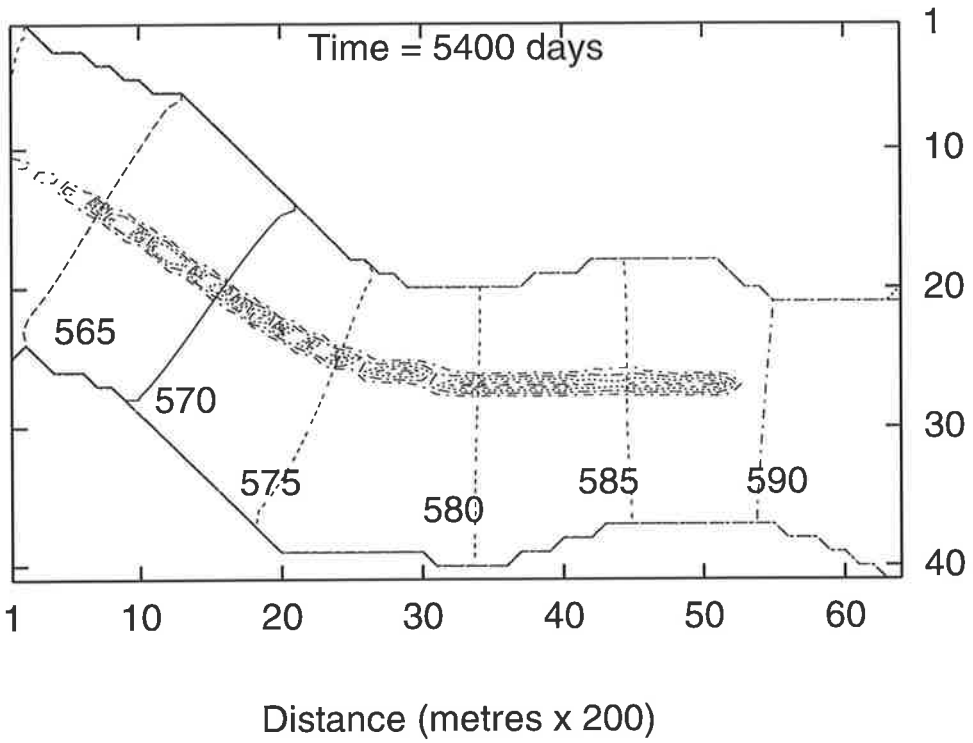

Figure 4.4: Computed chloride plume, initial results after 5400 days. Axes represent model coordinates.

the division of the model domain into two distinct zones of hydraulic conductivity, i.e. a northern and a southern zone, the division being made approximately along the centre of the model domain. Each of these zones was assigned a different hydraulic conductivity so as to encourage the plume to travel towards the northern extent of the aquifer. In this case, as an initial guess, the northern zone was assigned a hydraulic conductivity of 216 m/day (as used previously) and the southern zone a hydraulic conductivity of 10 m/day. This was not inconsistent with the situation as described in van der Kamp et al. [28] which showed the presence of an area of coarser, gravel-like material in the north west part of the aquifer.

The computed contaminant plume resulting from the use of these input parameters is shown in Figure 4.5. Clearly the path of the computed plume has moved such that it travels closer to the northern aquifer boundary consistent with the measured results. Additionally, it was found that the computed heads obtained using these modified parameters did not deviate significantly from those presented in Figure 4.3.

As detailed in van der Kamp et al. [28], the appearance of chloride at the

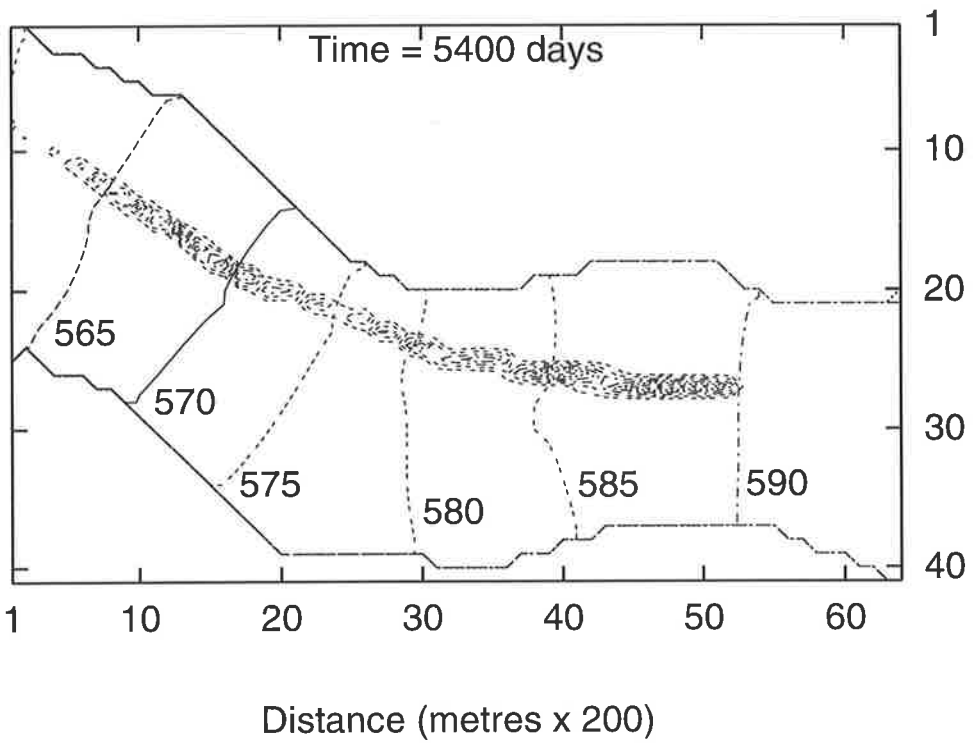

Figure 4.5: Computed chloride plume, using two hydraulic conductivity zones; results after 5400 days showing the plume moving closer to the northern model boundary. Axes represent model coordinates.

well R2 (labelled in Figure 4.2 at the end of the plume and located approximately at grid position (21,20) in Figure 4.3) has been well documented having been first observed in 1978, approximately twelve years after the initial introduction of chloride into the groundwater flow. The chloride breakthrough curve in Figure 4.6 was used in a further calibration procedure to match the rate of movement of the computed plume with the measured data. The aim was to produce a curve by the adjustment of parameters such that the concentration of particles at grid point (21,20) matched the concentration of chloride as shown in Figure 4.6. Comparison between the results shown in Figure 4.6 and the results from the model suggested that the plume moved too fast through the model aquifer, and thus steps would need to be taken to slow this movement.

By considering Equation 2.5 it was noted that the velocity of particles depends on the soil porosity, while in Chapter 3 it was shown that dispersivity is also used to determine a particle's movement. A number of dispersivity/porosity combina-

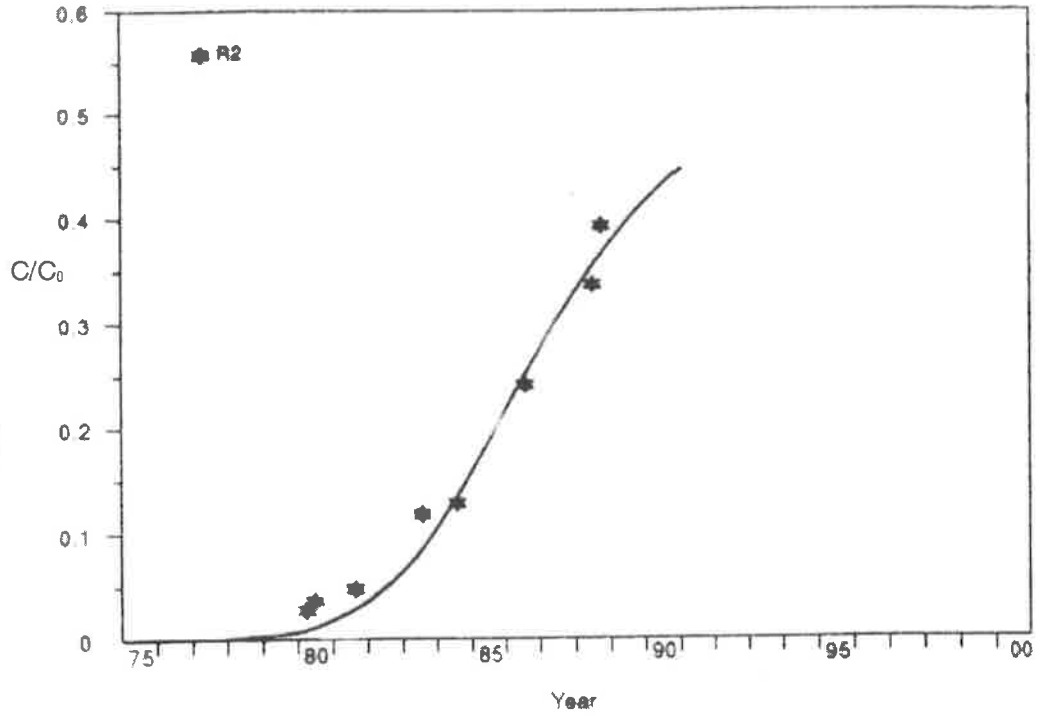

Figure 4.6: Measured breakthrough curve at well R2 [28]. The data points indicate measured concentrations of chloride at the well, while the continuous line shows a best fit solution for this data.

tions were tried using parameters which were within the ranges specified by van der Kamp et al. [28], all of which failed to reproduce the published measured results. Increasing the porosity to 0.48 and using a longitudinal dispersivity of 70 *metres* (close to the lowest value in the range specified by van der Kamp et al. [28]) produced a computed plume which reached the position of well R2 after a simulation time of approximately 12 years. Figure 4.7 shows the computed breakthrough curve for the model using parameters as shown in Table 4.2.

The value of porosity used in the model falls outside the range specified in van der Kamp et al. [28]. This indicated that there was some retardation of the plume while travelling in the aquifer, which was simulated via a slight increase in the porosity value.

4.4 Results

In this section the results of the simulations using the parameters shown in Table 4.2 are presented. Figure 4.8 shows the computed results using RNDWALK2D [23] for six times between $t = 600$ *days* and $t = 6000$ *days*.

For each of the time periods presented, the width of the computed plume re-

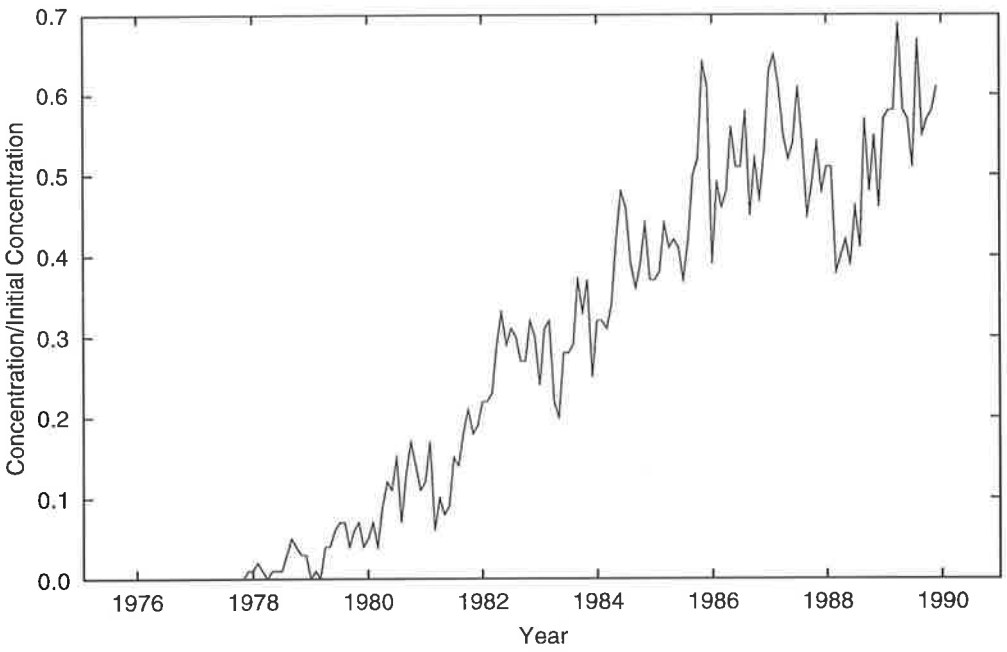

Figure 4.7: Computed breakthrough curve at well R2 using parameters from Table 4.2.

Parameter	Value
Northern hydraulic conductivity ($K_x = K_y$)	216 $m\ day^{-1}$
Southern hydraulic conductivity($K_x = K_y$)	10 $m\ day^{-1}$
Longitudinal dispersivity (d_L)	70 m
Transverse dispersivity (d_T)	0.10 m
Porosity	0.48

Table 4.2: Parameters used in the flow and transport models of Saskatchewan.

mains narrow, approximately one grid square (200 *metres*) wide; this is consistent with the measured results presented in van der Kamp et al. [28].

If the measured breakthrough curve for well R2 (Figure 4.6) is considered, it can be seen that the concentration at well R2 begins to rise in 1977 and starts to level out to approximately half of the concentration originally present under the sewage reservoir. Figure 4.7 shows that single particles arrive around 1978. The number of particles passing through the location of well R2 increases before starting to level out to approximately 40-70 particles (half the number present at the source) as in Figure 4.6, showing that this model is consistent with the measured results.

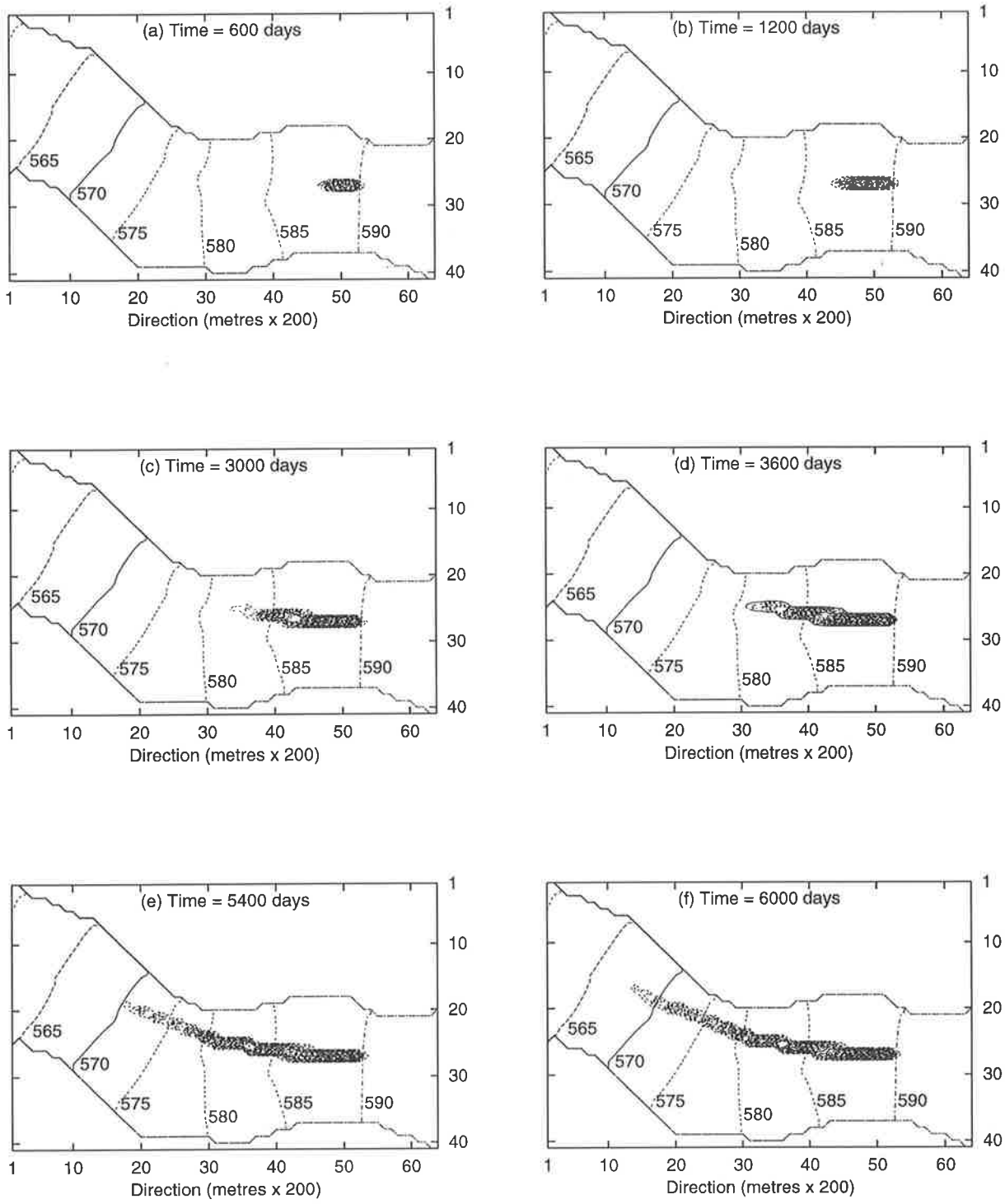

Figure 4.8: Results for the Condie Aquifer contaminant transport model using RNDWALK2D for six different time values with $d_L = 70$ metres and $d_T = 0.10$ metres. Labeled contours indicate groundwater head levels (metres).

4.5 Parameter Sensitivity.

Of interest is whether the accuracy of the computed solution is dependent upon specific parameter values. The parameters that are of most interest in this respect are those which effect the travel of the computed plume, specifically, longitudinal and transverse dispersivity and porosity.

As discussed in Section 4.3.2, the flow model is quite insensitive to changes in its parameters, with the model results being very similar even with large changes in model parameters.

This section determines whether the same is true of the transport model by considering a number of different values for each of the parameters that affect the transport of the plume and examining whether altering some of these parameters produces any unexpected results.

4.5.1 Changes to dispersion parameters.

In general the effect of changing the dispersion parameters in this model is quite small. Tests were conducted using different values of longitudinal and transverse dispersivities, with breakthrough curves being examined after each change of parameter. The results are shown in Figures 4.9 and 4.10. It can be seen by inspection that the more significant change occurs when the value of longitudinal dispersivity is changed.

Figure 4.9 shows the computed breakthrough curve at well R2 for three values of longitudinal dispersivity, $d_L = 60$ *metres*, $d_L = 120$ *metres*, the highest value in the range specified by van der Kamp et al. [28], and $d_L = 180$ *metres*, triple the lowest value specified by van der Kamp et al. [28]. It can be seen that the computed plume arrives at well R2 a few years ealier when using a value of $d_L = 180$ *metres* than with $d_L = 60$ *metres*. A smaller value (30 *metres*) was also tried, and as expected, the plume travelled more slowly. This shows that the value of longitudinal dispersivity can be close to the true value, but need not be exact, since a small increase in longitudinal dispersivity is likely to cause only minor increases (or decreases) in the distance travelled by the computed plume at a particular time.

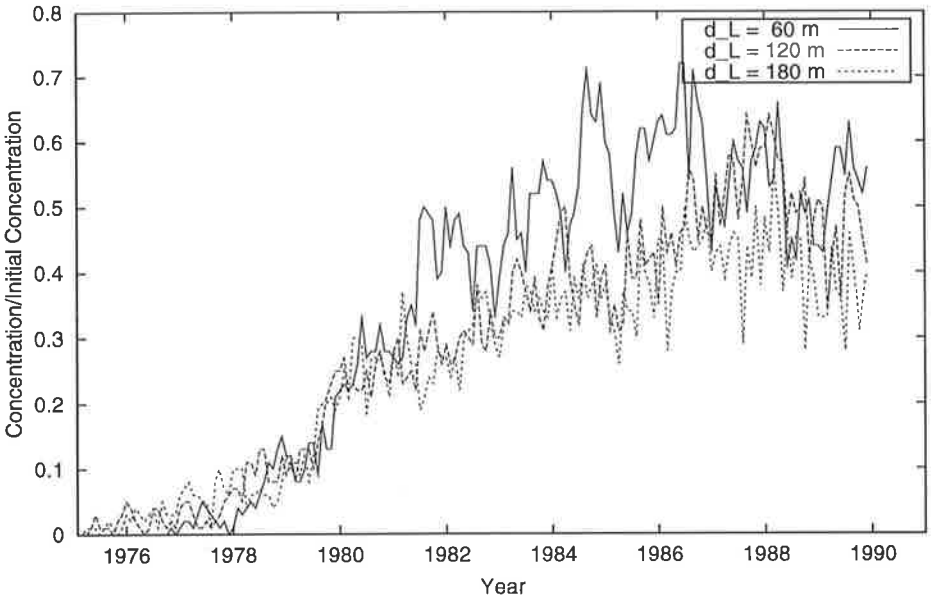

Figure 4.9: Breakthrough curves at well R2 using RNDWALK2D and three values of longitudinal dispersivity. The solid line shows the results for $d_L = 60$ *metres* and the dashed lines show the results for $d_L = 120$ *metres* and $d_L = 180$ *metres*. All other parameter values (K_x, K_y, d_T, *porosity*) are as shown in Table 4.2.

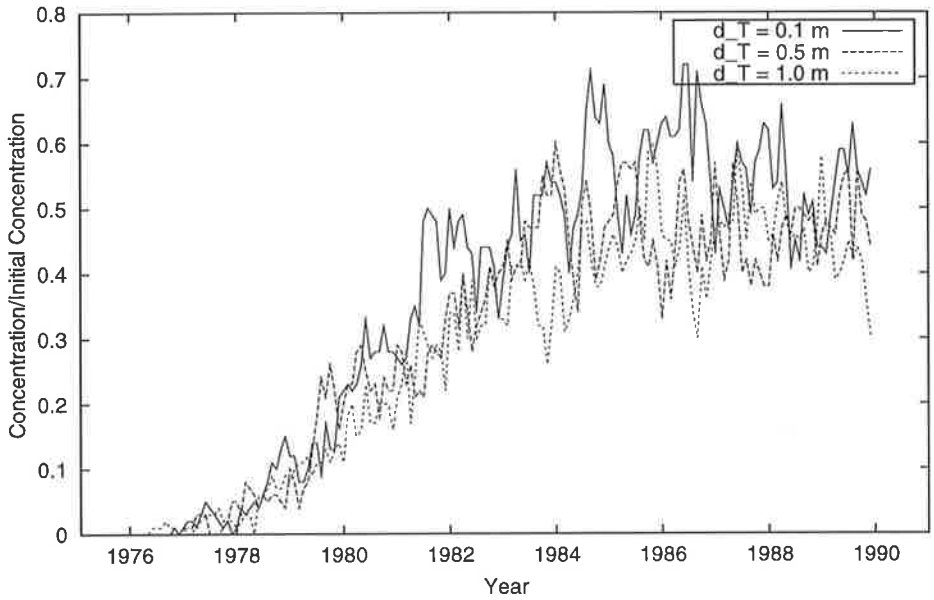

Figure 4.10: Breakthrough curves at well R2 using RNDWALK2D and three values of transverse dispersivity. The solid line shows the results for $d_T = 0.10$ *metres* and the dashed lines show the results for $d_T = 0.50$ *metres* and $d_T = 1.00$ *metres*. All cases used parameter values of K_x, K_y and *porosity* as shown in Table 4.2 and $d_L = 60$ *metres*.

Figure 4.10 shows three computed breakthrough curves generated as a result of three values of transverse dispersivity being used in the model, $d_T = 0.10$ *metres*, $d_T = 0.50$ *metres* and $d_T = 1.00$ *metres*. It can be seen that a ten times increase in transverse dispersivity produces a change in arrival time at well R2 of at most 2 years. Thus it would be anticipated that values of transverse dispersivity that deviate slightly from the true value would not markedly affect the end result.

It should be noted that these changes in longitudinal and transverse dispersivities did not significantly alter the number of particles arriving at well R2 in the model.

In general it was determined that changes in dispersivity values did not greatly effect the solution, with relatively high changes in dispersion values resulting in small changes in the computed results. It was noted that the effect of increasing the longitudinal dispersion had a greater effect on the computed plume, which was not entirely unexpected since it was in the direction of the flow. If the dispersion in any direction was allowed to vary by smaller amounts, the effect on the model was quite small, indicated that the model did not require dispersion coefficients of high accuracy to produce a model which reflected the observed situation in the field. The insensitivity to changes in dispersion values demonstrated in Figures 4.9 and 4.10 can be attributed to the high velocity of the groundwater, creating an advection-dominated system.

4.5.2 Changes to porosity

As mentioned in Chapter 2, the velocity of particles in the model is determined by Equations 2.4 and 2.5, shown below:

$$u = \frac{K_x}{porosity} \times \left(-\frac{dh}{dx}\right), \tag{4.1}$$

$$v = \frac{K_y}{porosity} \times \left(-\frac{dh}{dy}\right). \tag{4.2}$$

At a given point, the terms $\frac{dh}{dx}$ and $\frac{dh}{dy}$ are determined from the distribution of hydraulic head generated in the flow model. Additionally, the parameters K_x and K_y are used to determine the head distribution; thus the only parameters which may be altered by the user in the transport calibration process that will affect the velocity of the particles in the system, given some head distribution, is the porosity.

Values of porosity lie between 0 and 1. Clearly from Equations 4.1 and 4.2 a smaller value of porosity will increase the velocity of the particles in the system, and vice versa.

Figure 4.11 shows four computed breakthrough curves at well R2 using different values of porosity. It can be seen that by using a smaller porosity, the rate of movement of the plume is greater, and thus the plume reaches well R2 earlier than when a larger value is used. Conversely, when a larger value is used, the plume travels at a decreased rate. From this figure it can be seen that the value of porosity greatly effects rate of movement of the plume.

Given the results shown in Figure 4.11, a porosity value of approximately 0.50 should be used as this produced results that matched most closely with those presented in Figure 4.6.

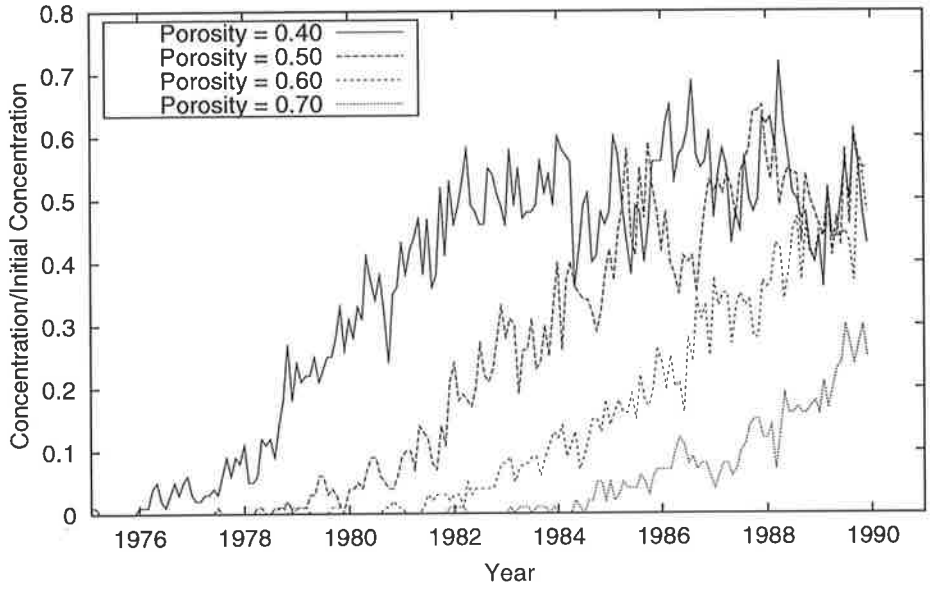

Figure 4.11: Breakthrough curves at well R2 using RNDWALK2D and four different values of porosity. The solid line shows the result for porosity = 0.40 while the dashed lines show the results for porosity = 0.50, 0.60 and 0.70.

4.6 Comparison with Other Methods

Applying the same parameters as presented in Table 4.2 to the Easton, Steiner and Zhang (ESZ) and Lewis, Noye and Evans (LNE) schemes, it was noted that the results differed from those produced by the Prickett, Naymik and Lonnquist (PNL) scheme; both the ESZ and LNE schemes showed a significant amount of additional dispersion near the tip of the plume, as shown in Figure 4.12, which highlights the large, and unexpected, spread of particles after the plume starts moving in a northerly direction.

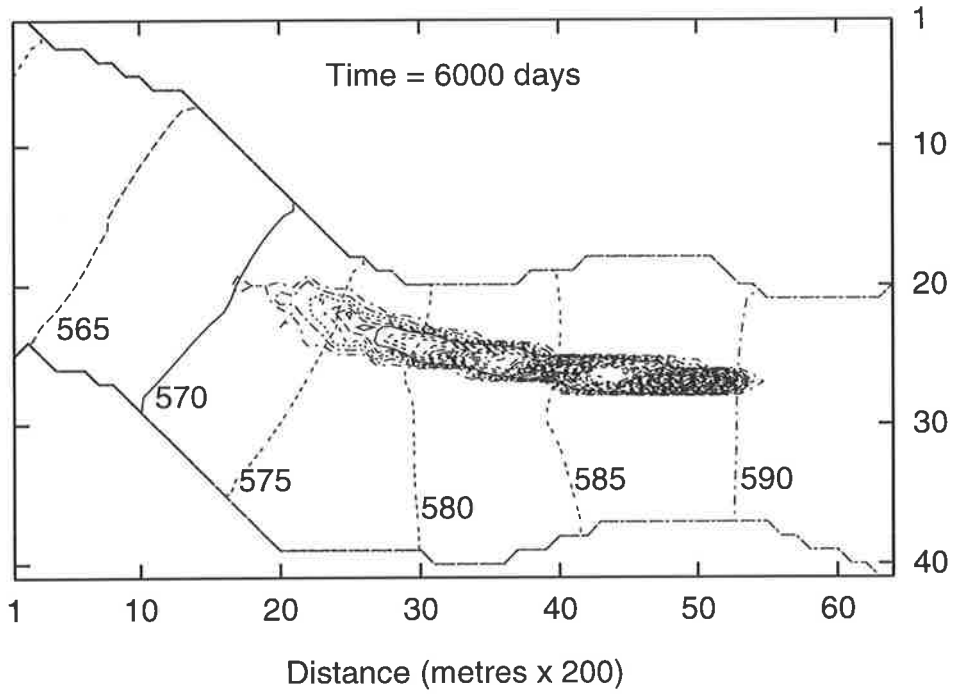

Figure 4.12: Example of the Lewis, Noye and Evans scheme prior to modification, showing the additional dispersion.

By examining the equations used and the preliminary results, it was determined that for proper operation the equations for each of the ESZ and LNE schemes were such that they required that the x axis of the model was aligned with the direction of travel, as was the case in the examples given in Chapter 3. Modifying the ESZ and LNE schemes to the more general case of the groundwater flow travelling in any direction was a simple procedure, applying a rotation to the dispersion terms in each scheme so that the longitudinal dispersion occurred in the same direction as the groundwater flow.

Following these modifications, each model was run again using the same parameters as used with the PNL scheme. The computed results are presented in Figures 4.13 and 4.14. It can be seen from inspection that the results obtained from these modified forms now match those given by the PNL scheme, verifying the assertion in Chapter 3 that all three schemes produce results that are very similar.

The primary differences between each of the three schemes is at the tip of the plume where a small number or particles has separated from the bulk of the plume. By considering the breakthrough curves at grid point (45,27) shown in Figures 4.15(a), (c) and (e), which lies 1400 metres downstream from the sewage reservoir, it can be seen that the plume arrives at this point at approximately the the same time for each of the three schemes and that the concentration of particles levels out at approximately the same value. This shows that the minor differences at the tip of each plume do not effect the overall results in any significant manner. It can also be seen that the time averaged concentrations are slightly above the initial concentration. As mentioned in Chapter 2, this is an idiosyncrasy of random walk models. The breakthrough curves in Figures 4.15(b), (d) and (f) show the arrival of particles at well R2, 6000 metres from the sewage reservoir. The similarity of these three results shows that the small differences that were seen in 4.15(a), (c) and (e) on the long term results are minimal.

It can be seen in Figures 4.15(b), (d) and (f) that there are differences at the end of the modelled time period. Namely, in Figure 4.15(b) the concentration appears to be increasing while in Figures 4.15(d) and (f) the concentration is decreasing. These differences are a result of using the random walk technique. Similar instances of the computed solutions being out of phase with each other can be seen at other times in Figures 4.15(a)-(f) without there being any significant differences in the overall solutions.

The time required to run these simulations using the PNL, ESZ and LNE schemes was 42 *seconds*, 49 *seconds* and 81 *seconds* respectively, showing that a computed solution for this problem can be generated using random walk techniques quickly and efficiently.

This chapter has shown the development, calibration and validation of a numerical model that simulates the transport of a plume of contaminant in a groundwater system. It has been shown that the three random walk schemes produce very similar results when applied to real-world problems, as was the situation for the test cases presented in Chapter 3.

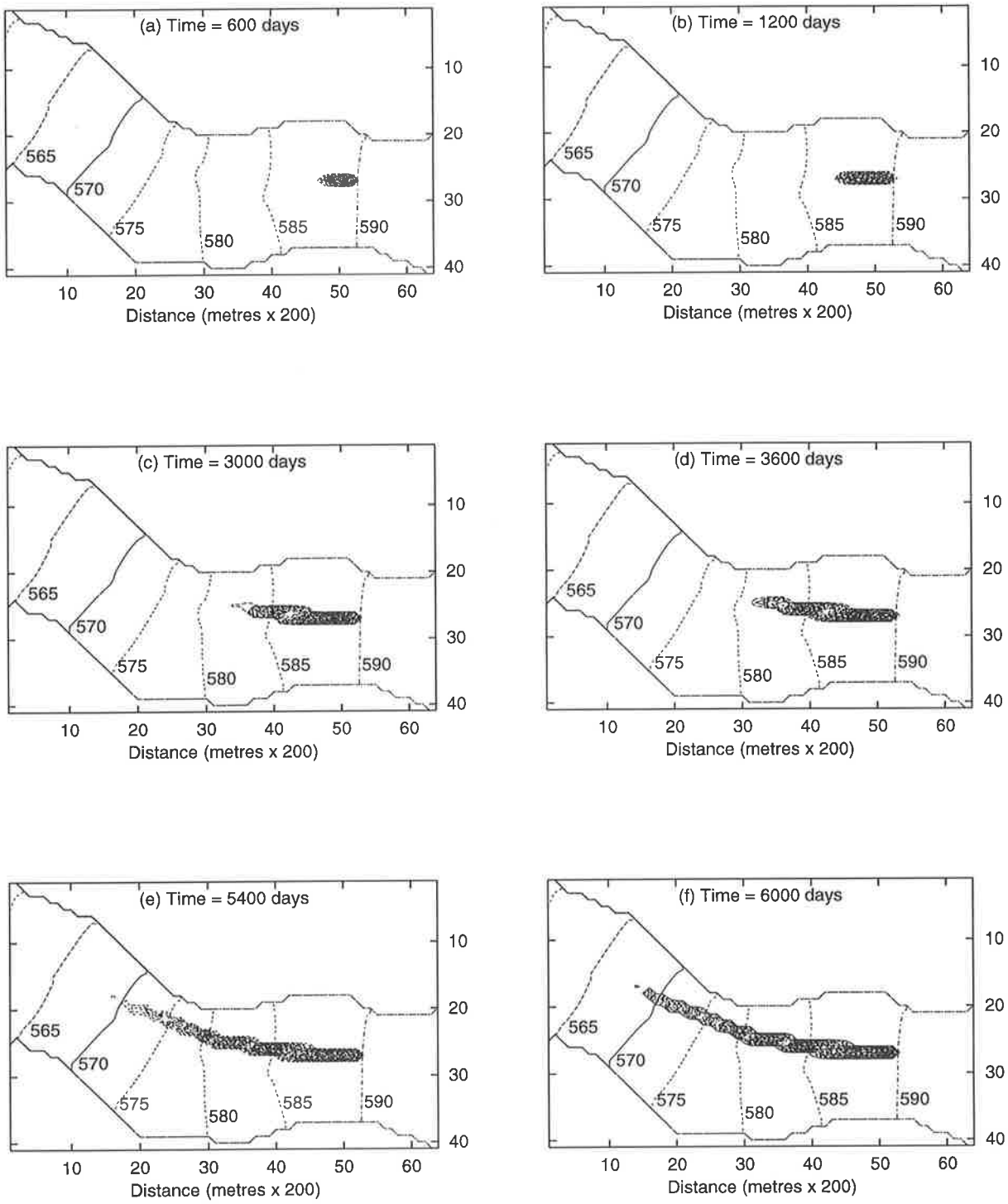

Figure 4.13: Results for the Condie Aquifer contaminant transport model using the Lewis, Noye and Evans scheme for the same six time levels as in Figure 4.8 using $d_L = 70$ metres and $d_T = 0.10$ metres. Labeled contours indicate groundwater head levels (metres).

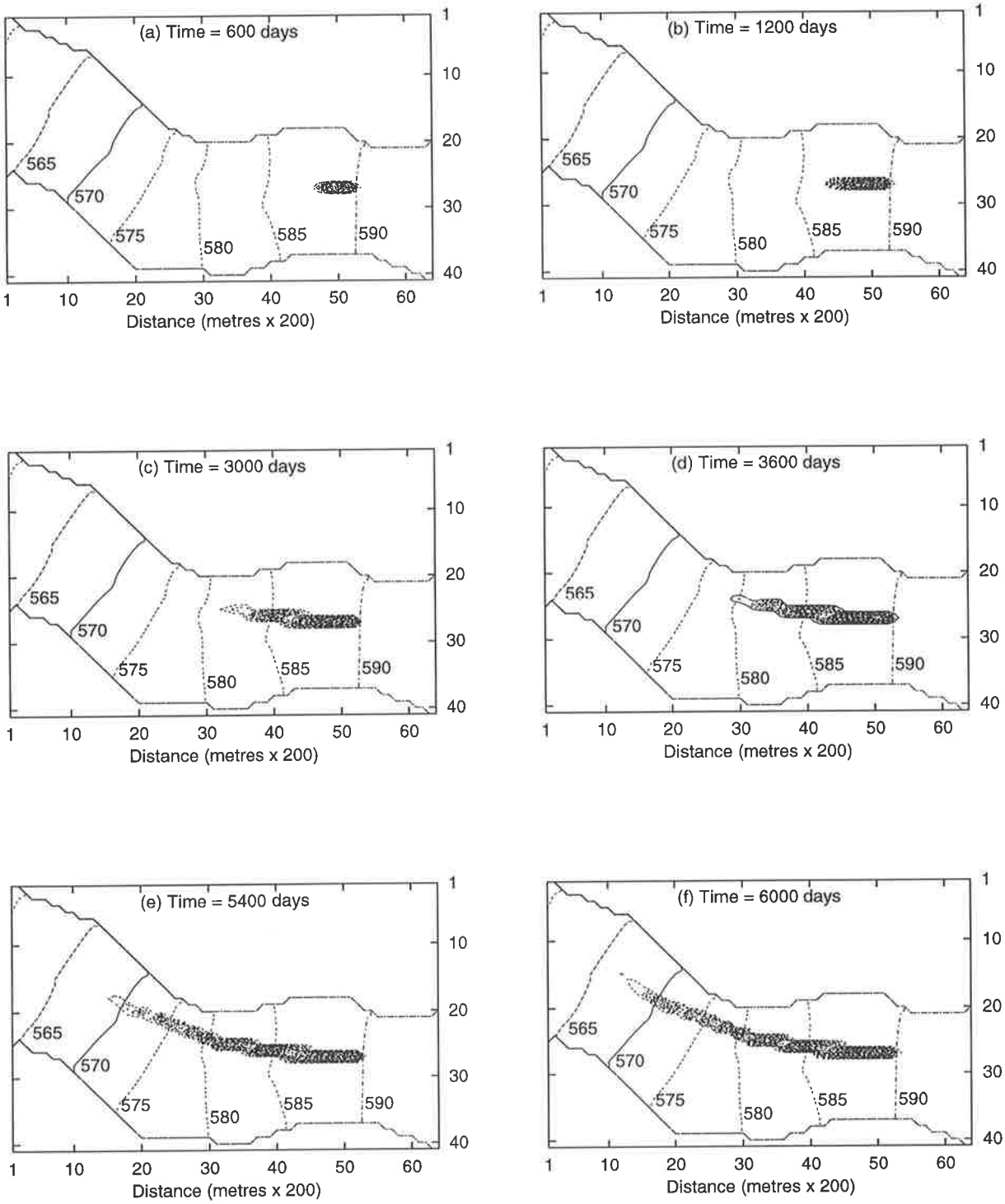

Figure 4.14: Results for the Condie Aquifer contaminant transport model using the Easton, Steiner and Zhang random walk scheme for six time levels using $d_L =$ 70 metres, $d_T = 0.10$ metres. Labeled contours indicate groundwater head levels (metres).

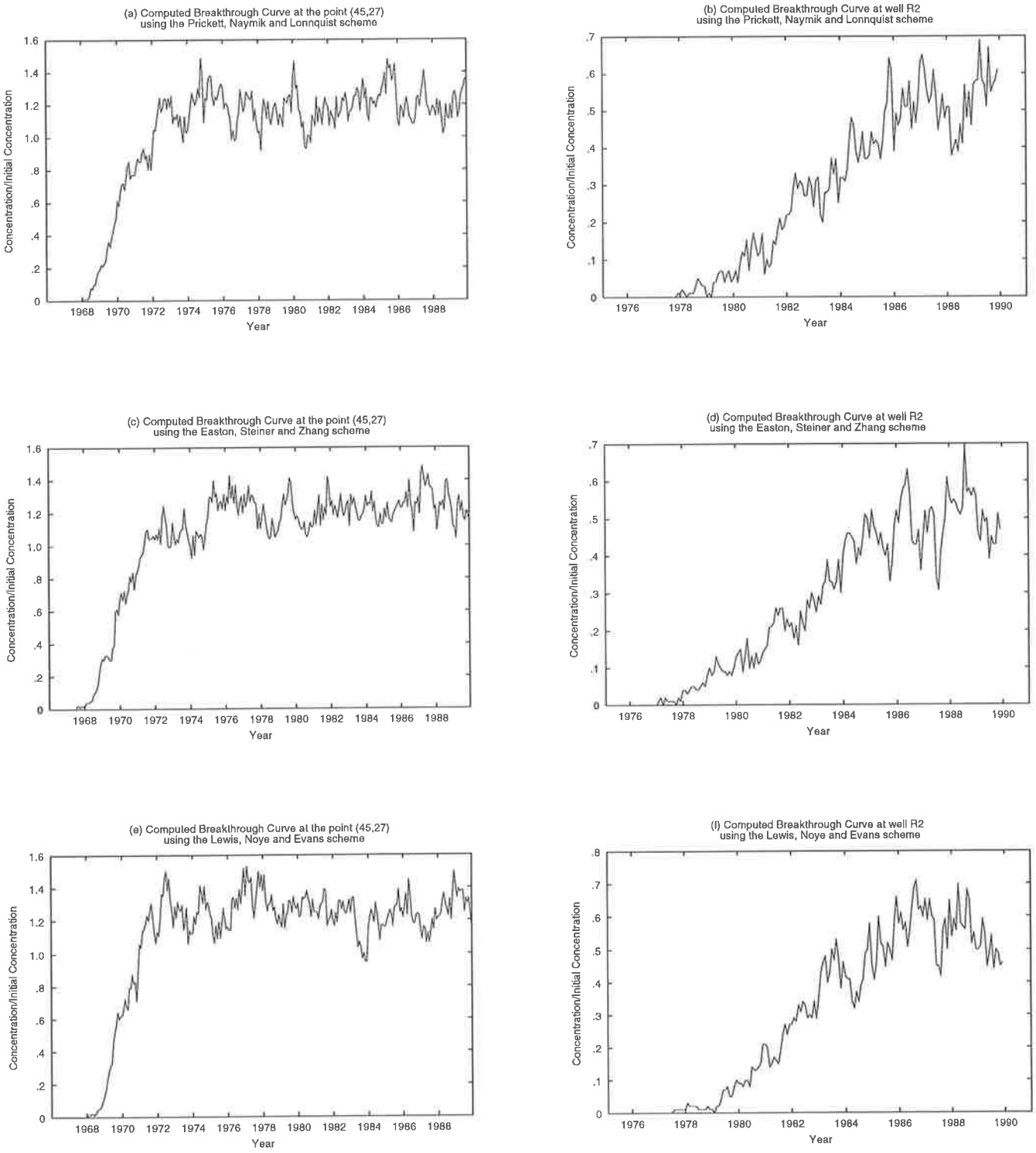

Figure 4.15: Time history plots at the point (45,27) (1400 m from the seepage point) and well R2 (near grid point $(21,20)$) for each random walk scheme.

Chapter 5

Salinity in the Southeast of South Australia

5.1 Overview and Objective

In this chapter the groundwater modelling program RNDWALK2D (with modifications) has been applied to a salinity problem in the south east of South Australia around Padthaway. The objective of this modelling effort is to use head and salinity data provided by the Department of Mines and Energy [5] to produce a model which simulates the increase in both water level and salinity in the region.

5.2 Background

The area of interest is located in the south east of South Australia, near the township of Naracoorte (see Figure 5.1), a region used extensively for the growing of vines for the production of wine. Due to the climate of the region, groundwater is used exclusively for irrigation during the months of November though to April [25], and therefore its quality is of prime concern.

Since the early 1980s the region has experienced increases in groundwater levels (Figure 5.2) as well as a steady increase in salinity levels within the local groundwater (Figure 5.3) primarily due to increases in irrigation in the area [25]. This increase in salinity has had an adverse effect on the yield within specific regions, and on the quality of the grapes produced since vines cannot tolerate high salinity irrigation water [25]. It is expected that continued increases in groundwater and salinity levels will only exacerbate this situation.

Figure 5.1: Map showing the location of the model area [27].

More recently, additional vines have been planted in the region, which has resulted in even more irrigation in the area, which in turn has an increasingly adverse effect on the level of the groundwater and its salinity.

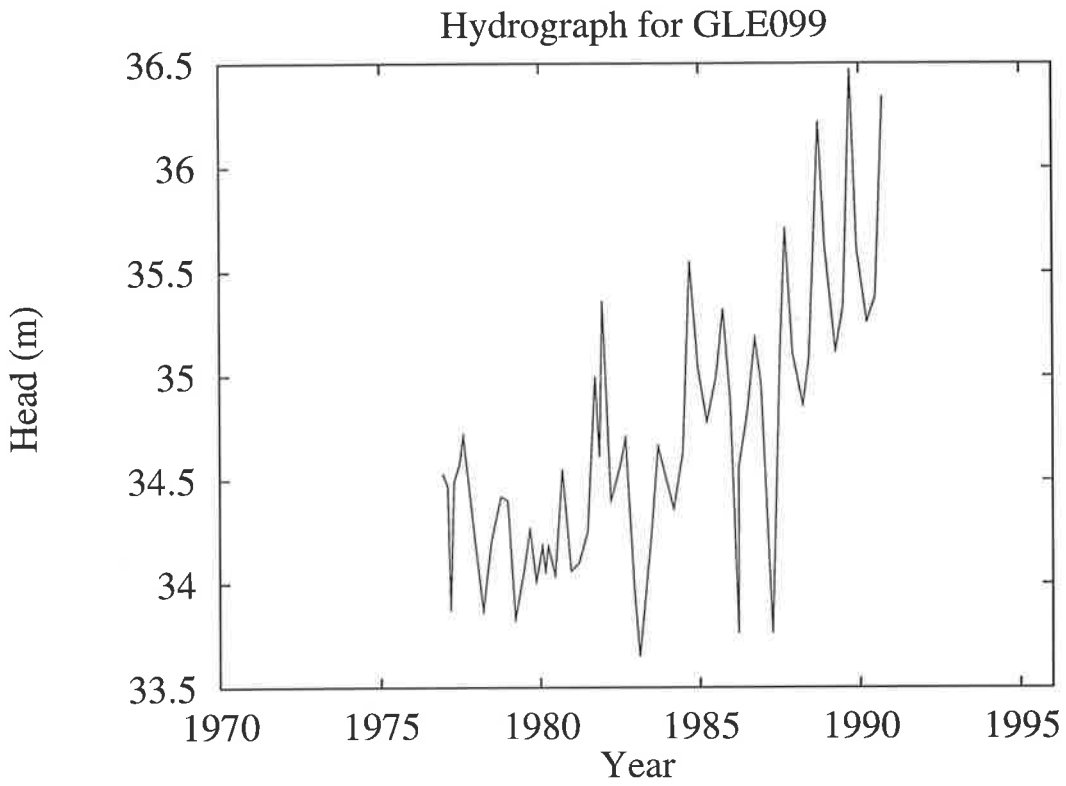

Figure 5.2: Hydrograph demonstrating the increase in ground water level at well GLE099 (located to the south-east of Padthaway) in the south east of South Australia [5].

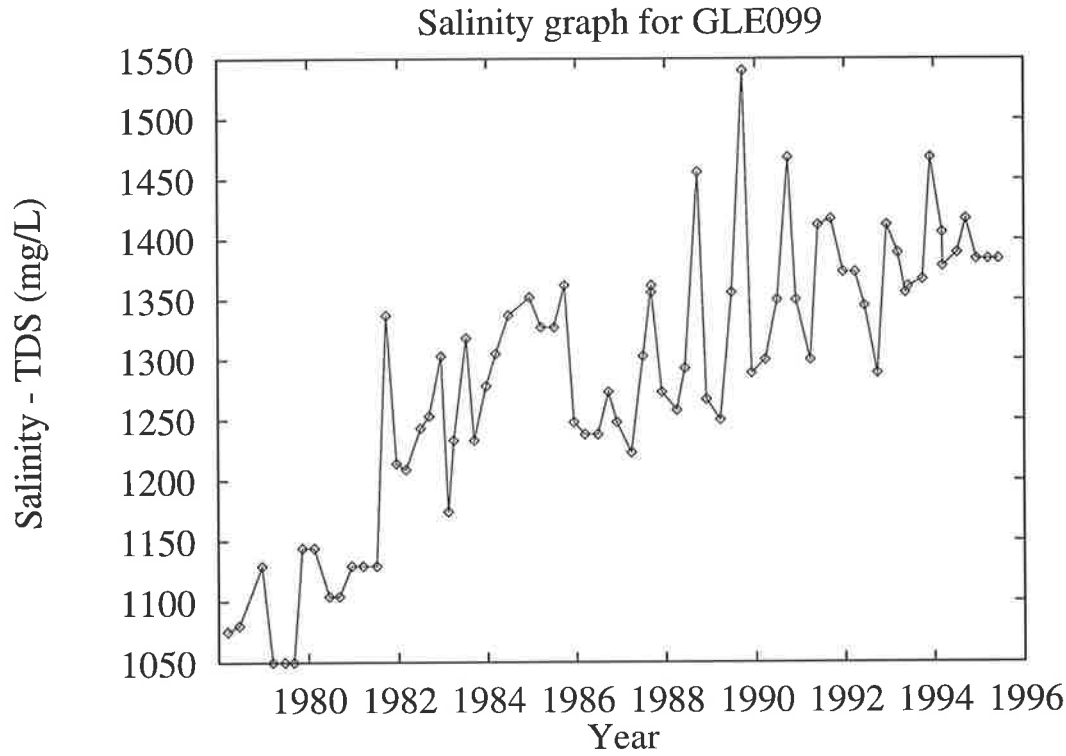

Figure 5.3: Time history plot showing the rise in salinity at well GLE099 in the south east of South Australia [5].

Topographically, the region is relatively flat, and is bounded by the Harper and Naracoorte Ranges, each running from the south east to the north west of the region. Figure 5.4 shows the topography of the lower portion of the model area, in particular the Naracoorte Range on the right, and the interdunal flat to the left.

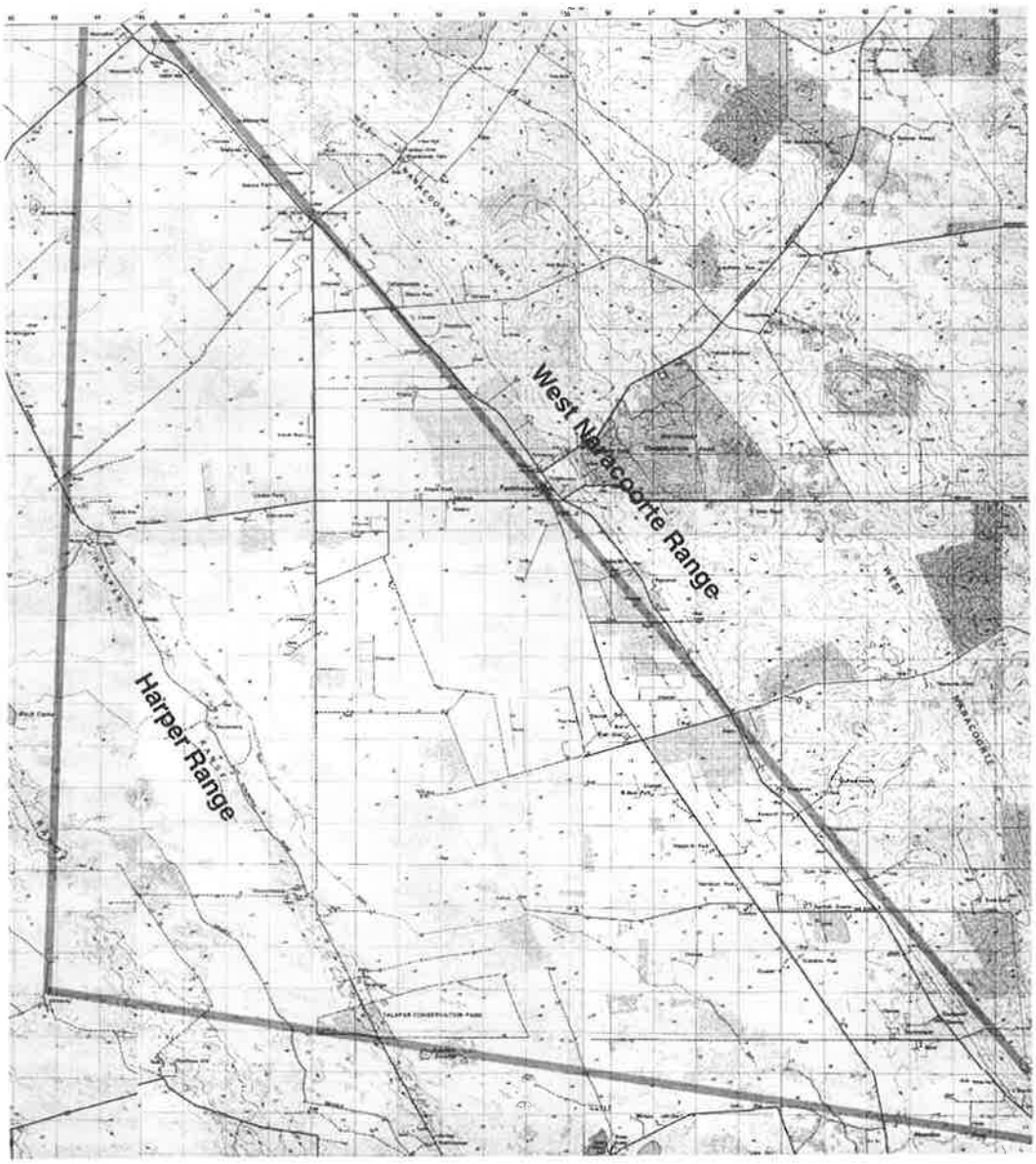

Figure 5.4: Topographic map showing the location of the model area, and the terrain. The thick lines indicate the model boundaries

Geologically, the region is dominated by the Padthaway and Bridgewater formations (Figure 5.5). The former consists of rubbly limestone, underlain by clay. The latter consists of sands and sandstones which are medium to coarsely grained [5]. Figure 5.5 shows that the Bridgewater formation is primarily confined to the sand hills, while the Padthaway formation occurs in the interdunal flats.

5.3 Model Development

Within this section, details of the development of the model which has been used to simulate the movement of salt in the groundwater in the south east of South Australia over the period 1980-1990 is presented.

5.3.1 Model Boundaries

Having identified the region of study in Section 5.2, the next task in developing a model is to identify the model domain, and to specify boundary conditions. The model domain, and the types of boundaries used, are shown in Figure 5.6. The model domain is the area contained within the boundaries shown.

Constant Head Boundaries.

From examining the water table elevation contours shown in Figure 5.6, it was determined that two constant head boundaries would be required. The first of these boundaries is aligned along the Naracoorte Range, and the second positioned in the interdunal flat near the wells MAR24, MAR27, MAR28 and MAR15. Figure 5.5 shows that the interdunal flat consists of the Padthaway formation and so, by positioning the eastern constant head boundary at the base of the Naracoorte range, areas containing the Bridgewater formation are excluded from the model domain, simplifying the model by enabling the use of a constant transmissivity throughout the domain. These constant head boundaries are illustrated in Figure 5.6.

The head values along the eastern and western boundaries were determined from observation wells which lay on, or close to, these boundaries, using measured data supplied by Brown [5]. Figure 5.6 shows that the values along the eastern boundary range from approximately 28 metres at the northern extent of the boundary to approximately 40 metres at the southern extent, while the values along the western boundary range from approximately 28 metres at the northern extent to approximately 30 metres at the southern extent.

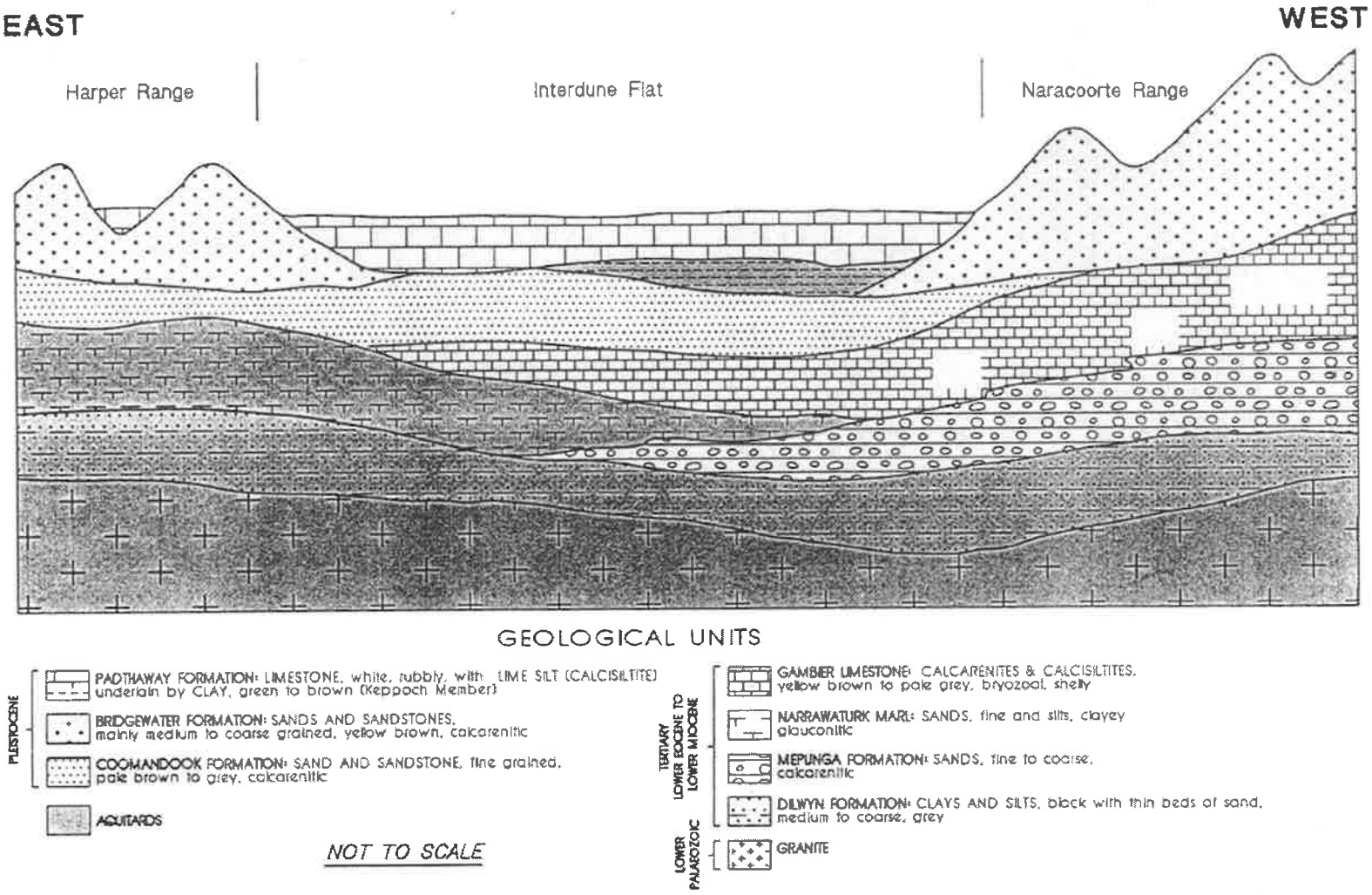

Figure 5.5: Geological cross section of the Padthaway region showing the different soils present in the region, in particular the Padthaway and Bridgewater formations in the top layer [5].

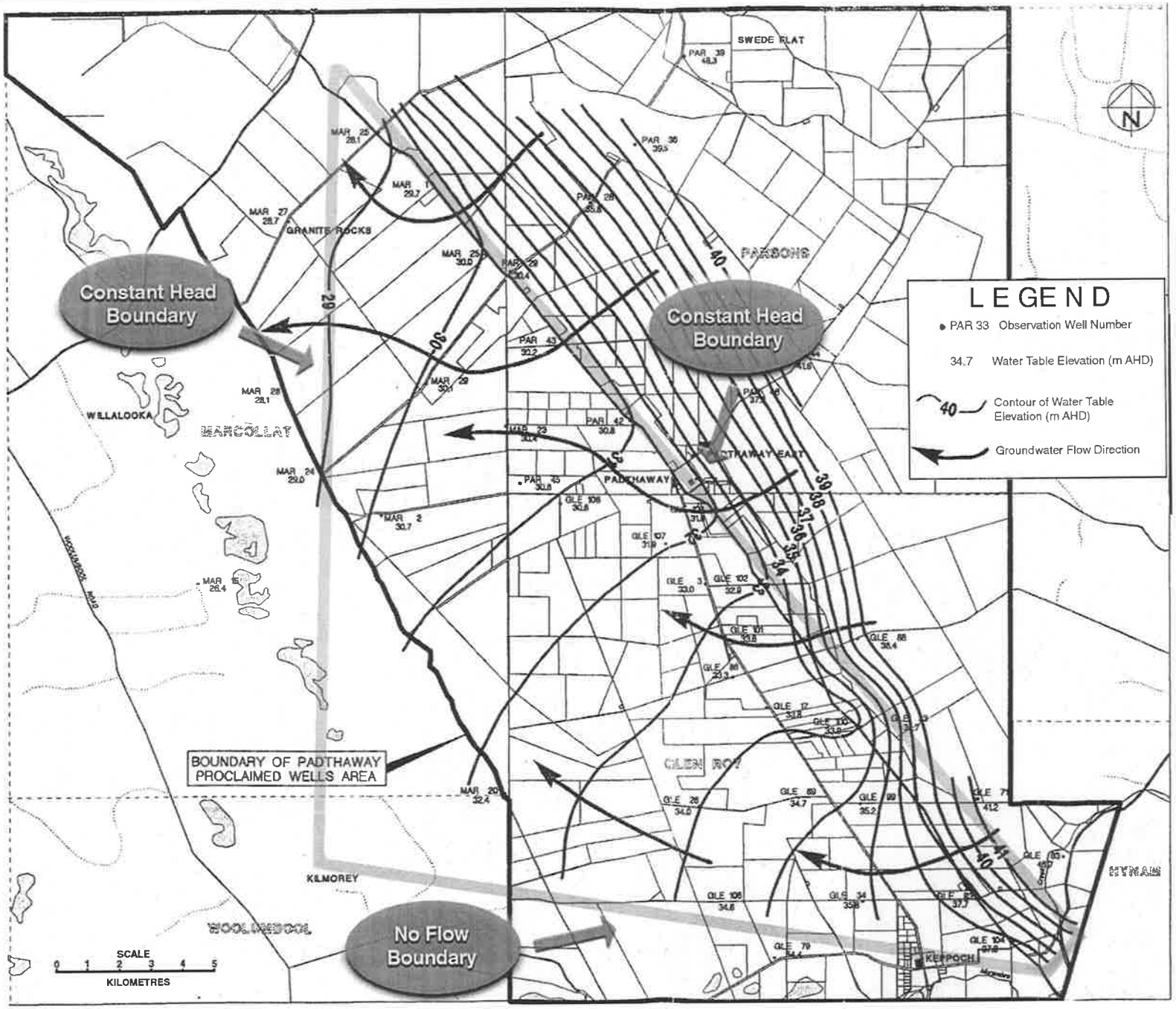

Figure 5.6: Measured heads for March 1994 (based on [5]), with model boundaries identified with a thick line and boundary conditions identified in ovals.

Monthly values were taken for the years 1980-1990 for each of the wells and applied to these boundaries. Head values for the grid points between these wells were determined via interpolation. A steady state head distribution was computed for each month, using these boundary values.

No Flow Boundary

Based on the head contour lines shown in Figure 5.6, which gives an indication of both the direction of groundwater flow and the head levels, a no flow boundary was positioned along the lower portion of the domain, perpendicular to the head contours.

5.3.2 Model Grid

With the model domain and boundaries chosen, a finite difference grid can be overlaid onto the model area. The choice of an appropriate grid is an important step, as it directly influences the maximum resolution achievable in the model results. Easton et al.[6] discusses problems related to grid size and particle numbers, with particular reference to problems relating to determining concentrations using a large grid spacing and smaller numbers of particles.

Since the area of interest was the whole of the domain, that is, there were no particular points in the domain that require additional resolution, a regular grid has been used. A grid size of 500 $metres \times 500$ $metres$ has been chosen since it was anticipated that this would give acceptable resolution, resulting in a domain contained within a 40×74 grid. It has been chosen to use a grid orientation such that the eastern grid boundary aligns with the constant head boundary (coinciding with the base of the Naracoorte Range). Figure 5.7 shows the grid and its orientation in relation to the physical terrain.

5.3.3 Model Parameter Values.

Model parameters were derived from Brown [5]. As mentioned in Section 5.2, the geologic properties of the region are dominated by two formations. However, the model boundaries were chosen such that only one of these formations (the Padthaway formation) was present in the modelled region. Therefore, the model parameters need only reflect the properties of this formation. The parameters used for the model are shown in Table 5.1.

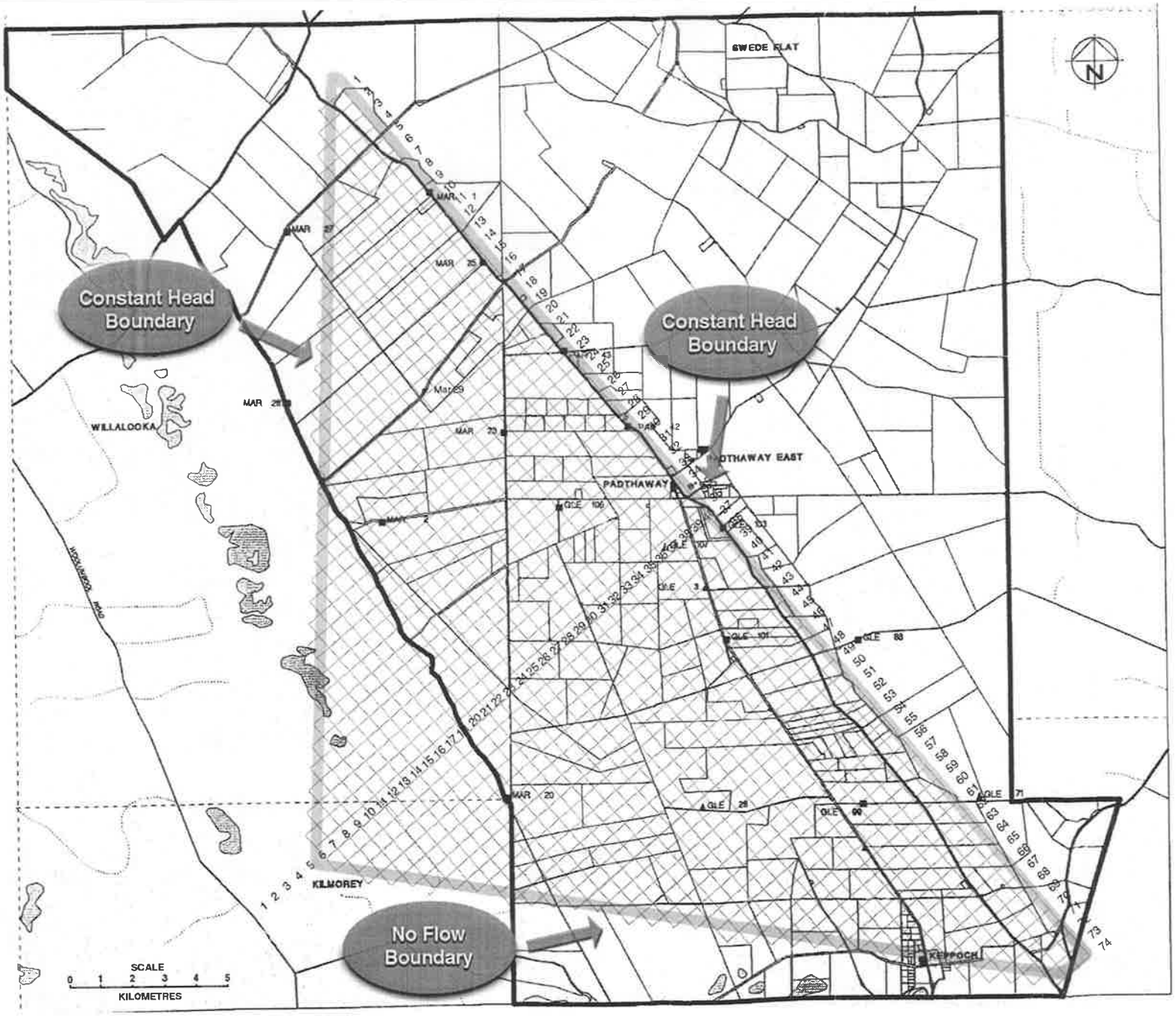

Figure 5.7: Numerical grid for the model of the south east of South Australia. Model boundaries are shown as thick lines and the type of boundary is shown in the ovals.

Parameter	Value
storage factor	0.3 (for unconfined conditions) [4]
pumping or recharge	none
bottom of aquifer	20 metres
top of aquifer	43 metres
porosity	0.2

Table 5.1: Model parameters for the model of the south east of South Australia [5].

In addition, transmissivity in the Padthaway formation ranges from 6000-14000 m^2/day [5], so a representative value of 10000 m^2/day was used as an initial value in the flow model for this formation. Hydraulic conductivity, which is required in the input for RNDWALK2D, was determined via the equation:

$$T = Kb, \tag{5.1}$$

where:

- T is the transmissivity,
- K is the hydraulic conductivity,
- b is the thickness of the aquifer.

In this model, it has been assumed that the aquifer is of a constant thickness of 23 *metres*. While not strictly accurate, there is little variation in the elevation of the bottom of the aquifer and the land surface over the model area. Thus, from Equation 5.1, it was determined that for the Padthaway formation, assuming a transmissivity of 10000 m^2/day, the hydraulic conductivity is 430 m/day.

For the contaminant transport model, an initial concentration of salt was distributed over the model domain based on information from Brown [5]. The eastern boundary was made a constant concentration boundary based on measured concentration data for the wells lying along this boundary, and a subroutine written and implemented in the RNDWALK2D code to ensure this boundary remained at the appropriate concentration. The western boundary was constructed such that particles hitting this boundary were removed from the model.

The following algorithm was applied to combine these models on an annual basis:

- Read in values for constant head boundaries for each month,
- Compute steady state head distribution for current month,

- Apply contaminant transport model
  - Check particle numbers are correct for the constant concentration boundary,
  - apply random walk to advect and disperse particles,
- increment current month.

5.4 Flow Model and Flow Model Calibration

One of the first steps in developing a contaminant transport model of the south east of South Australia was to produce a set of head levels (for each month modelled) which would be used to compute a velocity distribution for input to the particle tracking routines in RNDWALK2D. This required input at regular time intervals providing new boundary conditions every month and a steady state head distribution generated for each month. This was achieved by modifying RNDWALK2D to accept these input values at the time steps required.

Observation wells MAR27 and MAR28 (shown in Figure 5.8) were chosen to provide values for the constant head boundary to the west, while MAR1, MAR25, PAR29, PAR42, PAR43, GLE71, GLE88 and GLE103 were used to specify head values for the constant head boundary along the east. Hydrographs for these wells, sourced from [5], are shown in Appendix C.

The flow model was then applied, generating a steady state head distribution for each month during the period 1980-1990 which could be analysed and used in the calibration process.

Calibration of the flow model involved determining model parameters which would provide a head distribution which agreed (within acceptable tolerances) with the measured head values from Brown [5]. It was decided to calibrate the model against a head distribution from December 1984, owing to the availability of measured data from Brown [5], detailing head values at particular observation wells. Ten observation wells were chosen which were distributed throughout the domain (see Figure 5.8), the aim being to compare the computed head values with the measured values at these points and to reduce the differences between the two sets of values. The aim here was to apply a set of boundary conditions and parameters to the model, which would then reproduce the values at each of the chosen wells for any specified time.

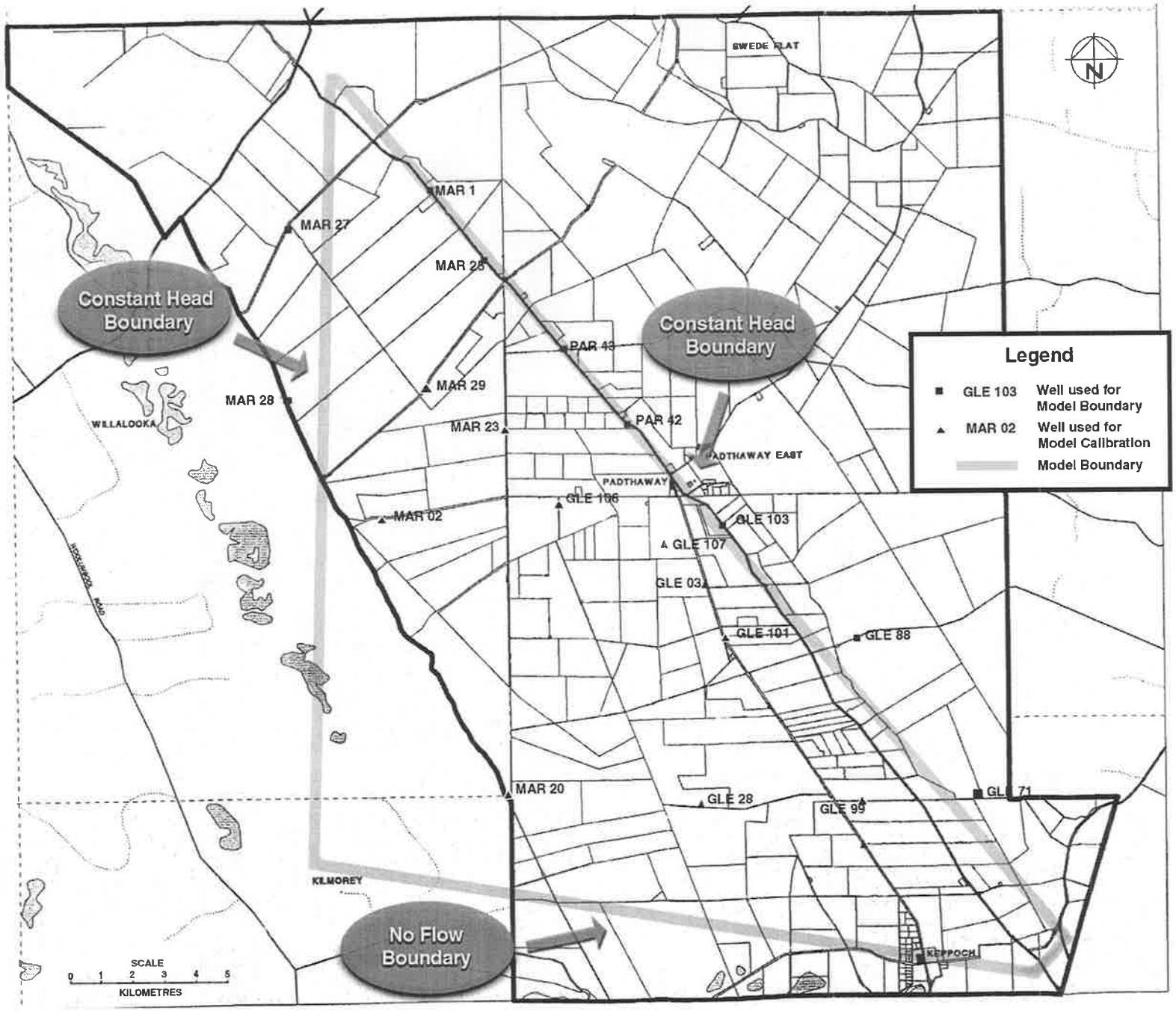

Figure 5.8: Location of the wells used to determine the head distribution for each time step in the flow model. Model boundaries are shown as thick lines.

Starting with the parameter values given in Section 5.3.3, the model was run and head values determined. Initially the greatest differences between measured and computed heads were occurring in the western part of the model (near wells MAR2 and MAR20), so efforts were concentrated on decreasing this difference.

It was noted that the computed head values in the middle of the model domain were a good match for the measured data, so it was thought that the western boundary conditions might not be accurate, primarily due to the sparseness of data in that area. The values on this constant head boundary were determined from the measured head values for wells MAR27 and MAR28. Since these wells did not lie on the boundary, the head values on the boundary were set approximately 1.5 metres higher than those at wells MAR27 and MAR28 to allow for the spatial difference. Additionally the head values were altered so as to provide higher head values at the southern end of the boundary and lower values to the north. By adjusting the values on this constant head boundary, the difference between the measured and computed heads was reduced, but it was clear that there was a limit as to how small this difference was likely to become, without adversely affecting other values in the model domain. The reason for this might be due to the close proximity of the constant head boundary, or more likely, that there was some local factors that had not been incorporated into the model.

Having tried a number of different transmissivity values in the range specified by Brown[5], it was found that a transmissivity of 11,000 m^2/day produced results closest to the measured head values for the wells used for calibration. Table 5.2 shows the final results from RNDWALK2D which shows the observed heads versus the computed heads and the error between the two values for the ten calibration wells.

These results were felt to be acceptable, despite the difference of 0.72 *metres* at well GLE03. Wells GLE107 and GLE101 are in close proximity to well GLE03 and each of these had much smaller errors, in particular GLE107. This shows that there may be some localised activity affecting the groundwater levels which may not be represented by the model, such as pumping. Another possibility, since well GLE03 is close to the eastern constant head boundary, is errors in the input data on the section of the constant head closest to well GLE03. A third possibility is that the use of a constant transmissivity throughout the model domain may not be a good approximation in this particular area.

Having produced an acceptable set of heads for the domain for a single time point the model can be extended to consider transient conditions and thus validate the model over the time period 1980-1990. This is achieved by reading in a set of

Head Calibration: Dec 1984

Well	observed	computed	error
MAR 02	30.35	30.45	-0.10
MAR 20	32.91	32.48	0.43
MAR 23	31.34	30.95	0.39
MAR 29	30.69	30.61	0.08
GLE 03	33.52	32.80	0.72
GLE 28	34.59	34.09	0.50
GLE 99	35.04	35.36	-0.32
GLE101	33.86	33.43	0.43
GLE106	31.76	31.51	0.25
GLE107	32.41	32.36	0.05

Table 5.2: Observed vs computed heads (m) for a selection of observation wells generated during the calibration of the flow model for the south east of South Australia.

boundary conditions, obtained from measured data (Brown [5]) for each month, and generating a head distribution for each month over the years 1980-1990.

Figure 5.9 shows the computed heads plotted against measured heads for each month during the years 1980-1990 for the ten calibration wells. These plots show that the head distributions used in the model are, in general, a good match for the measured heads. In particular, the computed results for the wells GLE106, MAR29 and MAR23 show excellent agreement with the observed values despite pumping being omitted in this model. Computed head levels at all wells show that the annual variation in head within each year is reproduced using this model, albeit in some cases with reduced amplitude with respect to the measured values. It should also be noted that the model reproduces the slight increase in head over the modelled time period.

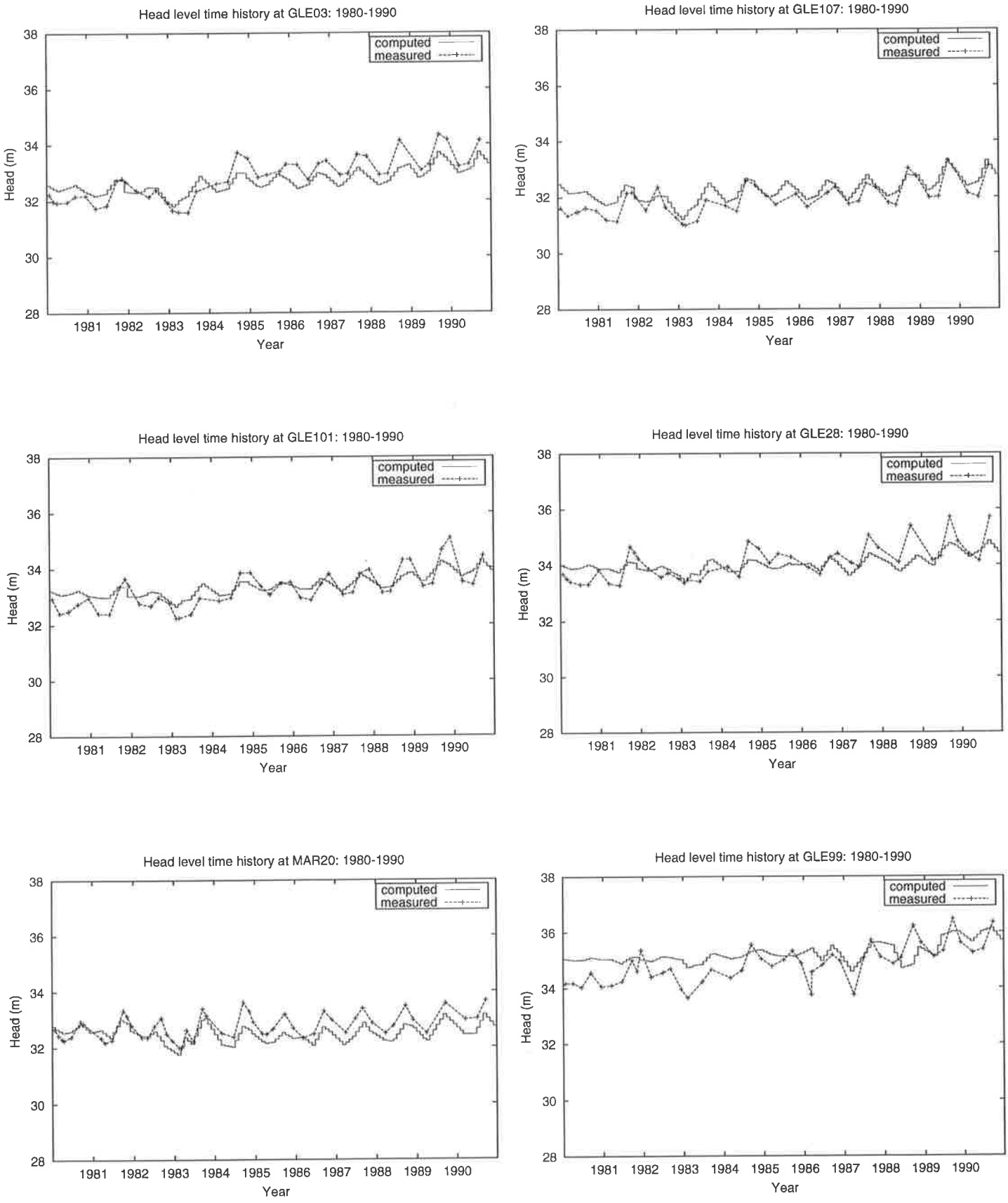

Figure 5.9: Computed heads plotted against measured heads for the period 1980-1990 for the ten observation wells.

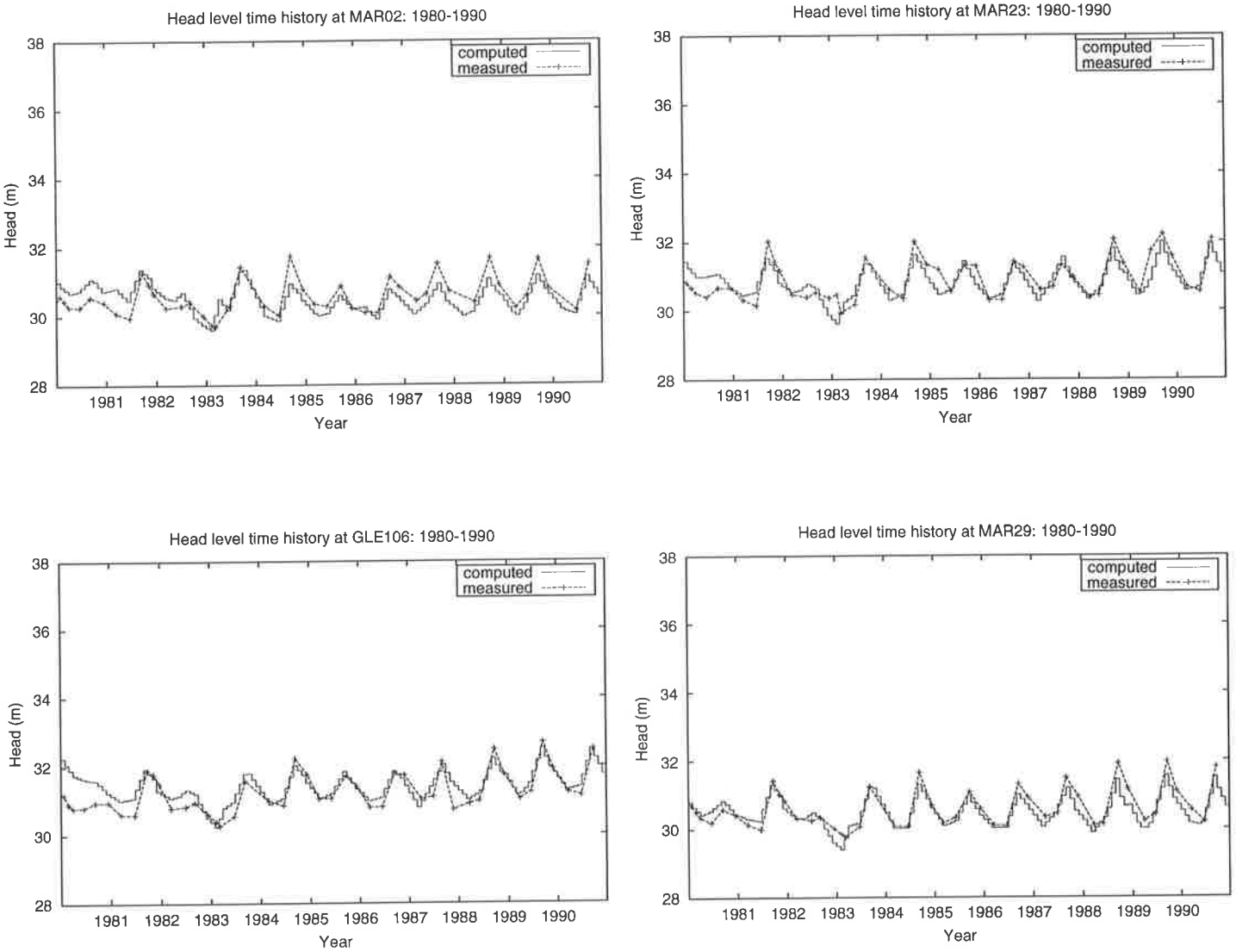

Figure 5.9(cont.): Computed heads plotted against measured heads for the period 1980-1990.

5.5 Transport Model and Transport Model Calibration

Having constructed an acceptably accurate flow model in Section 5.4, the transport of salt in the region was considered.

The tasks involved in the development of the transport model were to construct appropriate initial and boundary conditions, define the number of particles to be used and the concentration of salt that each particle represents.

The last two points above are important in the model since they directly determine the resolution, and hence accuracy, of the transport model as well as governing the speed of execution of the model. As was noted in Chapter 3 and in Prickett et al. [23], the greater the number of particles used, the more accurate the solution.

5.5.1 Transport Model Setup.

The maximum number of particles used in RNDWALK2D is a setting determined by the user as an upper limit for the model. Owing to the expanse of area which was required to be covered with particles, and the concentrations involved, the maximum number of particles (*"MAXP"*) was set to 100,000 after suitable modifications to the RNDWALK2D source code to allow this large number of particles. As a result, it was anticipated that the execution time for this model would be long, which was verified in practice. Smaller numbers of particles were tried, with the results showing larger deviations from the measured data. Similarly, some model runs were performed with substantially higher numbers of particles with noticeably more accurate results, but with *much* longer run times, as was expected.

In contrast to the model presented in Chapter 4 where the concentration was expressed as a fraction of some initial concentration, this model requires that the concentrations be expressed in parts per million (*ppm*). Therefore the amount of salt that each particle represents needs to be determined. This amount, referred to as the particle mass, was calculated as described in Prickett et al. [23]. Namely, the number of particles required by the user to represent a particular concentration is chosen and the particle mass is calculated via the equation:

$$PM = \frac{CONC \times \Delta x \times \Delta y \times (h - BOT) \times porosity \times WW}{10^6 \times NPART} \tag{5.2}$$

where:

$$
\begin{aligned}
PM &= \text{particle mass } (kg) \\
CONC &= \text{concentration required } (ppm) \\
BOT &= \text{height of the bottom of the aquifer above some datum } (metres) \\
NPART &= \text{number of particles required to represent "CONC"} \\
WW &= \text{density of water } (1000 \frac{kg}{m^3})
\end{aligned}
$$

From inspection of the model data, the minimum salt concentration in the area was approximately 1000 *ppm* (occurring on the eastern boundary) while the maximum concentrations occurred on the western boundary with values of between 8000 - 9000 *ppm*. The eastern boundary was chosen to compute the particle mass, so using Equation 5.2 with

$$
\begin{aligned}
CONC &= 1000 \text{ ppm}, \\
\Delta x &= 500 \text{ metres}, \\
\Delta y &= 500 \text{ metres}, \\
h - BOT &= 23 \text{ metres}, \\
porosity &= 0.2, \\
NPART &= 70 \text{ particles},
\end{aligned}
$$

resulted in a particle mass of approximately 16,400 *kg*.

It was expected that with this high particle mass the number of particles required for the whole domain would be close to the maximum number of particles (100,000). Coupled with the high particle mass the model is expected to give a rather coarse estimate of the salt concentration in the area. This coarseness could be reduced by the use of additional particles which would then result in longer execution times.

The next task in constructing the transport model was to define the initial conditions for the region. Given that the salinity of the area was only known for specific, and not equispaced, points, some method was required to determine the salinity values throughout the regularly gridded domain. For this, the package IDEC [11], which incorporates geostatistical techiques [17], was used to provide salinity values for a regular grid based on irregularly spaced data. Wells used to determine a set of initial conditions are shown in Figure 5.10. Although mostly successful in this role, the absence of any data in the west of the region produced

results which were not consistent with the known conditions. Adding some points on and near the western boundary, estimated by assuming that the salt concentrations in this region increased in a near linear manner, solved this problem and IDEC was able to produce a contour map of the initial salt distribution which was consistent with the known measured values for particular points and the known conditions. The initial distribution of salinity used in the model domain is shown in Figure 5.11. This initial distribution was then read into the model via a subroutine which then distributed appropriate numbers of particles throughout the domain.

This model assumes the inflow of salt occurs through the eastern boundary. This was modelled by the addition of particles at each time step along this boundary; the number of particles was determined by the measured data. The number released was controlled by the subroutine presented in Appendix D. This subroutine calculates the current concentration at the boundary grid points, reads in the concentration determined from the measured data, calculates the difference, and modifies the salt concentration by the addition or depletion of particles. Values for the salt concentration entering the model have been taken from Brown [5] using salinity data from the observation wells GLE93, GLE100, GLE103, MAR26, PAR42 and PAR43 which are on, or close to, the boundary and for which there exists good salinity data. Salinity graphs for these observation wells are presented in Appendix E.

5.5.2 Transport Model Calibration

Parameters which effect the transport of salt in the model are the porosity and the longitudinal and transverse dispersivities. The value of porosity was given by Brown [5] to be between 0.15-0.20, while no values for dispersivity were available. Initially, the porosity was assumed to be 0.2 and the longitudinal and transverse dispersivities were to be determined through the calibration process.

It was decided to calibrate the transport model against measured data from December 1984 provided by Brown [5] using eight calibration wells in the area (specifically, MAR02, MAR20, MAR22, MAR23, GLE89, GLE99, GLE101 and GLE106, the locations of which can be seen in Figure 5.10)

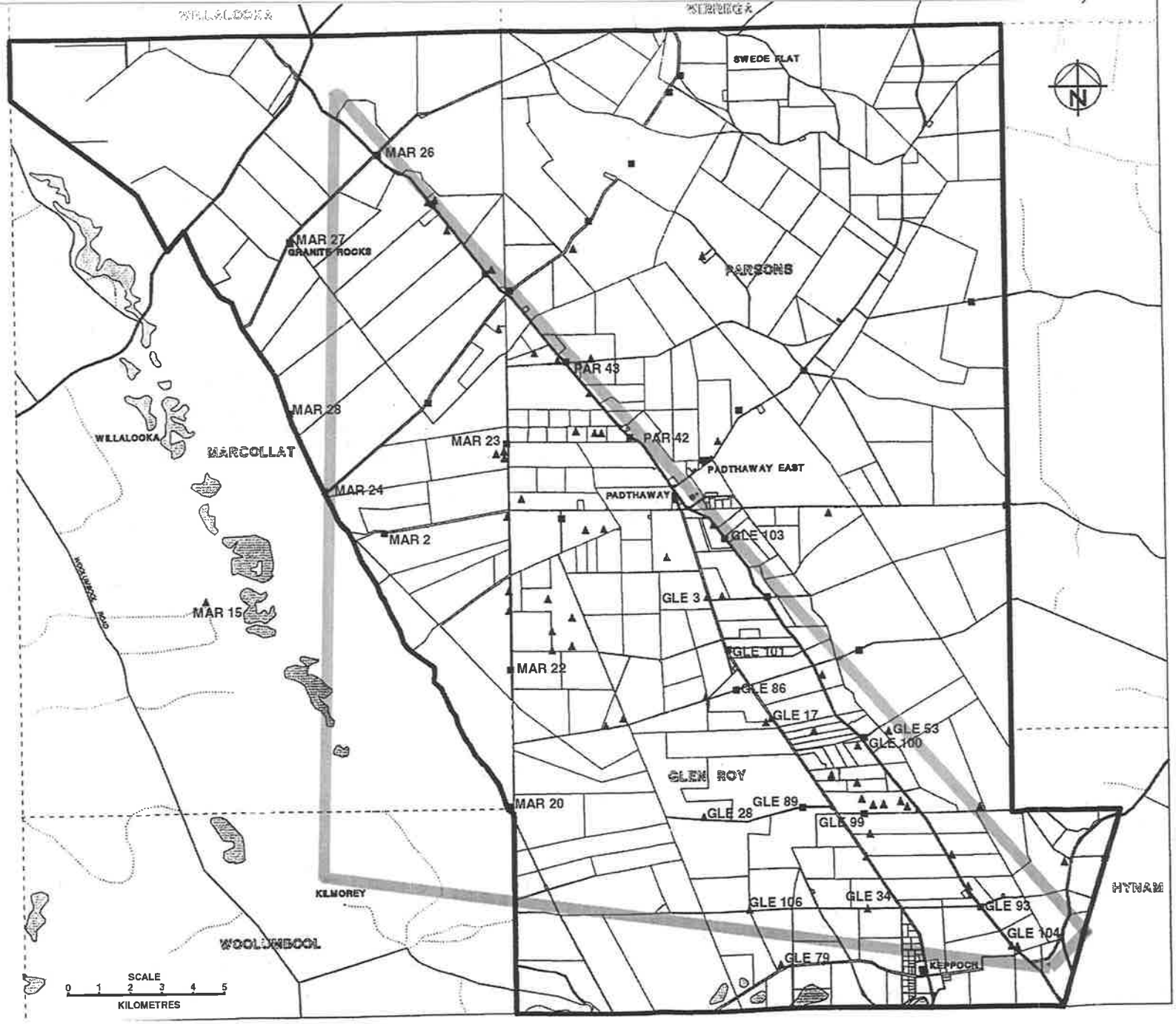

Figure 5.10: Wells used to determine the initial conditions for the model of salinity movement within the south east of South Australia. Thick lines indicate the model boundaries.

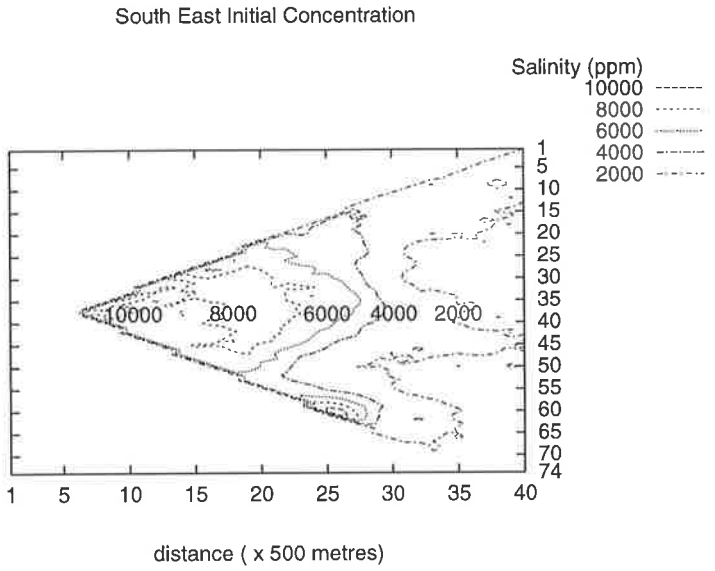

Figure 5.11: Initial concentration of salt used in the model of the south east of South Australia.

The model was run using a range of dispersivities (specifically d_L = 50-200 *metres*, d_T = 1-20 *metres)* and the salinity at each of the calibration wells observed. It was noticed that acceptable results were obtained for a range of dispersivities. Eventually, values of 90 *metres* and 9 *metres* were used in the longitudinal and transverse directions respectively. The computed salinity values using these dispersivity values for each of the calibration wells for December 1984 are presented in Table 5.3 and compared against the measured values from Brown[5].

It can be seen from Table 5.3 that the model results for most of the calibration wells show good agreement with the measured values, with most differing from the measured values by less than 10 per cent. The greatest relative difference for these wells is approximately 17 per cent for well GLE101, while the least difference is approximately 2 per cent at well MAR20

Having calibrated the transport model it was then possible to extend this to a full transient model for the time period 1980-1990. Figure 5.12 shows the time histories for six observation wells in the model area. It can be seen that there is particularly good agreement with the measured values for the wells GLE99 and MAR20. All other wells show good agreement with the measured values, with

Salinity Calibration: Dec 1984

Well	observed	computed	error	% error
MAR 02	3090.00	3246.79	-156.79	-5.07
MAR 20	5992.00	5876.67	115.33	1.92
MAR 22	5360.00	4845.45	514.55	9.58
MAR 23	953.00	914.46	38.54	4.04
GLE 89	1164.00	1251.72	-87.72	7.53
GLE 99	1352.00	1463.13	-111.13	-8.21
GLE101	1620.00	1335.05	284.95	-17.58
GLE106	1080.00	1122.79	-42.79	-3.96

Table 5.3: Observed vs computed salinities (ppm) for a selection of observation wells generated during the calibration of the transport model for the south east of South Australia.

some demonstrating larger differences in the later time steps. Given these results over the time period 1980-1990, it was felt that the model has been verified to produce computed results consistent with the available measured data during the same time period.

Due to the high number of particles used, this model required substantially longer time to run (approximately fifteen minutes) than the model developed in Chapter 4. This is due to the contaminant plume covering a larger proportion of the model domain, and hence requiring a large number of particles to produce a solution of acceptable resolution. This suggests that random walk techniques are not particularly favourable for problems of this type. That is, problems where the plume being modelled covers a large proportion of the model domain.

The model developed in this chapter simulates the movement of salt in the Padthaway region during the years 1980-1990 and could also be extended to predict the salt concentrations within the region for later years. This model could be used in the development and evaluation of remediation plans for the region, or to forecast problems which may occur so that action can be taken to avoid them. The benefit in using such a model in this way is that a number of scenarios may be tried before putting any plan into effect.

The primary limitations of this model are the absence of pumping and the

assumption of a constant transmissivity throughout the modelled region, both of which affect the head gradients in the region, and thus the transport of salt. However, the annual variations in computed head and salinity values are consistent with the measured values, suggesting that these limitations are not severe.

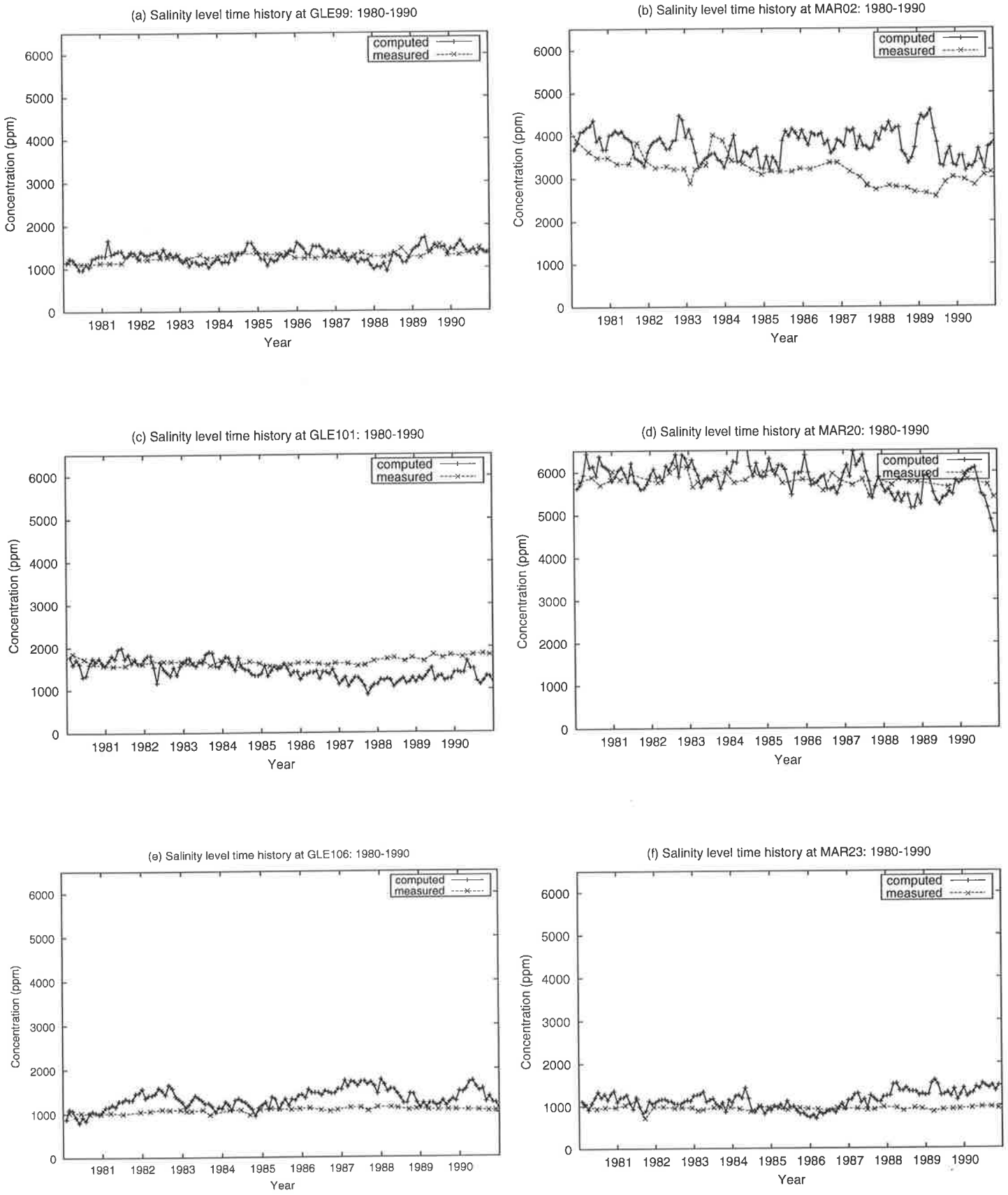

Figure 5.12: Computed and measured salinity plotted for the period 1980-1990 at six wells within the modelled region.

Chapter 6

Summary and Conclusions.

This thesis has examined techniques for simulating the transport of contaminants in groundwater. In particular, Lagrangian (or random walk) techniques have been examined. These techniques have been applied to a number of test cases and to two physical problems.

In Chapter 2 the equations governing the flow of groundwater and the transport of contaminants were presented. Methods for solving the advection dispersion equation were discussed, namely analytic, finite difference and random walk techniques. Results from the application of two finite difference methods were presented and compared with analytic solutions. It was shown that finite difference techniques could be used to numerically solve the advection dispersion equation; however, under certain conditions numerical diffusion made results inaccurate. Random walk techniques were introduced as an alternative method of solving the advection dispersion equation, using a technique that mirrored the physical processes involved in the transport of contaminants though porous media. Finally, the computer code RNDWALK2D [23] was introduced, a code which models the flow of groundwater and implements the random walk technique to model the transport of contaminants.

In Chapter 3, three random walk techniques were discussed and compared against analytic solutions for one and two dimensional dispersion and advection dispersion with the objective of determining whether the random walk technique could be used to simulate the movement of contaminants in these situations. Additionally, these computed results were compared against those in Chapter 2 which used finite difference methods. It was found that the numerical solution of the random walk techniques compared well to both the analytic solutions and the finite difference solutions. In particular, random walk techniques were not affected by numerical diffusion as was the case for the upwind finite difference scheme con-

sidered in Chapter 2. Thus it was concluded that random walk techniques can be used to numerically determine the solution to the advection dispersion equation.

In Chapters 4 and 5 the random walk technique was applied to two different groundwater systems, the first in Saskatchewan, Canada, the second in the south east of South Australia. In each of these situations the random walk technique was used to simulate the movement of contaminants in their respective systems, and the computed results analysed with respect to available measured values.

Chapter 4 considered the simulation of the movement of a plume of chloride in the groundwater system originating from a sewage reservoir. In this case, the plume that was modelled was long and narrow, occupying a small fraction of the model domain, an ideal situation for the random walk technique. The model developed was shown to produce computed results which were consistent with the measured data that was available.

In Chapter 5 the transport of salt was modelled using random walk techniques applied over a widespread area, in contrast to the model developed in Chapter 4.

In each case it was determined that the random walk technique was able to successfully model the transport of contaminant with the computed results consistent with the measured values.

During the use of random walk techniques, the advantages and limitations of this technique have been determined. The primary advantage of random walk techniques over finite differnce techniques is the lack of numerical diffusion. Another advantage is that in certain circumstances, such as when there is a large number of grid points compared to the number of particles present, using a random walk technique will require less computational effort and produce a computed result in less time.

The application of random walk techniques to the two problems in Chapters 4 and 5 highlights situations where random walk techniques are particularly applicable. In Chapter 4 random walk techniques were used to model a long, narrow plume which occupied a small fraction of the model domain. This is an ideal situation for random walk techniques, which was demonstrated by the low run times of the model. Additionally, if more nodes were added to the model domain, either by extending the domain or by using a finer grid, the number of calculations required to estimate the movement of the plume would remain the same for a given number of particles. On the other hand, using finite difference methods, the number of calculations required would be proportional to the num-

ber of nodes. Conversely, the model presented in Chapter 5 consisted of a plume which covered nearly the entire model domain, and required a large number of particles. The long run times of this model suggested that random walk was not ideally suited to this situation, and that perhaps a finite difference approach may have been more feasible. Nevertheless, the random walk technique produced results that were consistent with the available measured data.

These case studies indicated the strengths and weaknesses in using random walk techniques for simulating advection and dispersion in groundwater flow.

Appendix A

Program Listing for a Forward Time, Centred Space type Formula

```
*  ------------------------------------------------------------------------
*| This program solves the 2 dimensional advection-dispersion equation   |
*| using the FTCS type finite difference formula as discussed in         |
*| Chapter 2                                                             |
*  ------------------------------------------------------------------------


      program FTCS_program

      implicit none
      double precision C(30,30),C_old(30,30)
      double precision delx,dely,delt,u,v,D_x,D_y
      double precision c_x,c_y,s_x,s_y
      integer t

      delx=10
      dely=10
      delt=0.5
      D_x=4.5
      D_y=1.125
      u=1
      v=0

      print *,'FTCS type formula'
      print *
```

```
      print *,'Using the following paramters'
      print *,'Delta X = ',delx
      print *,'Delta Y = ',dely
      print *,'Delta T = ',delt
      print *,'   D_x  = ',D_x
      print *,'   D_y  = ',D_y
      print *,'X vel   = ',u
      print *,'Y vel   = ',v

      call initial(C)
      call boundary(C)
      call copy(C,C_old)
      call constants(delx,dely,delt,u,v,D_x,D_y,s_x,s_y,c_x,c_y)

      do t=1,3000
       call ftcs(C,C_old,c_x,c_y,s_x,s_y)
       if (delt*t .eq. 150) then
        call print_results(C)
       endif
       call copy(C,C_old)
      enddo


      end

*  /---------------------------\
*|    Initial Conditions       |
*  \---------------------------/
      subroutine initial(C)
      implicit none
      double precision C(30,30)
      integer i,j
      do i=1,30
       do j=1,30
        C(i,j)=0.0d0
       enddo
      enddo
      C(5,15)=300.0d0
      return
      end
```

```
* /--------------------------\
*|   Boundary Conditions      |
* \--------------------------/
      subroutine boundary(C)
      implicit none
      double precision C(30,30)
      integer j
      do j=1,30
        C(1,j) = 0.0d0
        C(30,j) = 0.0d0
        C(j,1) = 0.0d0
        C(j,30) = 0.0d0
      enddo
      return
      end


* /--------------------------\
*|    Copy C into C_old       |
* \--------------------------/
      subroutine copy(C,C_old)
      implicit none
      double precision C(30,30),C_old(30,30)
      integer i,j
      do i=1,30
       do j=1,30
        C_old(i,j)=C(i,j)
       enddo
      enddo
      return
      end

* /--------------------------\
*|    Compute constants       |
* \--------------------------/
      subroutine constants(delx,dely,delt,u,v,D_x,D_y,s_x,s_y,c_x,c_y
     & )
      implicit none
      double precision delx,dely,delt,u,v,D_x,D_y
      double precision c_x,c_y,s_x,s_y
```

```
      s_x = D_x*delt/delx/delx
      s_y = D_y*delt/dely/dely
      c_x = u*delt/delx
      c_y = v*delt/dely
      return
      end
*  /---------------------------\
*|   Apply the FTCS formula     |
*  \---------------------------/
      subroutine ftcs(C,C_old,c_x,c_y,s_x,s_y)
      implicit none
      double precision C(30,30),C_old(30,30)
      double precision c_x,c_y,s_x,s_y,A1,A2,A3,A4,A5
      integer i,j

      A1 = c_x/2.0d0 + s_x
      A2 = c_y/2.0d0 + s_y
      A3 = 1- 2.0d0*s_x - 2.0d0*s_y
      A4 = c_x/2.0d0 - s_x
      A5 = c_y/2.0d0 - s_y

      do j=2,29
       do i=2,29
          C(i,j)=A1*C_old(i-1,j)+A2*C_old(i,j-1)+A3*C_old(i,j)
     &  - A4*C_old(i+1,j) - A5*C(i,j+1)
       enddo
      enddo
      return
      end


*  /------------------------- \
*  |    Print the Results      |
*  \------------------------- /

      subroutine print_results(C)
      double precision C(30,30)
      open (unit=2,file='FTCS_output.out')
      do j=30,1,-1
        do i=1,30
          write (2,31)(C(i,j))
```

```
      enddo
     write(2,31)
    enddo
    close(2)
31    FORMAT(F20.10)


     return
      end
```

Appendix B

Program listing for an Explicit Upwind Formula

```
*  ------------------------------------------------------------------------
*| This program solves the 2 dimensional advection-dispersion equation   |
*| using the Upwind finite difference formula discussed in               |
*| Chapter 2                                                             |
*  ------------------------------------------------------------------------


      program Upwind_program

      implicit none
      double precision C(30,30),C_old(30,30)
      double precision delx,dely,delt,u,v,D_x,D_y
      double precision c_x,c_y,s_x,s_y
      integer t

      delx=10
      dely=10
      delt=0.5
      D_x=4.5
      D_y=1.125
      u=1
      v=0

      print *,'UPWIND type formula'
      print *
```

```
      print *,'Using the following paramters'
      print *,'Delta X = ',delx
      print *,'Delta Y = ',dely
      print *,'Delta T = ',delt
      print *,'   D_x  = ',D_x
      print *,'   D_y  = ',D_y
      print *,'X vel   = ',u
      print *,'Y vel   = ',v

      call initial(C)
      call boundary(C)
      call copy(C,C_old)
      call constants(delx,dely,delt,u,v,D_x,D_y,s_x,s_y,c_x,c_y)

      do t=1,3000
       call upwind(C,C_old,c_x,c_y,s_x,s_y)
       if (delt*t .eq. 150) then
        call print_results(C)
       endif
       call copy(C,C_old)
      enddo


      end

*  /---------------------------\
*|     Initial Conditions      |
*  \---------------------------/
      subroutine initial(C)
      implicit none
      double precision C(30,30)
      integer i,j
      do i=1,30
       do j=1,30
        C(i,j)=0.0d0
       enddo
      enddo
      C(5,15)=300.0d0
      return
      end
```

```
* /--------------------------\
*|   Boundary Conditions      |
* \--------------------------/
      subroutine boundary(C)
      implicit none
      double precision C(30,30)
      integer j
      do j=1,30
        C(1,j) = 0.0d0
        C(30,j) = 0.0d0
        C(j,1) = 0.0d0
        C(j,30) = 0.0d0
      enddo
      return
      end


* /--------------------------\
*|    Copy C into C_old       |
* \--------------------------/
      subroutine copy(C,C_old)
      implicit none
      double precision C(30,30),C_old(30,30)
      integer i,j
      do i=1,30
       do j=1,30
        C_old(i,j)=C(i,j)
       enddo
      enddo
      return
      end

* /--------------------------\
*|    Compute constants       |
* \--------------------------/
      subroutine constants(delx,dely,delt,u,v,D_x,D_y,s_x,s_y,c_x,c_y
     & )
      implicit none
      double precision delx,dely,delt,u,v,D_x,D_y
      double precision c_x,c_y,s_x,s_y
```

```
      s_x = D_x*delt/delx/delx
      s_y = D_y*delt/dely/dely
      c_x = u*delt/delx
      c_y = v*delt/dely
      return
      end
*  /--------------------------\
*|  Apply the Upwind formula   |
*  \--------------------------/
      subroutine upwind(C,C_old,c_x,c_y,s_x,s_y)
      implicit none
      double precision C(30,30),C_old(30,30)
      double precision c_x,c_y,s_x,s_y,A1,A2,A3,A4,A5
      integer i,j

      A1 = s_y + c_y
      A2 = s_x + c_x
      A3 = 1 - 2.0d0*s_x - 2.0d0*s_y -c_x - c_y

      do j=2,29
       do i=2,29
          C(i,j)=A1*C_old(i,j-1)+A2*C_old(i-1,j)+A3*C_old(i,j)+
     & s_x*C_old(i+1,j) + s_y*C_old(i,j+1)
       enddo
      enddo
      return
      end

*  ____________________________
*  |                          |
*  |    Print the Results     |
*  |__________________________|

      subroutine print_results(C)
      double precision C(30,30)
      open (unit=2,file='Upwind.output')
      do j=30,1,-1
        do i=1,30
          write (2,31)(C(i,j))
        enddo
       write(2,31)
```

```
      enddo
      close(2)
   31   FORMAT(F20.10)


       return
        end
```

Appendix C

Hydrographs for the model of the south east of South Australia

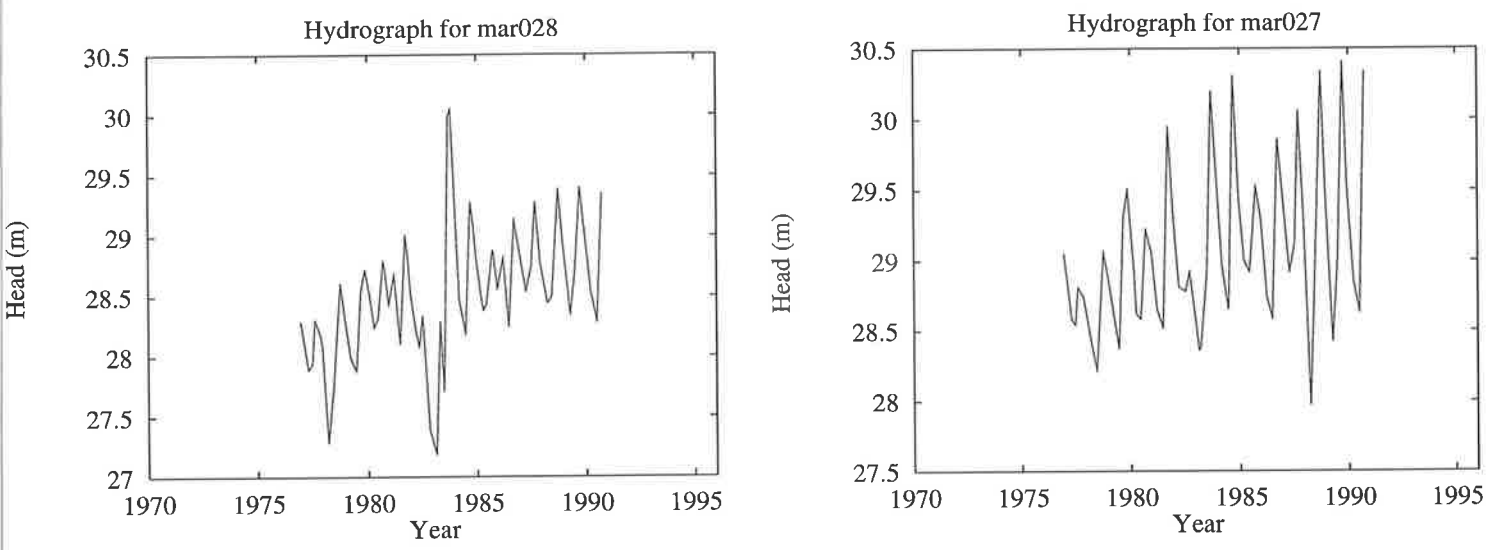

Figure C.1: Hydrographs used for determining heads for the western boundary in the model of the south east of South Australia [5].

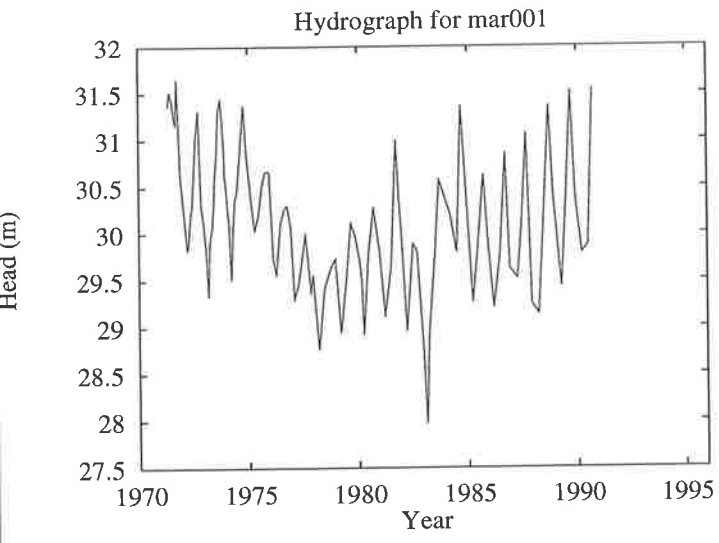

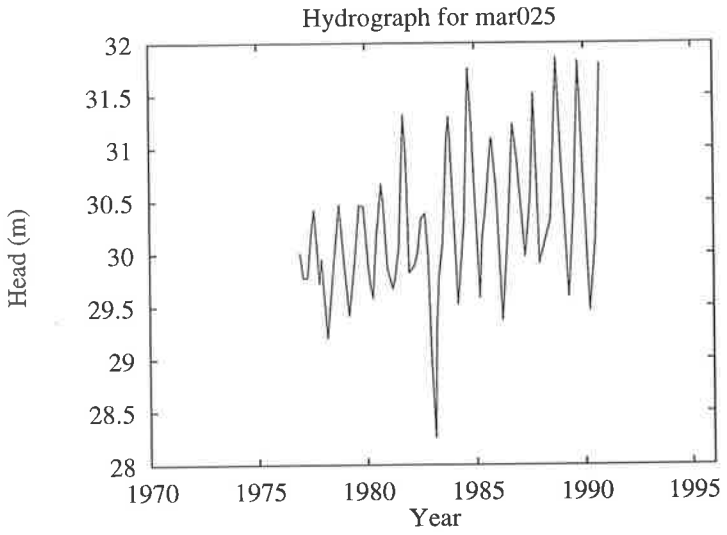

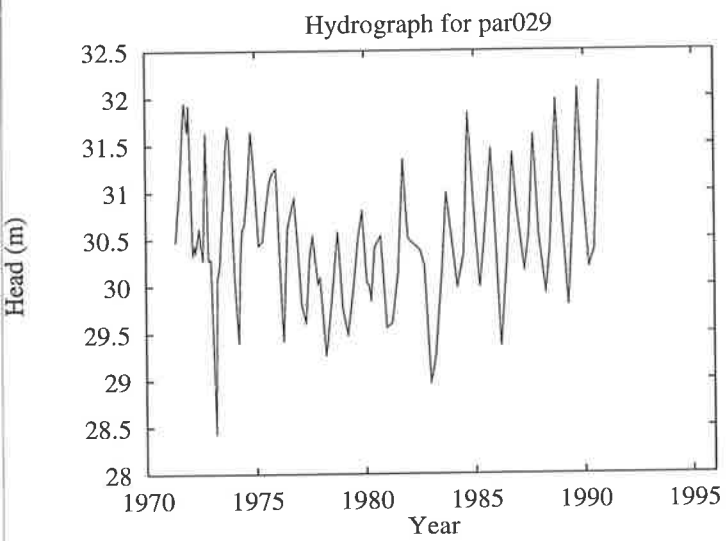

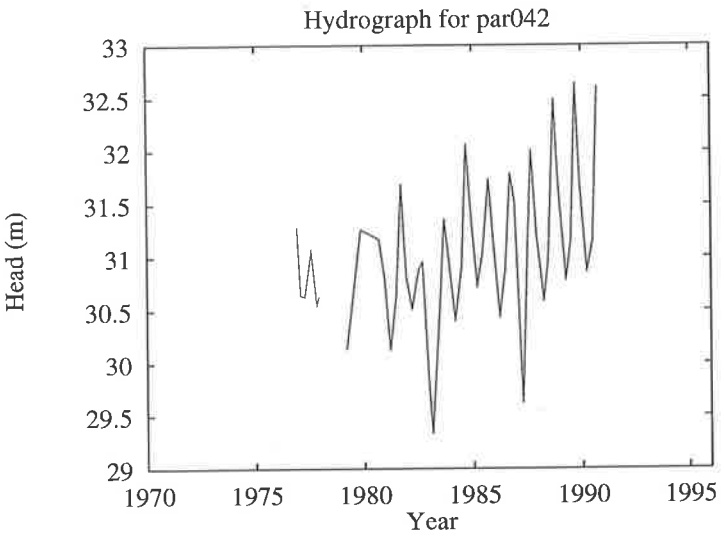

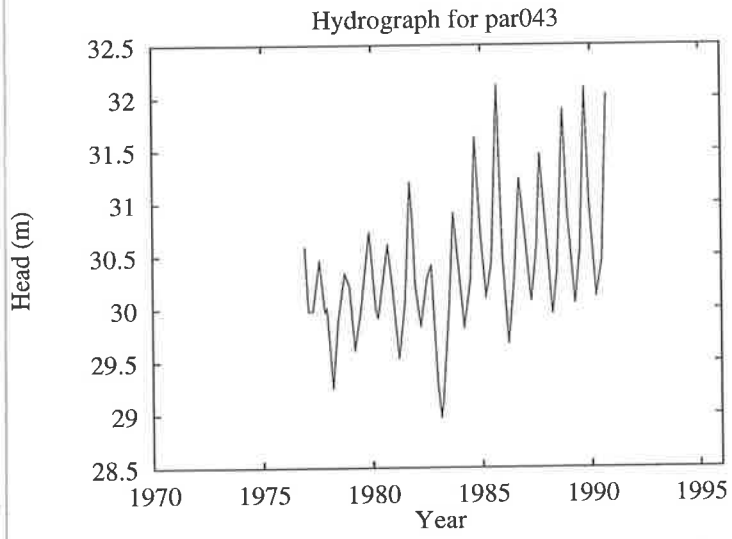

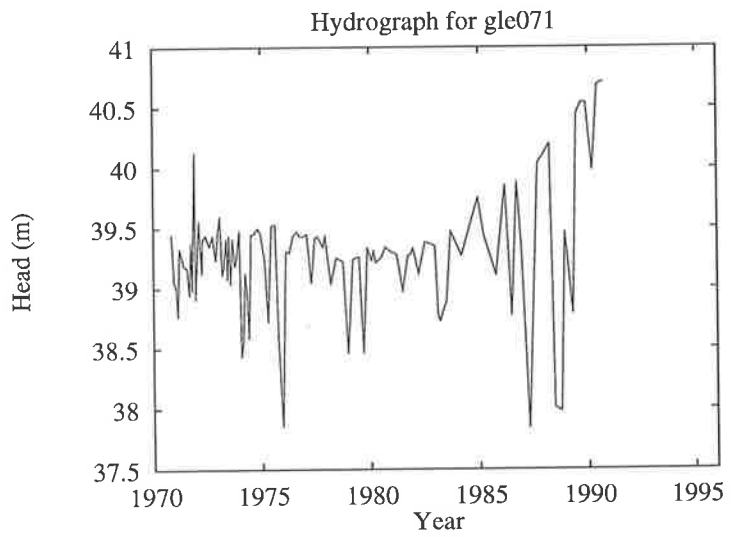

Figure C.1(cont.) Hydrographs used for determining heads for the eastern boundary in the model of the south east of South Australia [5].

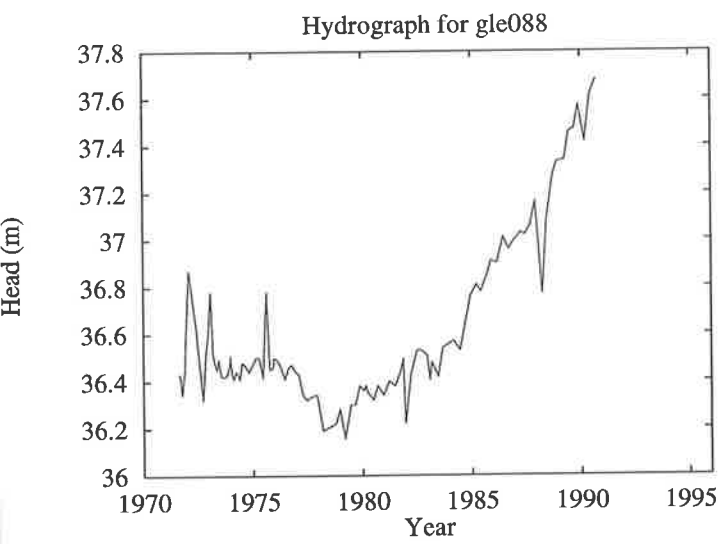

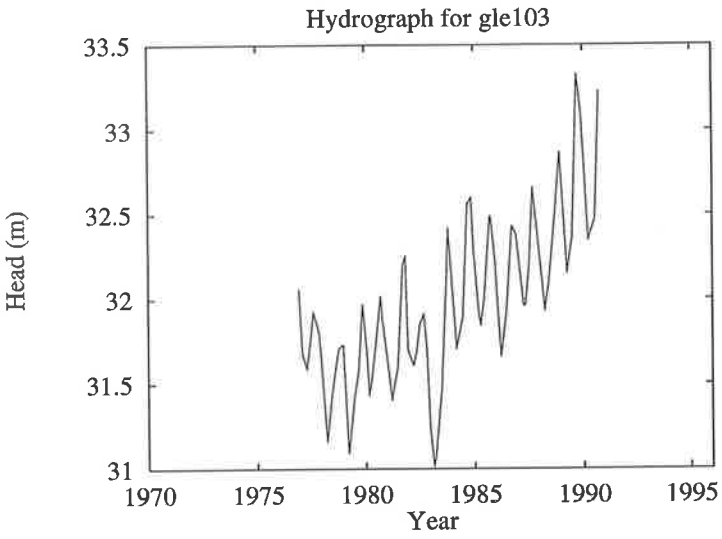

Figure C.1(cont.) Hydrographs used for determining heads for the eastern boundary in the model of the south east of South Australia [5].

Appendix D

Program listing for the subroutine controlling the inflow of particles in the model of the South East.

```
      subroutine SE_SOR
*****************************************************
* This subroutine generates the appropriate number *
* of particles based on a given concentration, eg  *
* given 200ppm at a source, this subr. will        *
* check the number already present in the grid     *
* containing the source, and add the appropriate   *
* number to give the required concentration        *
*****************************************************
       implicit none
       integer nc,nr,np,maxp,npart(90,90),i,j
       doubleprecision apor,epor,consor(90,90),pl,pm
       doubleprecision x1,dx,y1,dy,x(90001), y(90001)
       doubleprecision anc,anr,v(90,90,2),displ,dispt
       doubleprecision tmap,table(99),con_diff
       doubleprecision con_diff,conc(90,90)
       integer mark(90,90),req_part
       doubleprecision h(90,90),rh(90,90),delta,q(90,90),sor(90,90)
       doubleprecision rd(90,90),bot(90,90),delx(90),dely(99)
       doubleprecision x1,dx,y1,dy,delp

      COMMON/TRACE/NP,MAXP,PM,DISPL,DISPT,x(90001),
```

```
     1  y(90001),MARK(90,90),TMAP
      COMMON/AQUI/H(90,90),RH(90,90),
     1  DELTA,Q(90,90),SOR(90,90)
      COMMON/AQUI2/RD(90,90),BOT(90,90)
      COMMON /FORMS/TABLE(99),NPART(90,90)
      COMMON/VEL/NC,NR,ANC,ANR,V(90,90,2)
      COMMON/POR/APOR,EPOR,CONSOR(90,90)
      COMMON/VAR/DELX(99),DELY(99)
      COMMON/POL/X1,DX,Y1,DY,DELP

c this is the current concentration in the grid
         I=NC
       do  J=1,NR
       CONC(I,J)=NPART(I,J)*PM*1.0E6/(APOR*
     1 (H(I,J)-BOT(I,J))*(DELX(I)*DELY(J))*1000.0d0)

c this is the difference
       con_diff = consor(i,j) - conc(i,j)

c this is the number of particles we require
       req_part = con_diff*apor*(h(i,j)-bot(i,j))
     & *delx(i)*dely(j)*1000.0d0/(PM*1E6)

c Set up which grid should receive particles
             X1=I-0.5d0
             Y1=J-0.5d0
             DX=1.0d0
             DY=1.0d0

c  this is how much pollutant we need to put in
       pl = pm*req_part

c Call Subroutine GENP to insert the appropriate number of
c particles around grid X1,Y1
       if (pl .gt. 0.0d0) CALL GENP(PL)

       enddo
       return
       end
```

Appendix E

Salinity Graphs for the model of the south east of South Australia

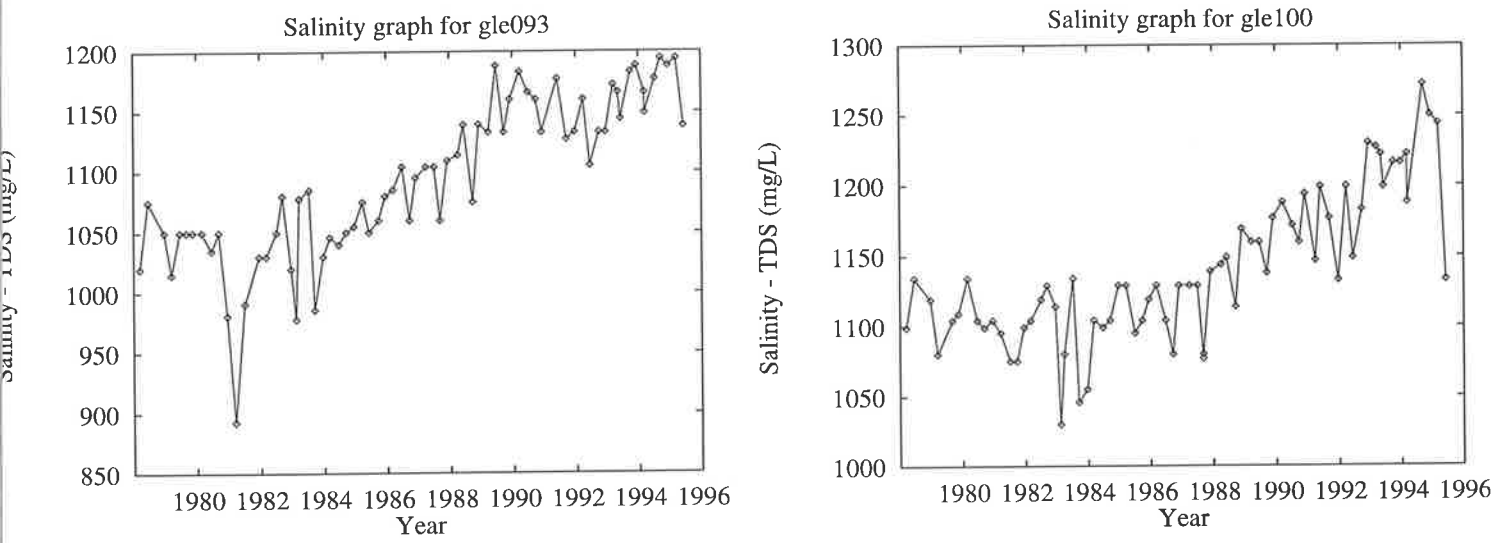

Figure E.1: Salinity graphs used to determine the concentration of salt entering the model of the south east of South Australia through the eastern boundary [5].

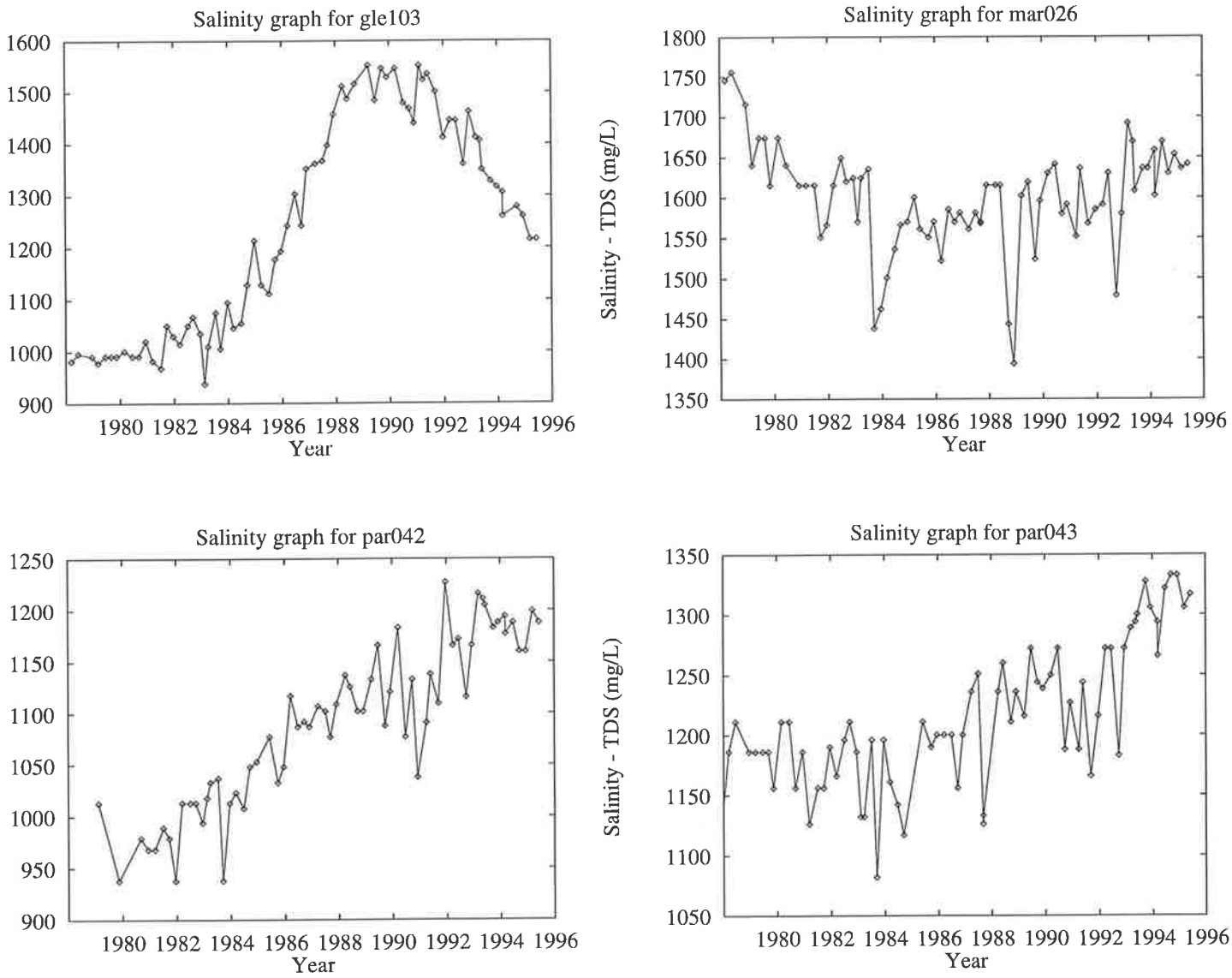

Figure E.1(cont.): Salinity graphs used to determine the concentration of salt entering the model of the south east of South Australia through the eastern boundary [5].

Appendix F

Supplement to the Random Walk Documentation

F.1 Introduction

This document is intended as a supplement to the documentation for RNDWALK2D [23], its purpose being to provide the reader with the basic knowledge required to compile, setup, modify and run the computer program. It is assumed that the reader has this reference available. The program RNDWALK2D can be used to simulate 1, 2, and quasi 3D steady and unsteady flow and solute transport in groundwater.

F.2 Compiling and Running Random Walk

The RNDWALK2D code as presented in [23] is written in FORTRAN IV, however this code has been successfully compiled under FORTRAN 77 using the command line:

```
f77 -f random_walk.f -o random_walk.out
```

which compiles the source code file `random_walk.f` and creates the executable file `random_walk.out` in the current directory.

To run RNDWALK2D the user uses the command line:

```
random_walk.out
```

The code was converted to use double precision variables to eliminate numerical underflow errors that were occurring during initial runs of the code.

F.3 Modifying RNDWALK2D

RNDWALK2D may be modified via the addition and/or modification of subroutines in the existing code. Routines which are used at every time step may be called by their inclusion in the input file. As standard, RNDWALK2D allows for eight such routines to be called at each time step, but this may be easily modified if required. Similarly, subroutines may be added to output files suitable for use in graphical output packages, such as GNUPlot, discussed below. Other modifications which might be employed are:

1. Alternative Random Walk schemes for simulating dispersion.
2. Inclusion of different head solving routines and/or head values derived from a known analytic solution,
3. Model specific routines to inject particles into the model.

F.4 Boundary Conditions

Four types of boundary condition are possible within RNDWALK2D, involving both the flow and transport models. Boundary conditions which affect the flow model are no flow boundaries and constant head boundaries while boundary conditions which affect the transport model are constant concentration and particle extraction boundaries. Specifying either of the flow boundaries types of boundary condition requires that we enter the appropriate values onto the node "card" for each of the nodes involved in the definition of such boundaries. Both types of transport boundary conditions are specified by calling the appropriate subroutines at each time step.

F.4.1 No Flow Boundaries

Boundaries through which no flow occurs may be specified by setting either transmissivity or hydraulic conductivity (or both) to zero on the appropriate node cards.

F.4.2 Constant Head Boundaries

Implementing a constant head boundary condition at a node (or nodes) requires that on the corresponding node card we specify the required head level, and set the storativity to some large value, typically 10^{30}.

F.4.3 Constant Concentration Boundaries and Nodes

A constant concentration boundary or node may be specified to simulate the inflow of a contaminant into the model through either a boundary of a point source. Either of these two situations may be modelled by using existing or custom subroutines which check the number of particles in the required grid squares remains at a specified constant number.

F.4.4 Particle Extraction Boundaries

As particles move through the model domain, it is possible that they may reach one or more of the model boundaries. To avoid a build up of particles at these boundaries a series of sinks can be set up to remove particles as they reach these boundaries.

F.5 Graphical Output with GNUPlot

To enable the production of graphical output of things such as head levels and contaminant plumes with the aid of a package such as GNUPlot, a subroutine must be added to RNDWALK2D to output the desired information into a file suitable for use by GNUPlot. This can be achieved via the addition of the following section of code:

```
      subroutine head_plot(H,nc,nr)
      doubleprecision H(90,90)
      integer nc,nr,i,j

      open (unit=3,file="heads.gnu")
      do j=NR,1,-1
        do i=1,NC
          write (3,114)(H(i,j))
        enddo
       write(3,114)
      enddo
      close(3)
  114   FORMAT(F10.3)
      return
      end
```

This subroutine can be called immediately after the head solving subroutine call via:

```
call head_plot(H,nc,nr)
```

Similarly, with the following additional piece of code, the number of particles at each grid point may be output for later plotting:

```
      Subroutine GNUPLO
       implicit none
      integer nc,nr,np,maxp,mark(90,90),npart(90,90),i,j,idigits,n
      doubleprecision anc,anr,v(90,90,2),pm,displ,dispt,x(5001),
     &  y(5001),tmap,table(90)
      character*20 filename, fmt

      COMMON/TRACE/NP,MAXP,PM,DISPL,DISPT,X(5001),
     1  Y(5001),MARK(90,90),TMAP
      COMMON /FORMS/TABLE(90),NPART(90,90)
      COMMON/VEL/NC,NR,ANC,ANR,V(90,90,2)
       n=TMAP
        if (n .gt. 0) then
          idigits = int(log10(n*1.0)+1)
          write (fmt, '(a,i1,a)') '(i', idigits, ',a)'
          write (filename, fmt) n, '.output'
        endif

      open (unit=2,file=filename)
      do j=NR,1,-1
        do i=1,NC
          write (2,31)(Npart(i,j))
        enddo
       write(2,31)
      enddo
      close(2)
   31   FORMAT(I3)
       return
        end
```

This subroutine should be called at each time step. (This subroutine could be modified so as to print out only at certain time steps). Note that this is simply a modification of the subroutine MAP.

F.6 Zonation patterns

The inputting of data into a data file for use in RNDWALK2D can be tedious and can also be the source of data entry errors which can be irritating and time consuming to eliminate. Examination of a typical RNDWALK2D input file shows that the user is required to input large amounts of data for each node which differs from the default values. For a large grid this could amount to a great many entries, each of which is a likely source of data entry error, even with the use of a cut-and-paste facility. Simplification of this data file can result in data files that are substantially easier to input, and more importantly, make it easier to track data entry errors. The method which I have employed to make this job easier is to assign the nodes of the problem domain into *zones* with the same values. In this way only the values which each zone takes must be specified, and for each node, which zone it belongs to. Use of this method means that for each zone the parameters are given and each node is assigned a zone, instead of listing all the parameters in the input file for each node.

For this purpose the pre processor program *rwpre.f* has been written; it takes a modified version of the standard type RNDWALK2D input file which includes the zonation information, and then outputs a data file for use in RNDWALK2D. The following command is used to compile this program under FORTRAN 77:

```
f77 -f rwpre.f -o rwpre
```

the executable *rwpre* is then run by issuing the command:

```
./rwpre
```

The program rwpre.f reads the data input file *pre.in* and writes the file *rndwalk.in* ready for use in RNDWALK2D.

This type of preprocessor could easily be modified to allow for zones of transmissivity, hydraulic conductivity, recharge, or any number of parameter. However it must also be noted that in doing so the input file would increase in size rapidly if this were undertaken for a number of parameters.

Bibliography

[1] A.H. Al-Rabeh and Gunay N. On the application of a particle dispersion model. *Coastal Engineering*, 17, 1992.

[2] M.P. Anderson and W.W. Woessner. *Applied groundwater modeling : simulation of flow and advective transport*. Academic Press, 1992.

[3] J. Bear. *Dynamics of Fluids in Porous Media*. American Elsevier, 1972.

[4] J. Bear and A. Verruijt. *Modeling Groundwater Flow and Pollution*. D. Reidel Publishing Company, 1991.

[5] K. Brown. *Personal Communication*. Department of Mines and Energy; South Australia, 1997.

[6] A.K. Easton, J.M. Steiner, and D.F. Zhang. Domain and cell effects in diffusion models for oil spills in the ocean. In T.H. Aung, editor, *Ocean and Atmosphere Pacific, Proceedings, International Conference, Adelaide*, pages 33–38, 1996.

[7] A.K. Easton, J.M. Steiner, and D.F. Zhang. Random walk methods for the solution of the diffusion equation. In R.L. May and A.K. Easton, editors, *Computational Techniques and Applications: CTAC95*. World Scientific, 1996.

[8] A. Emmett. *Groundwater Quality Protection*. Centre for Groundwater Studies, 1999.

[9] A.L. Fogelson. Particle-method solution of two dimensional convection-diffusion equations. *Journal of Computational Physics*, 100:1–16, 1992.

[10] R.A. Freeze and J.A. Cherry. *Groundwater*. Prentice Hall, 1979.

[11] A. Gill. IDEC (Inverse Distance Estimation and Cross Validation). *Personal Communication*, 1997.

[12] M. Grzechnik and B.J. Noye. Lagrangian-stochastic particle tracking applied to prawn larvae dispersion in Gulf St. Vincent, South Australia. In B.J. Noye, editor, *Modelling Coastal Sea Processes*, pages 219–246. World Scientific, 1999.

[13] M. Grzechnik and J. Noye. Alternative boundary conditions for a Lagrangian particle tracking routine for coastal seas. In E.O. Tuck and J.A.K. Stott, editors, *3rd Biennial Engineering Mathematics and Applications Confererence*. The Institution of Engineers, Australia, 1998.

[14] M. Grzechnik and J. Noye. A Lagrangian-stochastic particle tracking procedure for coastal seas. In J. Noye, M. Teubner, and A. Gill, editors, *Computational Techniques and Applications: CTAC97*. World Scientific, 1998.

[15] A.C. Hindmarsh, P.M. Gresho, and D.F. Griffiths. The stability of explicit Euler-time integration for certain finite difference approximations of the multi-dimensional advection-diffusion equation. *International Journal of Numerical Methods in Fluids*, pages 853–897, 1984.

[16] J.R. Hunter. The application of Lagrangian particle-tracking techniques to modelling of dispersion in the sea. *Numerical Modelling: Applications to Marine Systems*, 145, 1987.

[17] E.H. Isaaks and R.M.Shrivastava. *Applied Geostatistics*. Oxford University Press, 1989.

[18] L. Lapidus and G.F. Pinder. *Numerical solution of partial differential equations in science and engineering*. Wiley, 1982.

[19] G.D. Lewis, B.J. Noye, and P.L. Evans. A comparison of finite difference and Lagrangian-stochastic methods for oil slick tracking. In R.L. May and A.K. Easton, editors, *Computational Techniques and Applications: CTAC95*. World Scientific, 1996.

[20] B.J. Noye. Finite difference techniques for partial differential equations. *Computational Techniques for Differential Equations*, 1983.

[21] B.J. Noye and K.J. Hayman. Accurate finite difference methods for solving the advection-diffusion equation. In B.J. Noye and R.L. May, editors, *Computational Techniques and Applications: CTAC85*, pages 137–158. North-Holland, 1986.

[22] T.A. Prickett and C.G. Lonnquist. Selected digital computer techniques for groundwater resource evaluation. Technical Report 55, Illinois Department of Energy and Natural Resources, 1971.

[23] T.A. Prickett, T.G. Naymik, and C.G. Lonnquist. A "random-walk" solute transport model for selected groundwater quality evaluations. Technical Report 65, Illinois Department of Energy and Natural Resources, 1981.

[24] C. Purczel and M. Teubner. Comparison of three techniques for modelling the advection/dispersion equation. In E.O. Tuck and J.A.K. Stott, editors, *3rd Biennial Engineering Mathematics and Applications Confererence*. The Institution of Engineers, Australia, 1998.

[25] A.G. Smith and M.D. Teubner. Groundwater transport modelling of the Padthaway region. In J. Noye M. Teubner and A. Gill, editors, *Computational Techniques and Applications: CTAC97*. World Scientific, 1998.

[26] D.K. Todd. *Groundwater Hydrology*. John Wiley and Sons, 1980.

[27] Shaded relief map of Australia. The University of Texas at Austin Web Site. *http://www.lib.utexas.edu/Libs/PCL/Map_collection/australia.html*.

[28] G. Van der Kamp, L.D. Luba, J.A. Cherry, and H. Maathuis. Field study of a long and very narrow contaminant plume. *Groundwater*, 32(6):pages 1008–1016, 1994.

[29] W.C. Walton. *Numerical groundwater modeling : flow and contaminant migration*. Lewis Publishers ; National Water Well Association, 1989.

[30] J. Woods, C.T. Simmons, and K.A. Narayan. Verification of black box groundwater models. In E.O. Tuck and J.A.K. Stott, editors, *3rd Biennial Engineering Mathematics and Applications Confererence*. The Institution of Engineers, Australia, 1998.

[31] J. Woods, M.D. Teubner, C.T. Simmons, and K.A. Narayan. Numerical inaccuracy in groundwater modelling: Diagnosis and pathology. In *Water 99 Joint Congress*. The Institution of Engineers, Australia, 1999.

[32] D.F. Zhang, A.K. Easton, and J.M Steiner. Modelling the Kirki oil spill. In E.O. Tuck and J.A.K. Stott, editors, *3rd Biennial Engineering Mathematics and Applications Confererence*. The Institution of Engineers, Australia, 1998.

[33] C. Zheng. Analysis of particle tracking errors associated with spatial discretization. *Groundwater*, 32(5):pages 821–828, 1994.